Winter 2-2015

# ELUCIDATION OF THE CELLULAR AND MOLECULAR MECHANISMS OF MISSENSE MUTATIONS ASSOCIATED WITH FAMILIAL EXUDATIVE VITREORETINOPATHY AND CONGENITAL MYASTHENIC SYNDROME

Reham Mahmoud Mohammed Milhem

United Arab Emirates University

College of Medicine and Health Sciences

# ELUCIDATION OF THE CELLULAR AND MOLECULAR MECHANISMS OF MISSENSE MUTATIONS ASSOCIATED WITH FAMILIAL EXUDATIVE VITREORETINOPATHY AND CONGENITAL MYASTHENIC SYNDROME

Reham Mahmoud Mohammed Milhem

This dissertation is submitted in partial fulfilment of the requirements for the degree of Doctor of Philosophy

Under the Supervision of Professor Bassam R. Ali

February 2015

# Declaration of Original Work

I, Reham Mahmoud Mohammed Milhem, the undersigned, a graduate student at the United Arab Emirates University (UAEU), and the author of this PhD dissertation, entitled *"Elucidation of the cellular and molecular mechanisms of missense mutations associated with familial exudative vitreoretinopathy and congenital myasthenic syndrome"*. I hereby solemnly declare that this dissertation is an original research work that has been done and prepared by me under the supervision of Professor Bassam R. Ali, in the College of Medicine and Health Sciences at the UAEU. This work has not been previously formed as the basis for the award of any academic degree, diploma or similar title at this or any other university. The materials borrowed from other sources and included in my dissertation have been properly cited and acknowledged.

Student's Signature _____ Date _____

# Signatures

This Doctorate Dissertation is approved by the following Examining Committee Members:

1) Advisor (Committee Chair): Prof. Bassam R. Ali
Title: Professor
Department of: Pathology
College of: Medicine and Health Sciences

Signature: _____ Date: _____

2) Member: Prof. Abdul-kader Souid
Title: Professor
Department of: Pediatrics
College of: Medicine and Health Sciences

Signature: _____ Date: _____

3) Member: Dr. Samir Attoub
Title: Associate Professor
Department of: Pharmacology and Therapeutics
College of: Medicine and Health Sciences

Signature: _____ Date: _____

4) Member (External Examiner): Prof. Ineke Braakman
Title: Professor of Cellular Protein Chemistry
Department of: Bijvoet Center for Biomolecular Research
Institution: Faculty of Science, Utrecht University, The Netherlands

Signature: _____ Date: _____

This Doctorate Dissertation is accepted by:

Dean of the College of Medicine and Health Sciences: Professor Dennis Templeton

Signature _____ Date _____

Dean of the College of Graduate Studies: Professor Nagi Wakim

Signature _____ Date _____

Copy ____ of ____

# Abstract

The endoplasmic reticulum (ER), within eukaryotic cells, is a hub for protein folding and assembly. Misfolded proteins and unassembled subunits of protein complexes are retained in the ER and degraded by a process termed endoplasmic reticulum associated degradation (ERAD). Frizzled class receptor 4 (FZD4) and muscle, skeletal, receptor tyrosine kinase (MuSK) are Wnt receptors. These proteins contain the frizzled cysteine-rich domain (Fz-CRD) required for dimerization in the ER. Mutations in FZD4 and MuSK genes are known to cause familial exudative vitreoretinopathy (FEVR, an autosomal dominant disease) and congenital myasthenic syndrome (CMS, an autosomal recessive disease), respectively. It was hypothesized that missense mutations within Fz-CRD lead to misfolding of FZD4 and MuSK proteins and consequent ER-retention. Investigating the molecular mechanism of these mutations is important since misfolded protein and ER-targeted therapies are in development being developed. Wild-type and mutants of FZD4 and MuSK were expressed at 37 °C in HeLa, COS-7, and HEK293 cells and their subcellular localizations were investigated using confocal microscopy imaging and glycosidase treatments. Abnormal trafficking was demonstrated in 10 of 21 mutants studied; nine mutants were within Fz-CRD and one was distant from Fz-CRD. These ER-retained mutants were improperly N-glycosylated confirming ER-localization. They were tagged with polyubiquitin chains confirming targeting for proteasomal degradation. The half-lives of wild-type MuSK and P344R-MuSK were 45 and 37 minutes, respectively; the latter half-life improved on incubation with proteasomal inhibitor MG132. The P344R-MuSK kinase mutant showed around 50% of its *in vivo* autophosphorylation activity. Trafficking defects in three of the 10 mutants (M105T-FZD4, C204Y-FZD4, and P344R-MuSK) were rescued by expression at 27 °C and by chemical chaperones (2.5-7.5% glycerol, 0.1-1% dimethyl sulfoxide, 10 µM thapsigargin, or 1 µM curcumin). Trafficking of wild-type FZD4 was not affected by

co-expression with any of the nine ER-retained mutants, suggesting haploinsufficiency as the mechanism of disease. Thus, all nine Fz-CRD mutants of FEVR and CMS studied resulted in misfolded proteins. In contrast, only one of the 12 mutants outside Fz-CRD resulted in ER-retention. These findings demonstrate a common mechanism for diseases associated with Fz-CRD missense mutations. Disorders of Fz-CRD may be receptive to novel therapies that alleviate protein misfolding.

**Keywords:** Familial exudative vitreoretinopathy; congenital myasthenic syndrome; endoplasmic reticulum associated degradation; frizzled class receptor 4; muscle, skeletal, receptor tyrosine kinase; frizzled cysteine-rich domain.

# Title and Abstract in Arabic

## توضيح الآلية الخلوية والجزيئية للطفرات المغلطة المرتبطة بإعتلال الشبكية الزجاجي الوراثي (FEVR) ومتلازمة الوهن العضلي الخلقية (CMS)

## الملخص

تعتبر الشبكة الإندوبلازمية endoplasmic reticulum (ER) في الخلايا حقيقية النواة محور لطي البروتين وتجميعه. البروتينات ذات الطي الخاطئ وكذلك الوحدات الجزئية غير المجمعة من مجمعات البروتين تستقر في الشبكة الإندوبلازمية (ER) و تتدهور من خلال عملية تسمى التدهور المترابط في الشبكة الإندوبلازمية Endoplasmic reticulum associated degradation (ERAD). البروتين المستقبل فريزلد (FZD4) والبروتين المستقبل مسك (MuSK) يعتبران من مستقبلات وينت (Wnt). تحتوي هذه البروتينات على السستين frizzled cysteine-rich domain (Fz-CRD) الضروري لعمليات ربط جزيئات البروتينات (dimerization) في الشبكة الإندوبلازمية (ER). الطفرات في جين فرزلد (FZD4) وجين مسك (MuSK) هي المسببة لمرض familial exudative vitreoretinopathy (FEVR) ولمرض congenital myasthenic syndrome (CMS) على التوالي. لقد تم الإفتراض بأن الطفرات المغلطة في المجالات الغنية بفرزلد- السستين (Fz-CRD) تؤدي إلى الطي الخاطئ في بروتينات فرزلد (FZD4) ومسك (MuSK) وإلى الإستبقاء في الشبكة الإندوبلازمية (ER). البحث في الآلية الجزيئية لهذه الطفرات مهم كون والعلاجات المستهدفة للطي الخاطئ للبروتين و للشبكة الإندوبلازمية في تطور. تم إختبارالبروتين السليم والطفرات لكل من فرزلد (FZD4) و مسك (MuSK) عند درجة حرارة 37 سلسيوس في خلايا (HeLa و7- COS و HEK293) كما تم البحث في التمركز التحت خلوي (subcellular localization) لهما بواسطة التصوير المجهري متحد البؤر(confocal microscopy) وعلاجات غليكوزيداز (glycosidase treatments). ظهرت عمليات نقل غير طبيعية في عشرة طفرات من الطفرات الإحدى والعشرين التي تمت دراستها، حيث كانت تسع من هذة الطفرات ضمن المجالات الغنية بفرزلد السستين (Fz-CRD) وواحدة بعيدة عنها. هذة الطفرات المستقرة في الشبكة الإندوبلازمية (ER) كانت غير صحيحة الإرتباط الغليكوزيلي (N-glycosylated) مما يؤكد تمركزها في الشبكة الإندوبلازمية و كانت موسومة بسلسلة البوليوبيكويتين (polyubiquitin chains) مما جعلها هدف للتدهور البروتيزوملي (proteasomal degradation). كانت أعمار النصف للنوع الطبيعي من مسك (MuSK) و النوع المطفرن (P344R- MuSK) هي 45 و 37 دقيقة على التوالي، وقد تحسن نصف عمر الأخير خلال فترة الحضانة بواسطة استخدام المانع البروتيزوملي (proteasomal inhibitor MG132). أظهرت الطفرة مسك (P344R-MuSK) نحو 50% من نشاط الفسفرة الآلي في الجسم الحي (in vivo autophosphorylation). لقد تم تصحيح عيوب عملية النقل في ثلاث طفرات من العشر وهي (M105T-FZD4 و C204Y-FZD4 و P344R-MuSK) من خلال زراعة الخلايا المختبرة عند درجة حرارة 27 سلسيوس واستخدام المواد الكيميائية ( Chemical chaperones) الجلسرين و ثنائي ميثيل السلفوكسيد و ميكرومتر الثابسيجارجن و الكركمين ( 2.5-7.5% glycerol, 0.1-1% dimethyl sulfoxide, 10 µM thapsigargin, 1 µM curcumin). لم تتأثر عملية نقل البروتين السليم فرزلد (FZD4) بأي من طفرات فرزلد (FZD4) التسع عندما تم احتضانها بشكل ثنائي مع كل منها مما يدل على أن عدم كفاية الهابلو (haploinsufficiency) هي الآلية المسببة لهذا المرض. لذا فإن كافة الطفرات التسع الموجودة في (FZ- CRD) والمسببة لمرض (FEVR) ولمرض (CMS) تنتج عن الطي الخاطئ للبروتين. وعلى العكس من ذلك فإن واحدة فقط من الطفرات الإثنا عشر الموجودة خارج (FZ- CRD) أدت الى الإستقرار في الشبكة الإندوبلازمية (ER). أظهرت هذه النتائج وجود آلية مشتركة للأمراض المرتبطة بالطفرات المغلطة الموجودة في (FZ- CRD) مما يدل على امكانية علاج الإظطرابات الموجودة في (FZ- CRD) بإستخدام علاجات جديدة وغير مسبوقة تخفف من الطي الخاطئ للبروتين.

# Acknowledgements

I should like to thank my project supervisors, Professor Bassam Ali and Professor Lihadh Al-Gazali for giving me this once-in-a-lifetime opportunity to complete my PhD and to carry out research in their laboratory. I thank them for their support throughout. I should also like to show my gratitude to Professor Abdul-Kader Souid and Dr. Samir Attoub, members of the dissertation advisory committee, for their invaluable criticism, and their willingness to spend a lot of time giving me constructive criticism and feedback for my project.

I should like to the thank the Biochemistry Department at the College of Medicine and Health Sciences (CHMS) especially Zeina Al-Natour and Mustafa Ardah for their helpful discussions which allowed me to focus my attention on wider areas related to this project. This has allowed me to think critically and gain more experience in my field.

I am grateful to the United Arab Emirates University for offering me a PhD fellowship. I should like to thank members of the Graduate Studies Committee for their continuous efforts to improve the program.

I should like to thank all my colleagues from the Pathology Department laboratory for their moral support. I thank Hayat for taking the time to listen to my frustrations. I should especially thank Anne John for her efforts to ensure all my materials were ordered in a timely fashion and for showing me how to care for and culture cells. I should like to thank Mr. Tariq Saeed for his training with confocal microscopy imaging. I should truly like to thank everyone on the fourth floor of the CMHS building for their encouragement, willingness to lend a helping hand, their smiles and sense of humor.

I also need to thank a friend who gave me his precious time to listen to my burning issues, his encouragement and advice.

Lastly and most importantly, I wish to thank my children, Isra, Ala, Yaseen and Nour for their love and understanding. I owe my sincere gratitude to my husband, Mohammed, for without his understanding, encouragement, support and love, none of this would be possible.

# Dedication

*I wish to dedicate my PhD dissertation to*
*my husband Mohammed and*
*my children; Isra, Ala, Yaseen and Nour*
*for their unconditional love.*

*I also wish to dedicate this to the children suffering from*
*familial exudative vitreoretinopathy and*
*congenital myasthenic syndrome.*

# Table of Contents

# List of Tables

# List of Figures

# List of Abbreviations

| | |
|---|---|
| AAA ATPase | ATPases Associated with diverse cellular Activities |
| ACVRL1 | activin receptor-like kinase (ACVRL1) |
| Aha1 | Hsp90 co-chaperone ATPase regulator (Aha1) |
| AMDM | acromesomelic dysplasia type Maroteaux |
| AMP | adenosine mono-phosphate |
| ATF6α | activating transcription factor 6 α (ATF6α) |
| ATP | adenosine tri-phosphate |
| BAP | BiP associated protein |
| C | cysteine |
| $Ca^{2+}$ | calcium |
| cAMP | cyclic adenosine monophosphate |
| cAMP | cyclic adenosine monophosphate |
| CD | cluster of differentiation |
| CF | cystic Fibrosis |
| CFM | confocal fluorescence microscopy |
| CFTR | cystic fibrosis conductance regulator |
| CHOP/GADD153 | CCAAT enhancer-binding protein (C/EBP) homologous protein |
| CHX | cycloheximide |
| CMS | congenital myasthenic syndrome |
| COPII | cytosolic coat protein complex II |
| COS-7 | fibroblast-like cell line derived from monkey kidney tissue |
| CPY | carboxypeptidase Y |
| CRISPR | clustered regulatory interspaced short palindromic repeats)/cas9 systems |
| CRT | calreticulin |
| CXN | calnexin |
| DDR2 | discoidin domain receptor tyrosine kinase 2 |
| DERL1/DER1 | der1-like domain family, member 1 |
| DMEM | dulbecco’s modified Eagle’s medium |
| DMSO | dimethylsulfoxide |
| DNA | deoxyribonucleic acid |
| DTT | dithiothreitol |
| E1 | ubiquitin activating enzyme |

| | |
|---|---|
| E2 | ubiquitin conjugating enzyme |
| E3 | ubiquitin ligase enzyme |
| EDEM | ER degradation-enhancing α-mannosidase I–like protein |
| EGFP *HRAS* | enhanced green fluorescent protein-Harvey rat sarcoma viral oncogene homolog |
| eIF2 α | eukaryotic translational initiation factor 2 α |
| Endo H | endo-β-N-acetylglucosaminidase H |
| ENG | endoglin |
| ER | endoplasmic reticulum |
| ERAD | endoplasmic reticulum associated degradation |
| ERAD-C | ERAD-cytoplasmic |
| ERAD-L | ERAD-luminal |
| ERAD-M | ERAD-intramembrane |
| ERdj(1-7) | HSP40's J-domain containing proteins |
| ERLEC1/XTP3-B | ER lectin 1 |
| Ero1 | ER oxidase 1 |
| ERQC | endoplasmic reticulum quality control |
| Erv2 | essential for respiratory and vegetative growth 1 |
| FCMD | Fukuyama-type congenital muscular dystrophy |
| FEVR | familial exudative vitreoretinopathy |
| FZ-CRD | frizzled cysteine–rich domain |
| FZD4 | frizzled class receptor 4/frizzled family receptor 4 |
| GAPDH | glyceraldehyde-3-phosphate dehydrogenase |
| GI /GII | α-glucosidase I and II |
| GlcNAc | N-acetylglucosamine |
| Golgi Man I /II | alpha-mannosidases I and II |
| GPI | glycosylphosphatidylinositol |
| GQC | glycoprotein quality control |
| GRP | glucose-regulated protein |
| GRP94 | GRP170 alongside HSP90-like chaperones |
| GSSG | oxidized glutathione |
| GTP | guanosine-5'-triphosphate |
| HEK293 | human embryonic kidney cell Line 293 |
| HeLa | Henrietta Lacks (human epithelial adenocarcinoma cell line) |

| | |
|---|---|
| HHT | hereditary hemorrhagic telangiectasia |
| hKv1.5 | human cardiac Kv1.5 |
| Hmg2p | 3-hydroxy-3-methylglutaryl-CoA reductase |
| HMG-CoA | 3-hydroxy-3-methylglutaryl coenzyme A |
| hPAH | human phenylalanine hydroxylase |
| HSPA5/BiP | heat shock 70kDa protein 5 (glucose-regulated protein, 78kDa) |
| IF | immunofluorescence |
| IGF2R | insulin-like growth factor 2 receptor |
| IRE1α | inositol requiring transmembrane kinase/endoribonuclease 1 α |
| kDa | kiloDalton(s) |
| MHCI | class I major histocompatibility complex |
| MRH | mannose-6-phosphate receptor homology |
| mRNA | messenger ribonucleic acid |
| MuSK | muscle, skeletal, receptor tyrosine kinase |
| NDP | Norrin |
| NFM | non-fat dry milk |
| N-glycan | Glu(3)Man(9)GlcNAc(2) |
| *NPR-B* | natriuretic peptide receptor B |
| OS9/OS-9 | osteosarcoma amplified 9, endoplasmic reticulum lectin |
| PDI | protein disulfide isomerase |
| PDIA3/ERp57 | protein disulfide isomerase family A, member 3 |
| PERK | PKR-activated protein kinase-like eukaryotic initiation factor 2 α kinase |
| PN | proteostasis network |
| PNGase F | peptide-N(4)-(N-acetyl-beta-glucosaminyl) asparagine amidase |
| PPIs | peptidyl prolyl isomerases |
| PPP1R15A | protein phosphatase 1, regulatory subunit 15A |
| PUCs | polyubiquitin chains |
| QC | quality control |
| RDH12 | retinol dehydrogenase 12 (RDH12) |
| rHBCK | human brain-type creatine kinase |
| RING | really interesting new gene |
| RNA | ribonucleic acid |

| | |
|---|---|
| RNAi | ribonucleic acid interference |
| ROR2 | receptor tyrosine kinase-like orphan receptor 2 |
| S. cerevisiae | saccharomyces cerevisiae |
| SBP | substrate-binding pocket |
| SDS-PAGE | sodium dodecyl sulfate-polyacrylamide gel electrophoresis |
| Sec23/Sec24 | sec23/24 homolog (S. cerevisiae) |
| SEL1L | sel-1 suppressor of lin-12-like (C. elegans) |
| siRNA | small interfering RNA |
| SP | signal peptide |
| SQLE | squalene monooxygenase |
| SRP | signal recognition particle |
| SVIP | small VCP/p97-interacting protein |
| SYVN1 | synovial apoptosis inhibitor 1, synoviolin |
| TALEN | transcription activator-like effector nucleases) |
| TBS | TRIS-buffered saline |
| T-cell | thymus lymphocyte |
| TEK | TEK tyrosine kinase, endothelial |
| UAE | United Arab Emirates |
| Ub | ubiquitin |
| UDP | uridine diphosphate |
| UGGT1 | UDP-Glc:glycoprotein glucosyltransferase 1 |
| UPR | unfolded protein response |
| VMCM | cutaneomucosal venous malformation |
| Wnt | wingless-type mouse mammary tumor virus integration site family |
| XBP1 | X-box binding protein-1 |
| α-Gal A | α-galactisidase A |
| ΔF508 CFTR | deletion of phenylalanine (F) at position 508 in the CFTR protein |

# Chapter 1: Introduction

## 1.1 Problem statement and motivation

Folding and processing of proteins destined for the secretory pathway takes place within the endoplasmic reticulum (ER) as a specialized series of events resulting in the expression of bona fide proteins. The primary amino acid sequence inherent in the polypeptide backbone and multiple post-translational modifications indicate the folding status of polypeptides in the ER [1-3]. The fidelity of protein folding and assembly is mediated by cellular proteins that are collectively referred to as molecular chaperones which function together as “quality control monitors” [4]. The chaperones are capable of distinguishing between native and non-native states of the polypeptide.

Glycoproteins incapable of reaching their native states, either due to a mutation or an error in the folding, trigger a signal to the glycoprotein quality control (GQC) system [5, 6] which utilizes protein *N*-glycosylation and N-glycan trimming [7] to dislocate nascent glycopolypeptide substrates from the ER via extremely complex ER-machinery. The mechanism of ER-misfolded protein recognition, targeting, retrotranslocation and cytosolic degradation by the ubiquitin-proteasome has been collectively termed endoplasmic reticulum-associated degradation (ERAD) [8-13].

Over the past 30 years, the cellular pathogenesis of multiple genetic disorders caused by single amino acid substitutions (missense mutations) has been directly linked to altered protein folding and/or abnormal protein maturation [1, 8, 14, 15]. These ER-retained proteins are either susceptible to aggregation [16] or up-regulation of the unfolded protein response (UPR) within the cell resulting in cell death [17] or elimination of the protein by ERAD.

ER-retained misfolded proteins caused by missense mutations are not well represented in extant literature. Bioinformatic tools have predicted that proteins, in

the human genome, with ER-targeting signals that enter the secretory pathway *en route* to their final destinations, are more than stated in the literature (45 versus 30%) [18]. The extant literature appreciates that 85% of proteins harboring signal peptides come from known disease-associated genes and have been shown to be authentic ERAD substrates. Therefore, the pathological cellular and molecular mechanism of many human genetic diseases where ERAD is the cause of the loss-of-function of the protein remains to be elucidated.

More importantly, little is known about inherited missense mutations located within the conserved frizzled cysteine-rich domain (Fz-CRD) of proteins. The Fz-CRD is a mobile evolutionary unit that has been found mainly in Wnt (wingless-type mouse mammary tumor virus integration site family) receptors. Fz-CRD families are named so because they possess 10 conserved cysteine motifs. Fz-CRD attains a correct fold in the ER alongside homo-and/or hetero-dimerization [19-23]. The major cell surface receptors for Wnts are the seven-transmembrane frizzled proteins [24], certain receptor tyrosine kinases such as muscle, skeletal, receptor tyrosine kinase (MuSK) [19, 21] and receptor tyrosine kinase-like orphan receptor 2 (ROR2) [25]. Missense mutations in frizzled class receptor 4 (*FZD4*) and *MuSK* genes are known to cause familial exudative vitreoretinopathy (FEVR, an autosomal dominant disease) and congenital myasthenic syndrome (CMS, an autosomal recessive disease), respectively. It was hypothesized that missense mutations within Fz-CRD lead to misfolding of FZD4 and MuSK and their retention in the ER. They would consequently be degraded by ERAD leading to loss-of-function at the cell surface.

Cystic fibrosis (CF) is a well-known hereditary disorder that affects 1 in 2500-4000 newborns [26] of Caucasian descent. Patients mainly suffer from thick mucous secretions in both the lung and the intestine which leads to repeated lung infections. Fifty years ago, the life expectancy of CF patients was about six months but they

can now live up to 37 years [27]. Correction of the molecular defect offers the maximum potential for improving CF patients' quality of life and life expectancy [27]. Observations were made that the deletion of phenylalanine at position 508 (ΔF508) in the cystic fibrosis conductance regulator protein (CFTR) causing CF appears to reach the native state, move out of the ER to the plasma membrane and function as a cyclic adenosine monophosphate (cAMP)-stimulated chloride channel [28, 29].

Therefore, knowledge of the cellular and molecular mechanisms underpinning a disease is vital and serves to facilitate understanding of both the pathology of the disease and the selection and development of appropriate therapeutic targets. Lower-temperature incubation has been shown to slow down cellular processes assisting folding. These temperature-sensitive misfolded proteins are salvageable and can be further manipulated using chemical compounds referred to as chemical chaperones. Chemical chaperones work in different ways to assist the folding, stabilization and/or exit of mutant proteins out of the ER [28, 30-32]. Some misfolded proteins targeted by the ERAD machinery have been shown to be biologically functional if allowed to exit from the ER and pass further on in the secretory pathway to their final destinations [33-35].

This raised the possibility that strategies that influence the protein folding environment inside cells might prove to have therapeutic value [8, 29, 31]. Manipulation by silencing of the messenger RNA (mRNA), siRNA of prominent ERAD machinery components responsible for the ubiquitination or handling of the misfolded protein before it is dislodged out of the ER and transferred to the proteasome system, could also correct and rescue the misfolded protein. This has encouraged researchers to manipulate the ER folding and GQC machinery in ways that offer novel therapeutic approaches in some diseased states.

## 1.2 Objectives

Some disease-causing missense mutations in selected Wnt genes namely: *FZD4* and *MUSK* were potential candidates for retention in the ER and handling by ERAD. Another gene, TEK tyrosine kinase endothelial (*TEK*), was also a potential candidate. These candidates can be examined by analyzing the effect of the mutations on the protein structure using bioinformatics tools and evaluated experimentally using cell line model systems. These proteins are functionally diverse and each possesses a unique tertiary structure with different interacting partners.

The specific objectives that I set out to seek in my dissertation research are highlighted below:

Firstly, to characterize the cellular, biochemical and molecular mechanisms underlying disease-causing mutations in the following genes:

1. Muscle, Skeletal, Receptor Tyrosine Kinase (*MuSK)* gene causing Congenital Myasthenic Syndrome (CMS)
2. Frizzled Class Receptor 4 (*FZD4*) gene causing Familial Exudative Vitreoretinopathy (FEVR)
3. TEK Tyrosine Kinase, Endothelial *(TEK)* gene causing Multiple Cutaneous and Mucosal Venous Malformations (VMCM)

Secondly, to evaluate the effects of manipulating the ER cellular environment to assist correct folding of ER-retained mutant proteins. The effect of varying culturing temperatures and incubation with different chemical chaperones on the selected mutants was evaluated by confocal microscopy and protein expression studies. Changes in the trafficking, judged by confocal imaging, deglycosylation assays and cell-surface protein biotinylation, were evaluated by immunofluorescence, immunoprecipitation and western blotting [18].

Initially, transient transfection allowed for screening of a larger number of mutants. These preliminary results showed which mutants were thermosensitive, hence, can be manipulated to traffic normally to the cell surface. Chemical chaperones reported in the literature and found to affect the folding of ΔF508-CFTR and other ER-retained proteins were evaluated.

Thirdly, to generate stably transfected cell lines of a model ERAD substrate. The aim was to generate stably expressing cells for a thermosenstive mutant, its wild-type and an empty vector. A kill curve was generated to determine the lowest concentration of antibiotic necessary to maintain the stable cell lines. Stable cell lines allowed for more consistent reproducible results and therefore were also used to look at *N*-glycosylation profiles, chemical chaperone treatment and siRNA knockdown treatment.

Finally, to assess the knockdown of some ERAD machinery components using siRNA. RNAi and siRNA technologies have emerged in recent years to be the methods of choice for downregulation/knock out of specific genes expressed in cultured cells, tissues and even whole animals [36]. This project aimed to downregulate a set of proteins involved in the degradation of ERAD substrates. Based on work carried out in this area, prominent ERAD machinery components were chosen for siRNA knockdown.

## 1.3 Dissertation structure

This dissertation is divided into five chapters. Chapter 2 contains the background biology and literature about the GQC system and ERAD as a disease causing mechanism for numerous human diseases. It also contains research that is being adapted to help misfolded proteins exit from the ER mimicking the chemical chaperones in this regard, as well as offering misfolded protein and ER-targeted therapy. Silencing has emerged as a useful tool to observe the knockout effect of

ERAD machinery components and their effect on proteins. A brief description shows how silencing can be used as a target to promote the rescue of misfolded proteins.

Chapter 3 outlines the materials and research methods used in the dissertation. Chapter 4 presents and discusses the results and provides the bulk of the dissertation. A brief literature background on the genes and/or proteins utilized in this research. More importantly each section includes the results obtained together with brief discussion. Designing and making the mutant and wild-type constructs, expression of these constructs within mammalian cell lines and observing their effects *in vitro* allowed the mechanisms of disease to be elucidated. Further work such as chemical chaperone treatment carried out *in vitro* and observing the effects provide the groundwork for potential therapeutic interventions.

Chapter 4, section 4.1 focuses on FZD4, the gene and protein that effects many missense mutations scattered throughout the protein studied. The subcellular localization of mutants within mammalian cell lines and FZD4's pathological cellular and molecular mechanism in FEVR will be explained. Chapter 4, section 4.2 discusses MuSK, the gene and protein will also be discussed. The localization of six reported missense mutations will be observed. One vital disease causing mutation, found within the Fz-CRD, will be studied in detail with biochemical and functional *in vitro* analysis showing the involvement of ubiquitin/proteasome in loss-of-function of the misfolded protein as the cause for CMS. Chapter 4, section 4.3 will briefly discuss TEK; the gene and protein. The results exclude TEK disease-causing inherited mutations from being ERAD substrates. Chapter 4; section 4.4 will discuss the effects of silencing the ERAD machinery components on stable cell lines expressing a selected ERAD substrate. Silencing of ERAD machinery components *in vitro* is to observe any rescue effect on the misfolded protein. Chapter 5 will briefly summarize the findings, provide a general disussion, highlight the conclusions, outlook and perspectives for future directions.

# Chapter 2: Literature Review

## 2.1 The ER as a hub for protein folding

### 2.1.1 History of the endoplasmic reticulum and disease

Thymus lymphocyte (T-cell) receptor was seen to be rapidly degraded in cells independent of lysosomal proteases. This observation by Lippincott-Schwartz in 1988 led to the proposal that the ER organelle had some uncharacterized proteolytic activity towards misfolded proteins. In yeast *Saccharomyces cerevisiae* (*S. cerevisiae*), a component of the ubiquitin conjugation machinery [37] further confirmed this observation when a short-lived misfolded ER membrane protein's degradation was blocked in Ubc6 deficient yeast cells. Ubc6, a component of the ubiquitin conjugation machinery [37] is involved in the covalent attachment of the 76 amino acid ubiquitin (Ub) protein acting as a degradation signal and targeting them to ubiquitin activating (E1), ubiquitin conjugating (E2) and ubiquitin ligase (E3) enzymes [38]. These ubiquitin tagged proteins are then targeted for proteasomal degradation [39].

The ubiquitin-proteasome systems' involvement in CFTR degradation was shown when proteasome inhibition resulted in the accumulated polyubiquitinated CFTR [40, 41]. In addition, luminal misfolded proteins such as carboxypeptidase Y (CPY*) yeast mutants [39] defective in the breakdown of a mutated soluble vacuolar protein, [38, 39] were also studied as a prototype ERAD substrate. Collectively, these studies resulted in the understanding that aberrant misfolded proteins were disposed of by an ubiquitin-proteasome system in the cytosol.

### 2.1.2 ERAD regulates and maintains homeostasis of the cell

ERAD has been shown to be involved in the regulation of metabolic pathways in the presence of a specific signal. The key enzyme in sterol biosynthesis, 3-hydroxy-3-methylglutaryl coenzyme A (HMG-CoA) reductase, was found to be tightly

regulated through ERAD degradation when the level of cholesterol in the cell is adequate i.e. intracellular cholesterol homeostasis, thereby preventing atherosclerosis [42]. Yet another enzyme of the sterol biosynthetic pathway, squalene monooxygenase (SQLE), also an ERAD substrate, orchestrated through a feedback inhibition system to prevent the accumulation of toxic intermediate sterol metabolites [43]. Synthesis of sterols and other sterol-derived metabolites is regulated by ERAD in mammals, yeasts and plants [44] indicating a role for the evolutionary conservation of this mechanism.

Viral and bacterial toxins such as the human cytomegalovirus and cholera toxin, hijack the ERAD machinery to degrade host defense proteins such as the major immunohistocompatibility complex class I (MHC I) or CD4 complexes and, as a result, they escape surveillance mechanisms and consequently gain access to the cell [45]. Several soluble and cytoplasmic proteins have also been subjected to protein turnover by ERAD machinery [43].

Subsequent genetic and biochemical studies in both mammalian cells and budding yeast identified many ERAD components and the organization of the ERAD machinery. Taxis et. al., [46] identified distinct specificity for different classes of misfolded proteins and the differentiated substrate approach taken by ERAD machinery leading to multiple branches of this pathway [47].

### 2.1.3 Protein translocation and folding in the endoplasmic reticulum

The ER is an essential cellular organelle which maintains lipid biosynthesis, redox and calcium homeostasis and more importantly protein folding and secretion. Approximately one third of all open reading frames code for proteins which enter the ER [48]. The folding of proteins is very complex yet intriguing and is discussed in the next few sections.

Nascent secretory pathway targeted polypeptides translated on ribosomes in the cytoplasm are co-translationally translocated into the ER lumen via a translocon [49] (Figure 2.1.1). When the polypeptide sequence emerges from the ribosome exit tunnel, an N-terminal hydrophobic signal peptide (SP) sequence of 20-30 amino acids exposes itself to the cytoplasm. This SP targets the polypeptide to the ER for further processing and the nature of the SP is vital for further processing of the polypeptide [50].

Polypeptides destined to the ER harboring this signal peptide are recognized and captured by a ribonucleoprotein complex, the signal recognition particle (SRP) [51] using guanosine-5'-triphosphate (GTP) as energy. This complex of translating ribosomes and SRP causes translational arrest, and concomitantly targets the complex to a translocon channel via SRP receptor located on the cytosolic face of the ER. Binding of the complex to the SRP receptor stimulates GTP hydrolysis and the release of SRP, allowing translation to resume and the polypeptide to enter the ER lumen [48].

Protein folding always starts during translation [52], but the vast majority of folding takes place when the polypeptides enter the ER lumen where the signal peptide is cleaved by a signal sequence peptidase complex. Timing of signal peptide cleavage is not the same for different proteins. For example, tyrosinase's SP is cleaved when the polypeptide chain reaches ~ 120 aminoacids [53] and the human immunodeficiency virus (HIV) envelope glycoprotein has its SP cleaved post-translationally after initial folding has started [54]. Inefficient cleavage also results in proteins with different features from a single transcript. When the ER protein, ER degradation-enhancing alpha-mannosidases-like protein 1 (EDEM1) undergoes an inefficient SP cleavage, a soluble EDEM1 is formed. When the SP is not cleaved, a type II membrane ER anchored protein is formed. Inherited mutations in the insulin

SP result in ER-localization and as a consequence, early-onset diabetes in patients [55].

Therefore, the SP targets the polypeptide, influences folding and the features of a protein, further modifications and localization. Other major post-translational ER modifications include *N*-linked glycosylation, *O*-glycosylation, disulfide-bond formation and glycosylphosphatidylinositol (GPI)-anchoring [56, 57]. Both covalent linked *N*-glycosylation and disulfide-bond formation play crucial roles in the folding of numerous secretory and membrane proteins. In addition, assembly of multi-subunit complexes takes place within the ER.

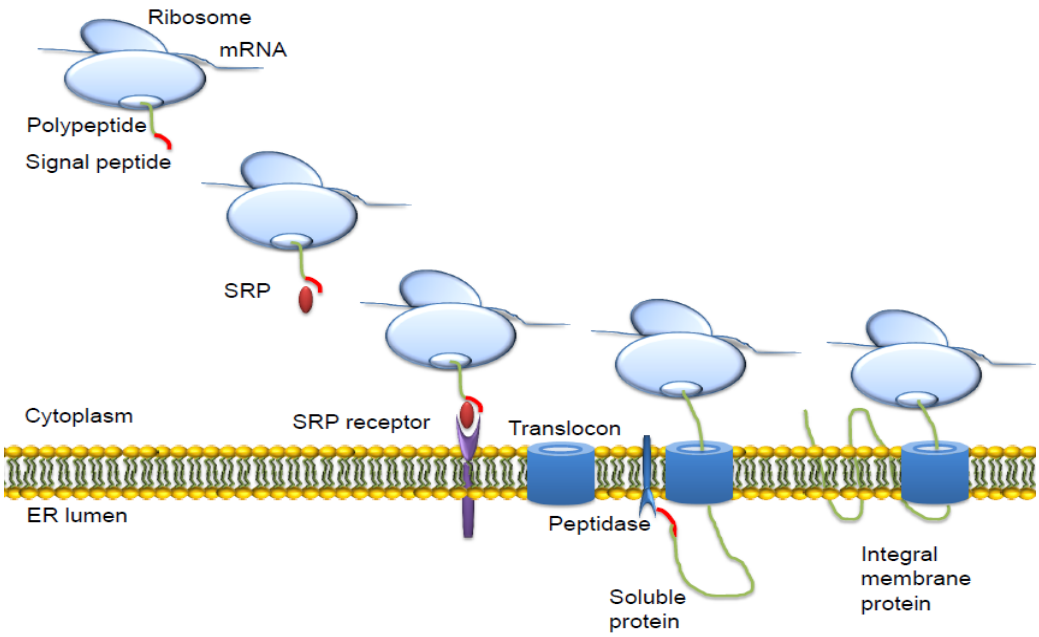


Figure 2.1.1. Polypeptides enter the endoplasmic reticulum *en route* through the secretory pathway. Appearance of the signal sequence found on a nascent polypeptide (shown in orange) prompts the signal recognition particle (SRP) portrayed as a red oval. Binding of SRP to the signal sequence initiates two signals. First it slows down translation of the mRNA found within the ribosome and second it binds the signal sequence to the dimeric SRP co-receptor and in doing so, escorts the nascent polypeptide to the ER membrane. The SRP is then released for recycling and translation ensues and a nascent soluble polypeptide enters the ER lumen via a translocon. An integral membrane protein is incorporated into the membrane also by the translocon complex. Once settled, the soluble proteins and some membrane proteins have their signal sequences cleaved by the ER localized signal peptidase complex portrayed as a blue snipping tool. Redrawn from reference [8].

### 2.1.4 The ER lumen

Protein folding is dependent on the internal chemical environment of the ER lumen. Folding chaperones are the gatekeepers for protein folding and quality control [58, 59]. The ER lumen is relatively oxidative in nature and contains millimolar calcium ($Ca^{2+}$) concentrations and lipophilic content compared to the cytoplasm and plasma membrane, respectively [60]. This calcium content is required for cellular signaling and as a cofactor for chaperone function. Folding chaperones residing in the ER lumen are numerous reaching up to 0.1-1.0 mM concentrations.

Proteins destined for secretion or insertion into the membrane enter the ER in an unfolded form and generally leave only after they have reached their native folded states. Protein concentration can reach up to >100 mg/ml in the ER lumen [2] and as a result, folding in the ER is often slow and inefficient, with a substantial fraction of polypeptides failing to reach their native states as the protein concentration has been seen to reach 300-400 g/L [61]. Quality control occurs at every stage of protein biosynthesis in the ER. These include co-translational translocation, post-translational modification, chaperone-assisted folding, assembly of multi-subunit complexes, trafficking and export. Protein folding rates are altered for different proteins ranging from a few minutes to hours. Some proteins fold quickly however, linger inside the ER lumen before moving on through the secretory pathway [2].

Within the ER, the folding cascade of the polypeptide is challenged and dependent on the kinetic and thermodynamic stability of polypeptides in the oxidizing and relatively calcium rich environment of the ER. However, it is the rich ER lumen milieu, alongside chaperones, that assist the newly synthesized proteins to form disulfide bonds and fold into their native three-dimensional structure based on the primary structure inherent in their amino acid sequence. These nascent polypeptides fold and assemble into proteins and undergo modification within the

ER lumen and are then targeted for expression at the plasma membrane, directed to intracellular organelles or destined for secretion.

The cell must continuously assess the pool of folding proteins and remove polypeptides that are terminally misfolded. This process of culling is critical to protect the cell from the toxic effects of misfolded proteins. As a consequence, misfolded proteins and orphaned subunits of protein complexes are targeted for degradation [7].

### 2.1.5 Folding chaperones

ER-folding chaperones form networks and complexes that collaborate and propagate folding. Chaperones residing in the ER lumen include but are not limited to protein disulfide isomerase (PDI) enzymes, heat shock protein like HSP70 (HSPA5/BiP), heat shock protein like HSP90, HSP70/HSP110 and the lectin chaperones, calnexin (CXN) and calreticulin (CRTN), UDP-Glc:glycoprotein glucosyltransferase 1 (UGGT1) and the peptidyl prolyl isomerases (PPIs) such as cyclophilin B (CypB) [2, 8].

These chaperones exist in complexes in the ER-lumen when assisting the folding of proteins. For example, the thyroglobulin protein complexes with the HSPA5/BiP, heat shock protein 90kDa beta (Grp94), member 1 (HSP90B1), hypoxia up-regulated 1 (HYOU1/Grp 170) and the PDIs and protein disulfide isomerase family A, member 4 (PDIA4/ERp72) forms a mutimeric complex in the ER lumen [62]. Characteristics of the folding protein determine which chaperone complex is recruited to the nascent chains. For example immunoglobulins bind to HSPA5/BiP then CNX or CRT [2].

Chaperones promote efficient folding by supporting polypeptide native folding. Chaperones prevent the aggregation of exposed hydrophobic residues. They survey

the ER-lumen for immature, abberant or aggregation-prone proteins and promote their disposal to maintain proteostasis.

### 2.1.6 Post-translational modification in the ER

Glycosylation of asparagine (Asn) residues is an essential protein modification reaction that occurs in 90% of proteins that enter the secretory pathway in eukaryotic cells [63]. A core unit of 14 saccharides (Glu(3)Man(9)GlcNAc(2)) (Figure 2.1.2) is synthesized as a dolichol pyrophosphate precursor by enzymes located in the ER membrane. Asparagine-linked *N*-glycans are transferred *en bloc* onto polypeptides in the lumen of the rough endoplasmic reticulum (RER) by the oligosaccharyltransferase (OST), found close to or on the translocon complex, using a dolichol pyrophosphate-linked oligosaccharide (OS-PP-Dol) as the donor substrate [64]. This addition occurs when the polypeptide is ~ 13 amino acids into the ER lumen and the Asn residue aligns correctly with OST [50]. OST's subunit Ost3/6p has been found to contain an active thioredoxin-like domain possessing oxidoreductase activity. Oxidation of substrate proteins has been shown to negatively impact glycosylation efficiency [65], therefore covalent tethering of nascent chains to the Ost3/6p subunit can impact glycosylation transfer efficiency in polypeptides [64, 66].

### 2.1.7 *N*-glycosylation

*N*-glycosylation is unique to the ER and marks the initiation of protein folding of glycoproteins. Congenital disorders of glycosylation represent a large number of diseases resulting from improper *N*-glycosylation [67]. This type of glycosylation involves the *en bloc* transfer of a glycan complex Glu(3)Man(9)GlcNAc(2) from the lipid-linked sugar donor Glu(3)Man(9)GlcNAc(2)-diphosphate dolichol by the OST complex to selected asparagines at canonical consensus tripeptide sequon motifs of Asn-Xxx-Ser/Thr or more rarely Asn-Xxx-Cys, Asn-Xxx-Val, or Asn-Gly sequons

within the sequence of the polypeptide (where X can be any amino acid except proline) [68-70].

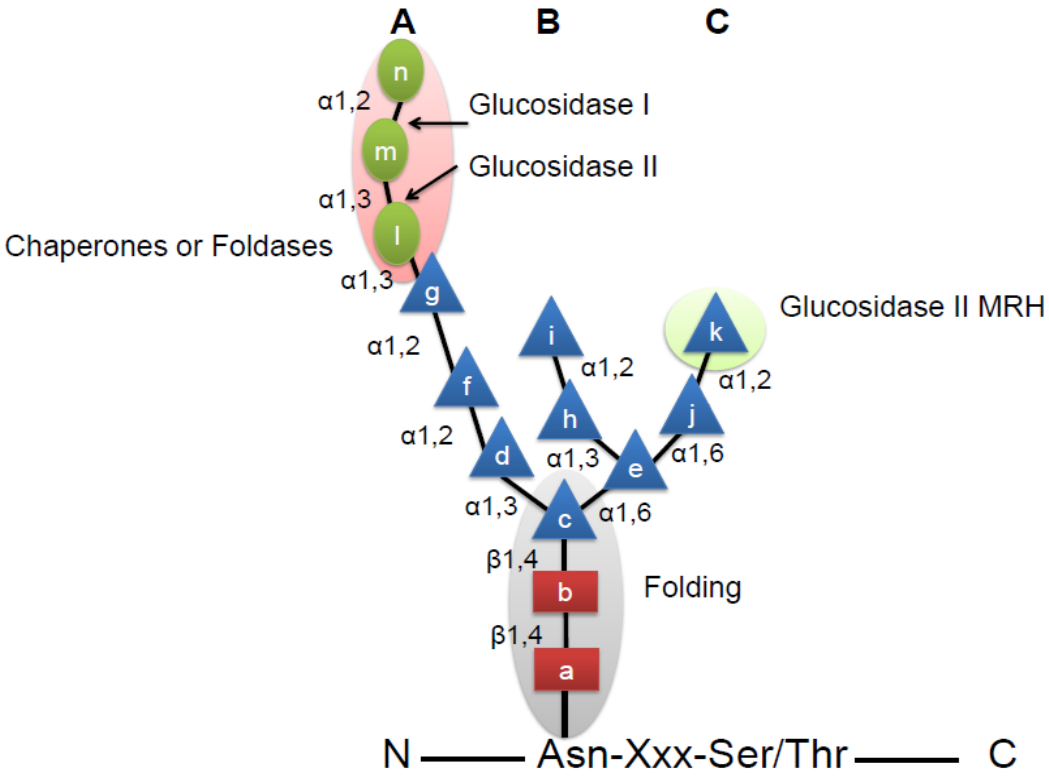


Figure 2.1.2. The composition of *N*- glycans attached to a tripeptide sequon motif. The 14-member carbohydrate is covalently linked to Asn residues of the consensus sequence Asn-Xxx-Ser/Thr as shown above. The glycan is comprised of three branches depicted as A, B and C corresponding to the 3 mannose branches. 3 glucoses (G) (green circles), 9 mannoses (M) (blue triangles), and 2 N-acteylglucosamines (GlcNAc) (red squares). Saccharide units are labeled a-n. The orientation of the glycosidic linkages is shown as either α or β with the corresponding numbers each G, M or GlcNAc. The sites of cleavages of glucosidase I and II are indicated by arrows, the mannose K recognized by the glucosidase II mannose 6-phosphate receptor homology (MRH) domain is highlighted in light green and the region important for folding kinetics of the protein is indicated in shaded grey. *N*-glycans are crucial to the stability and conformation of proteins. Redrawn from reference [71].

Glycans are hydrophilic modifications added to the folding peptide, to protect and stabilize the unstructured polypeptides from hydrophobic aggregations [72] and increase their solubility and interaction with chaperones. *N*-glycans enhance the kinetics and thermodynamics of folding (Figure 2.1.2; highlighted in shaded grey).

This was seen with the human immune cell receptor cluster of differentiation 2 (hCD2ad) folding energetics. It was observed that the first saccharide accounted for a 2/3 accelerated folding and stabilization of the polypeptide. The next two saccharides further potentiated and completed the stabilization effect. The core (ManGlcNAc(2) was shown to have intrinsic benefits to folding energetics [73].

Little is known about how chaperones in the ER are organized into complexes to assist in the proper folding of secreted proteins. However, it was established that glycans act as substrates for the lectin chaperones CNX and CRT [57, 74], which are part of the ER folding and quality control machinery.

### 2.1.8 Trimming of the N-glycan

The A-branch or glucose-containing arm of N-linked glycans (Figure 2.1.2) recruits molecular chaperones that assist in the efficient folding of glycoproteins [72, 75]. The terminal glucose residue (n) of the transferred triglucosylated glycan is rapidly removed by α-glucosidase I (GI), which is associated with the translocon complex. Malectin, a $Glc_2$-binding protein, might then intervene to retain immature and/or misfolded polypeptides in the ER [76]. Trimming of the final glucose (m) by the α-glucosidase II (GII), a luminal heterodimeric enzyme, supports co- or post-translational association of folding polypeptides with the ER lectins CNX and CRT. GII contains an MRH domain which requires the presence of mannose residue k on branch c. The MRH domain makes GII a key regulator of the QC mechanism of glycoprotein folding. It has been shown that a decrease in N-glycan mannose content results in lower GII enzymatic activity [77].

### 2.1.9 The calnexin cycle

Glycoprotein association with CNX or CRT marks the beginning of the ‘calnexin cycle’ [78]. CNX is a membrane-anchored protein and CRT is a luminal homolog (Figure 2.1.3). Both proteins consist of: (1) a globular domain that harbors both the

oligosaccharide- and calcium-binding sites; and (2) an elongated arm, also known as the P domain because of its proline-rich sequence motifs [79, 80]. The oligosaccharide-binding site in the globular domain of CRT has been well established [81]; yet, how polypeptides bind CNX and CRT is less clear. CNX and CRT are structurally similar with different preferences to substrates [82]. CRT forms complexes with HSPA5/BiP and Grp94 and the former two are close to the translocon pore on the luminal side of the ER [83].

Recent structural studies have identified possible peptide-binding sites in both the lectin and arm domains of CRT [84]. The P domain binds to a luminal thiol-disulfide oxidoreductase, ERp57, an accessory protein (Figure 2.1.3) [85] and a PPI, CypB [86]. Together, CNX or CRT (CNX/CRT), protein disulfide isomerase family A, member 3 (ERp57) and CypB assist the nascent glycoproteins in achieving a native conformation with the correct disulfide bonds. Affiliated with PPIase CypB, CNX and CRT have been shown to promote proline isomerization [86]. The duo also retain misassembled or non-native protein conformations to allow more time for proper folding and prevent aggregation and turnover of non-native proteins allowing for proteostasis within the ER [50].

The ER enzymes, GI and GII, remove the two terminal glucose residues of the glycan moiety from the nascent polypeptides forming (Glu(1)Man(9)GlcNAc(2) (Figure 2.1.3). Then the lectin chaperones, membrane bound-CNX and its lumen soluble homolog CRT [72], both in complex with the glycan directed oxidoreductase PDIA3/ERp57, modulate enzymatic change to form disulfide bonds within the monoglucosylated glycan client (Glu(1)Man(9)GlcNAc(2). Interestingly, these lectin proteins slow down folding to allow more efficient folding to take place.

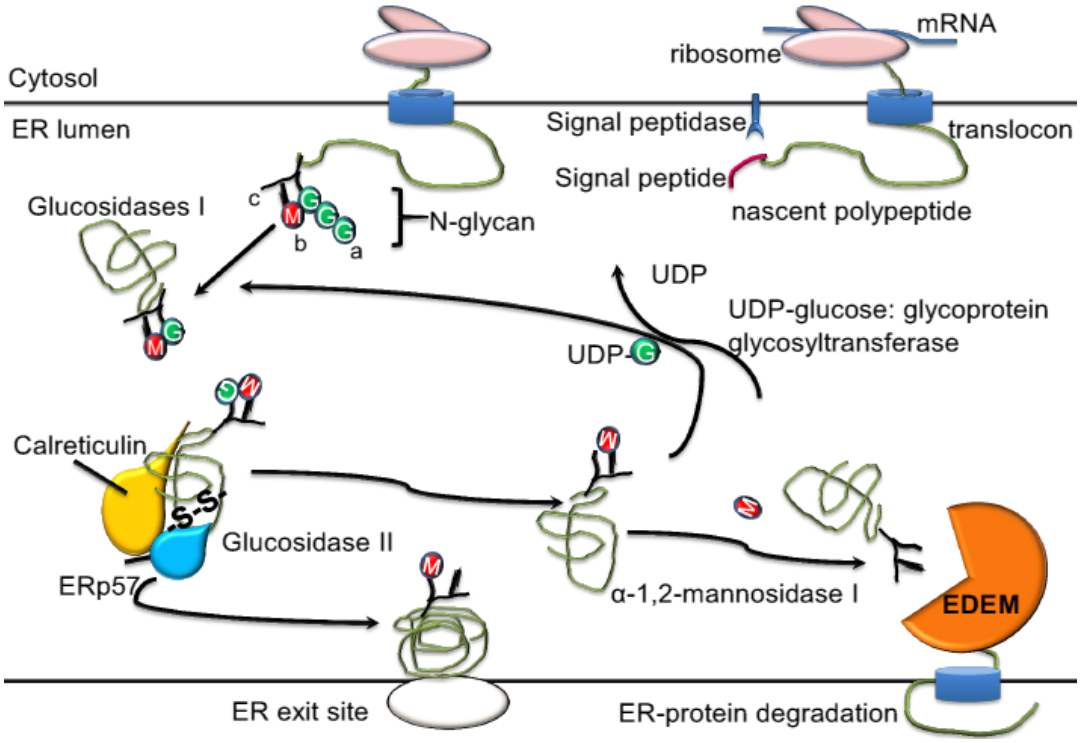


Figure 2.1.3. The glycoprotein folding cycle within the endoplasmic reticulum lumen. As the polypeptide enters the ER, an *en bloc* transfer of the core oligosaccharide (Glc(3)Man(9)GlcNAc(2)) where glucose is represented as green and mannose as red circles and N-acetylglucosamine is Y-shaped attached to the nascent polypeptide chain. Glucosidases I and II remove two of the three glucoses generating a monoglucosylated glycoprotein. This monoglucosylated protein is a signal for interacting with CNX and CRT, both lectins bound to thiol-disulphide oxidoreductase (ERp57). For simplicity and representation purposes; CRT is shown. CRT is the soluble form of CNX and they form interchain disulfide bonds (S-S) with the bound glycoproteins. Removal of the final glucose by glucosidase II allows the glycoprotein to be released from the chaperones and leave the ER through ER exit sites to the Golgi Apparatus. In the event that the protein has not been processed correctly, UDP-glucose-glucosyltransferase re-adds a single glucose on to the glycan and the cycle of protein folding is repeated. If the glycoprotein is permanently misfolded, the terminal mannose α1–2Man from the central arm of Man(9)GlcNAc(2), shown as a red circle, from the b branch of the oligosaccharide is removed by α-1,2-mannosidase I yielding a Man(8)GlcNAc(2) b-isomer. A second ER resident α-mannosidase I–like protein which lacks enzyme activity known as ER degradation-enhancing α-mannosidase I–like protein (EDEM), recognizes misfolded glycoproteins and targets them for ERAD. Redrawn from reference [56].

### 2.1.10 HSPA5/BiP chaperone

Being true chaperones to their polypeptides, the first ER-resident molecular chaperone (HSPA5/BiP), interacts with the hydrophobic stretches on the polypeptide with its substrate-binding pocket (SBP). HSPA5/BiP is the most abundant of ER chaperones. HSPA5/BiP is a peptide-dependent adenosine triphosphatase (ATPase) that can either increase or decrease the folding rate of protein ligands [87]. It binds with low ATPase activity and affinity. HSPA5/BiP has co-chaperone partners that regulate binding of the glycoprotein substrate to HSPA5/BiP. These regulatory proteins such as DnaJ (Hsp40) homolog, subfamily C, member 1-7 (DNAJC/ERdj1-7) proteins which harbor thioredoxin domains [7], and the guanine nucleotide exchange factor BiP associated protein (BAP) [87] and glucose-regulated protein (GRP) GRP170 alongside HSP90-like chaperones (GRP94), stimulate ATP hydrolysis on BiP [10]. The resultant ADP-BiP binds to the polypeptide with high affinity resulting in a tight BiP-substrate complex that is locked into the SBP [8]. This allows BiP to hold the substrate while it interacts with other chaperones such as the protein disulfide isomerases and attains its native conformation. This ATP binding and hydrolysis regulates cyclic binding to glycoproteins thereby assisting their protein folding.

### 2.1.11 Protein disulfide isomerase enzymes

Oxidized glutathione (GSSG) enters the ER from the cytosol and generates oxidizing and buffering conditions pertaining to the ER environment [88]. Proteins depend on their disulfide bonds for their stability, maturation and function. Disulfide-linked folding has been reported to be slow due to its dependence on a redox reaction in the ER. Mispairing of cysteine residues can be detrimental by preventing proteins from attaining their native conformations consequently leading to misfolding [88].

PDIs are enzymes which contain cysteines (CXXC) motifs and thioredoxin-like domains [89, 90]. PDIs are oxidoreducatase enzymes which have the J-domain and multiple thioredoxin domains necessary for disulfide exchanges. ERdj5 has been shown to be involved in reducing disulfide bonds for proteins destined for ERAD and in certain proteins it is needed for efficient folding of a protein [90]. These motifs and domains utilize paired cysteine residues to reduce (donate electrons) and oxidize free thiols (accept electrons) on cysteine residues of the proteins forming disulfide bridges. PDI protein can rearrange incorrect disulfides as well by breaking incorrectly formed disulfide bonds and remaking them [3, 8, 88]. The oxidative potential of the ER is largely generated by ER oxidase 1 (Ero1) to regulate the balance of oxidized and reduced PDIs by transfer of electrons to oxygen [1, 91, 92].

A novel oxidoreductase, ERp44 has been shown to act specifically on plasma cell protein folding such as the IgM J-chain, heavy chain and light chain proteins [93]. Substrate specificity and cell-type specificity of these oxidoreductases remains to be determined. ERp57 interacts with CNX and CRT and PDIs have a b'domain containing an inactive thioredoxin fold able to bind hydrophobic stretches of a polypeptide in complex with CRT and CNX [50, 94]. In this regard, PDIs are considered to possess both chaperone-like qualities and an oxidoreductase activity. Correct disulfide bond formation is crucial for proper folding and provides stability for the protein in the extracellular environment and proteins are then allowed to proceed along the ER-to-Golgi anterograde trafficking pathway.

### 2.1.12 Peptidyl prolyl isomerases

Another set of ER catalyst enzymes, PPIs rotate the peptide [95], which is immobilized by the interaction of proline side chains within the peptide backbone. PDI's and PPIs have been shown to catalyze proline *cis-trans* isomerization [50], the latter being a very important feature for proper and correct folding of polypeptides. Proline residues are found in *trans* conformations as the enter the ER-lumen. Trans-

prolines are then converted to *cis*-prolines in the native protein. This is a rate-limiting step in protein folding and slows down folding [50, 96]. This substrate-chaperone interaction guides folding of the polypeptides within the ER. To terminate the folding process, GII can remove the remaining glucose residue and abolish the binding site for CNX and CRT to the glycoprotein. This prevents rebinding of the glycoprotein to the CNX/CRT-ERp57 complex [97].

### 2.1.13 Glucosyltransferase

In the event that a polypeptide has been incompletely folded, the ER enzyme UGGT1 recognizes structured, hydrophobic patches in folding intermediates and re-glucosylates the Man(7-9)GlcNAc(2) to restore the binding site for CXN and CRT to re-guide folding again (Figure 2.1.3). UGGT1 is a folding sensor and to re-glucosylate, it has been shown that the glycoprotein substrates must have at a minimum the innermost GlcNAc residue of the N-glycan and hydrophobic amino acids exposed in denatured conformations. More disordered conformations, i.e. those exposing more hydrophobic amino acids, were found to have a higher glucose acceptor capacity [98].

UGGT1 has been found to reglucosylate *N*-glycans only on the misfolded half [99], suggesting that the *N*-glycans must be near the misfolded region of the substrate. UGGT1 has also been reported to reglucosylate *N*-glycans that were more distant (40 Å) from local hydrophobic regions [100]. Despite these substrate-specific differences, it seems that UGGT1 can survey glycoprotein substrates for misfolded regions and reglucosylate attached *N*-glycans when appropriate. UGGT1 was able to sense an unfolded dimer within a heterodimer of the ribonuclease, RNase B (RNAse B) and specifically reglucosylates it [99]. Reglucosylation mediated by UGGT1 can promote association with CNX/CRT-ERp57 and the thiol-disulfide isomerase activity of ERp57 can promote proper disulfide bond formation [101].

It has been shown recently that proteins that linger in the ER undergo O-mannosylation in yeast [102]. O-mannosylation involves the addition of a mannose residue to an oxygen atom on serine or threonine amino acids. This in turn acts as a cell timer to prevent further unproductive folding cycles for a non-glycosylated protein and targets it for ERAD. Two key players contribute to yeast O-mannosylation; protein O-mannosyltransferases 1 and 2 (Pmt1 and Pmt 2). The importance of this finding is that this modification to the non-glycosylated protein renders it soluble for ER exit through the translocon. It has been proposed that it stimulates unfolding of the protein [103] and it may be the first step in the elimination process of misfolded or unassembled proteins.

### 2.1.14 The mannosidases

Unfortunately, this cyclic quality control can be disrupted by the prolonged retention of the glycoprotein in the ER lumen so that the removal of mannose residues from the b and c branches of Man(9)GlcNAc(2) by ER mannosidases I and II form Man(7-8)GlcNAc(2), is not recognized by GII and UGGT1, hence this glycoprotein has a different fate. ER lectins of the ER degradation-enhancing alpha-mannosidases-like protein (EDEM) family (EDEM1-3) also act as mannosidases and recognize the mannose trimmed *N*-glycans that have an energetically unstable conformation. Unfortunately, these partially folded proteins are targeted for ERAD. Interestingly, studies have shown that proteins that are kinetically stable and thermostable in the ER, but do not conform to a proper conformation, can still progress to the secretory pathway [57, 104].

### 2.1.15 Glycoprotein export out of the ER

Following this close scrutiny, bona fide synthesized proteins may exit the ER to set off for their final destinations within the cell, or are secreted into the extracellular

environment [12, 13, 105]. Two different mechanisms have been proposed (1) bulk-flow and (2) receptor-mediated transport [106].

Glycoproteins are sent to the Golgi complex where they are demannosylated by one or more of the resident mannosidases: alpha-mannosidases I and II (Golgi Man I-(A, B, C)) and (Golgi Man II) [107]. These Golgi mannosidases can remove mannoses from glycopeptides with a range of attachments to the *N*-glycans: Glc(0-3)Man(8-9)GlcNAc(2), allowing for their processing. Natively folded, demannosylated substrates are glycosylated and transported to their final destination. Like the ER, the Golgi complex may also make conformation-based sorting decisions leading to disposal of selected proteins. Misfolded glycoproteins scrutinized by Golgi complex quality-control systems are either sent back to the ER to be degraded by the proteasome or more often re-directed to lysosomes for degradation [108].

The proteins that assume a stable conformation are recognized and sorted into secretory vesicles by the cytosolic coat protein complex II (COPII). The formation of the COPII coat on ER membranes drives vesicle budding [109]. This occurs due to sequential binding of at least five soluble components, including the small GTPase Sar1p and two cytosolic heterodimeric protein complexes, Sec23/24 homolog (*S. cerevisiae*) (Sec23/Sec24) and Sec13/31 homolog (*S. cerevisiae*) Sec13/Sec31. Budding from the ER involves activation of the SAR1 homolog A (*S. cerevisiae*) pseudogene 1 (SAR1AP1/Sar1) GTPase by the ER-resident protein Sec12, a Sar1-specific guanine nucleotide exchange factor (GEF).

The binding of Sec23 to GTP bound Sar1 recruits Sec23/24 to the membrane and these constitute the inner-layer membrane of the coat. The extended surface of this Sar1-Sec23/24 complex has binding pockets. Cargo proteins interact with these binding pockets directly via receptors or indirectly with low affinity and high specificity and enter the budding vesicles at ER exit sites. Sec13/31 subunits are recruited to the membrane through interactions of Sec31 with Sec23/24 and Sar1. A molecular cage is formed by the Sec13/31 subunits to form the outer coat. Soon after formation and trafficking, COPII vesicles shed their coat, and then fuse with the cis-Golgi compartment [56, 109]. On the other hand, the stringent quality control system of the ER detects misfolded proteins, unmodified or orphaned subunits of protein complexes from properly folded proteins and targets them for retention and degradation by ERAD [56, 105, 110-112].

## 2.2 Homeostasis of the proteome

The ER prevents retained misfolded proteins from forming aggregates in the ER lumen and thus reducing their deleterious effects on the cell. Accumulation of misfolded proteins can lead to an overwhelming ER which disrupts its function and is known as ER stress [113]. Proteome stability and functionality is maintained by constant homeostasis of the proteome (proteostasis network) (PN).

Besides, protein synthesis, the PN regulates the retention, folding and/or degradation of unfolded, misfolded and/or non-native proteins within the ER and protein ubiquitination and/or proteasomal degradation on the cytosolic side of the ER. It is vigilant for cell stress and adapts it’s mechanism to avoid it at all costs. It adjusts the expression and activity of molecular chaperones at both the transcriptional and post-translational level [114] ensuring cross-talk between mechanisms is tightly regulated. The main outcome of the PN is to detoxify cells from non-repairable proteins.

The ER employs two main mechanisms in response to the presence of misfolded and/or unfolded proteins. One mechanism is an ER-adaptive stress response termed the unfolded protein response (UPR) outlined in Figure 2.2.1 [56, 57, 115]. The UPR acts to remodel the ER so that it increases its folding capacity. The other mechanism is ERAD, which eliminates misfolded proteins retained in the ER after surveillance systems scrutinize proteins by ER quality control mechanisms. ERAD is equally important to maintain the turnover of specific proteins to establish the PN within the cell [116]. ERAD tuning has also been defined as an ER-adaptive pathway regulated by misfolded protein loads [117]. Proteins may also aggregate in the ER and get cleared by cell apoptosis or lysosomal autophagy.

### 2.2.1 The unfolded protein response

Misfolded or aggregated proteins are potentially cytotoxic and consequently the cell needs to remove these aberrant proteins as early as possible. Because aberrant proteins may expose hydrophobic regions as well as free cysteine residues, they have a tendency to aggregate and ER molecular chaperones play key roles in ERQC because they recognize misfolded and aggregation-prone proteins [118]. Accumulation of misfolded proteins elicits an apoptotic response, the unfolded protein response (UPR), by proapoptotic genes which lead to cell death.

The UPR shown in Figure 2.2.1 involves at least 3 signaling pathways stemming from the ER. The three integral ER membrane proteins acting as ER stress sensors are: inositol requiring transmembrane kinase/endoribonuclease 1 α (IRE1α), PKR-activated protein kinase-like eukaryotic initiation factor 2 α kinase (PERK) and activating transcription factor 6 α (ATF6α). The activation of these proximal sensors is dependent on dissociation from ER chaperone HSPA5/BiP. When the proximal sensors are bound to HSPA5/BiP, their dimerization and activation is turned off [119]. As misfolded proteins accumulate in the ER, HSPA5/BiP is sequestered from

these sensors [120] unmasking their dimerization motifs thereby allowing their oligomerization, transphosphorylation and activation.

The UPR is activated by IRE1α, which when activated cleaves a 26-base fragment from the mRNA encoding X-box binding protein-1 (XBP1) [121]. Spliced Xbp1 mRNA is translated into potent transcription factor XBP1s which targets proteins involved in protein folding, protein secretion from the cell and ERAD. PERK is the second arm, which phosphorylates the α-subunit of eukaryotic translational initiation factor 2 α (eIF2 α). eIF2 α generally decreases protein influx into the ER lumen. The PERK-eIF2α-ATF4 pathway also induces CCAAT enhancer-binding protein (C/EBP) and homologous protein (CHOP/GADD153), a pro-apoptotic factor induced by ER stress [122]. During severe ER stress, CHOP up-regulates apoptosis related genes to promote cell death. Cell survival is the purpose of the UPR though prolonged or persistent stress results in the activation of pathways that ultimately lead to cell death [60, 115, 119].

ATF6α, a transcription factor, is the third arm of the mammalian UPR. When ATF6 dissociates from HSPA5/BiP, it moves to the Golgi apparatus and undergoes regulated intramembrane proteolysis releasing its cytoplasmic domain. This in turn translocates to the nucleus and activates gene transcription [123]. Activated ATF6α transcribes unspliced XBP1. When Ire1α is dimerized and transphosphorylated, Ire1α's endonuclease activity specifically splices XBP-1 mRNA and induces the translation of the active form of XBP-1 [115].

Multiple perturbations can cause accumulation of unfolded proteins in the ER and activate UPR. Other cellular conditions such as hypoxia, glucose deprivation, oxidative stress, viral infection, high fat or cholesterol also upregulate the UPR. All in all, the UPR regulates transcription and translation of genes such as ER chaperones and components of the ERAD pathway to restore ER homeostasis and prevents protein translation.

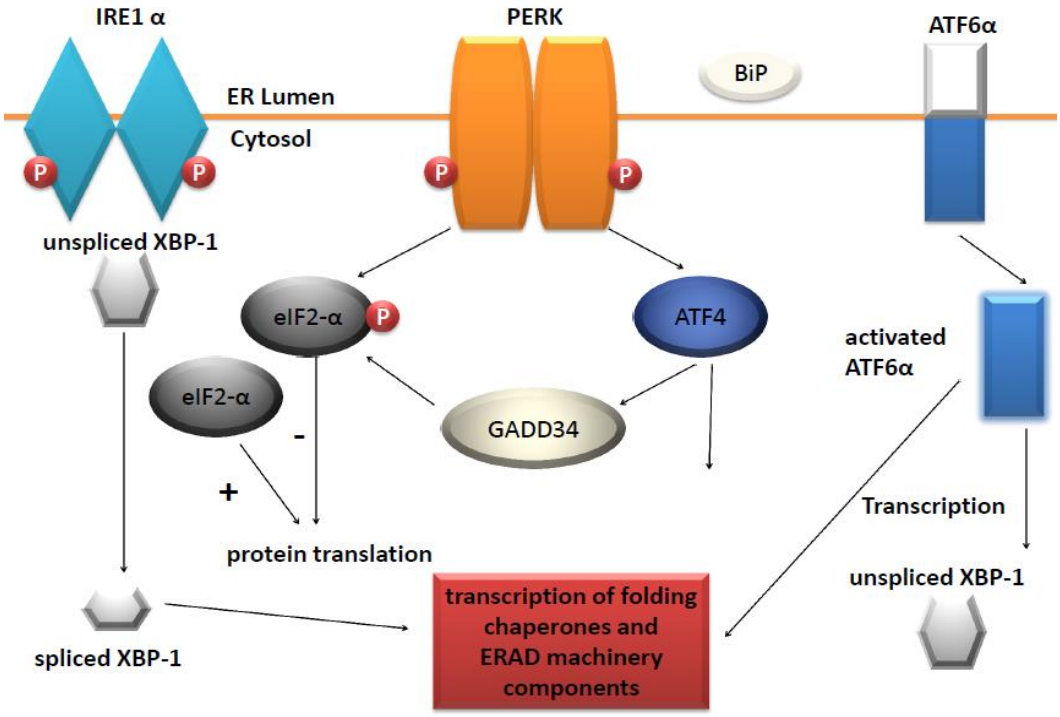


Figure 2.2.1. The three arms of the unfolded protein response (UPR) include IRE1α, PERK and ATF6α. When misfolded proteins accumulate in the ER, the three arms IRE1α, PERK and ATF6α are released from the HSPA5/BiP chaperones. This in turn is the signal for activation of the UPR. PERK phosphorylates eIF2α and the latter inhibits protein translation. PERK also activates ATF4 leading to the synthesis of protein phosphatase 1, regulatory subunit 15A (PPP1R15A) which then targets protein phosphatase I (PPI) to dephosphorylate eIF2α-P resuming protein translation. ATF6 is mobilized to the Golgi where it is activated producing an unspliced XBP1 which is then activated by IRE1 to further transcribe folding chaperones and ERAD machinery components. Redrawn from reference [115].

### 2.2.2 Endoplasmic reticulum associated degradation (ERAD)

Proteins that fail the stringent ERQC checkpoints are initially retained in the ER. This retention-based ERQC system is made up of ER-resident chaperones such as HSPA5/BiP, Ero1, PDIs, and ER lectins and members of the EDEM family (EDEM 1–3). Proteins of the Der1-like domain family, member 1 (DERL1-3) also interact with EDEM proteins that monitor the folding of N-glycoproteins [124]. A misfolded BACE457 substrate was found to interact with PDI and EDEM. It may be possible

that chaperones, co-chaperones and oxidoreducatases work together collectively on ERAD [2]. ERAD is a process in which misfolded retained proteins are consequently retrotranslocated back to the cytoplasm for degradation by the ubiquitin/proteasome systems [7, 12, 13, 18, 56, 125-127]. These interactions provide a direct link between the quality control system within the ER and cytosolic proteasomal degradation machinery.

#### 2.2.2.1 Mannose trimming

ER mannosidase I (ERMan I) catalyzes the removal of the terminal mannose of the B chain of the *N*-glycan residue (i) shown in Figure 2.1.2. This tags polypeptides for disposal [128]. This mannose removal also occurs for native polypeptides selected for secretion. This step is a pre-requisite for the intervention of EDEM, which removes mannose (k) displayed on misfolded polypeptides [129] (Figure 2.1.2). Removal of the mannose residue (g) prevents the substrate from UGGT1-mediated re-glucosylation and re-entry into the CNX cycle. Removal of the terminal mannose residues from the B and C chains, residues (i) and (k) respectively, allows binding of the *N*-glycan by the ERAD lectins osteosarcoma amplified 9, endoplasmic reticulum lectin (OS9/OS-9) and endoplasmic reticulum lectin 1 (ERLEC1/XTP3-B), promoting degradation [77]. OS-9 containing MRH domain binds Man7 oligosaccharides exposing the terminal α-1,6-bonded mannose (j). This now signals this glycoprotein as a substrate for ERAD retrotranslocation and degradation [130, 131] as outlined below.

### 2.2.3 The main steps of ERAD

ERAD is primarily involved in protein QC, since most ERAD substrates are damaged, misfolded or orphan proteins. ERAD pathways involve the ubiquitin-proteasome pathway to execute degradation marking the substrates by covalent addition of multiubiqutin chains, leading to destruction by the 26S proteasome.

There are four main steps in ERAD as depicted in Figure 2.3.1 [12, 13, 18, 56, 125, 126].

ERAD starts with a recognition of ER-retained substrates known as “Step 1: substrate recognition”. Here proteins which have misfolded cytoplasmic, ER luminal or transmembrane domains are recognized by ER luminal or cytoplasmic chaperones, depending on the site of the lesion in the protein. As mentioned, these consist of the HSPA5/Bip, CXN, CRT and PDIs. The misfolded protein is now targeted to the dislocation/retrotranslocation machinery and/or to the E3 ligases [10]. The E3s have variable numbers of transmembrane domains and a cytosolic Really Interesting New Gene (RING) finger domain on their cytosolic C-terminus which catalyzes the transfer of ubiquitin (Ub) from the E2 directly on to the substrate [132]. They catalyze substrate ubiquitination [133] and organize the complexes that coordinate events on both sides of and within the ER membrane “Step 2: Ubiquitination”.

Ubiquitination is a post-translational modification taking place in both the cytosol and nucleoplasm of cells. It serves to add Ub moieties to the substrate for recognition by the proteasome as an ERAD substrate. An ubiquitin-activating enzyme (E1) transfers ubiquitin via ATP to an active site cysteine [134] in an ubiquitin-conjugating enzyme (E2). Ubiquitin ligase (E3) acts as a platform for Ub moieties and then transfers ubiquitin from E2 to a lysine residue on the misfolded protein. Substrates are first monoubiquitinated and then they are further modified by the addition of additional Ubs leading to the formation of polyubiquitin chains (PUCs). Polyubiquitination occurs at the ER membrane via cytoplasmic or ER-localized E3 ligases [110].

E3 ligases are numerous in number and make up approximately 600 in mammalian cells probably due to specificity for one or a few particular substrate(s)

[135, 136]. Once substrates are polyubiquitinated, they become exposed to the cytosol where they are recognized for early retrotranslocation.

Self-ubiquitination of the E3 ubiquitin ligase is reversible. Ub moieties attached to substrates are not a permanent modification. They serve to promote the late steps of retrotranslocation by recruiting the ATPases associated with diverse cellular activities (AAA ATPase) via binding to its adapter protein [137]. Machinery involved in ubiquitination is recruited to the misfolded protein either within the membrane or by cytoplasmic chaperones.

Ubs can attach to one another in different ways forming PUCs with different chain conformations [135, 138]. The C-terminal glycine of the donor Ub can be attached to the α-amino group of the N-terminus of the acceptor Ub. Alternatively, the C-terminal glycine of the donor Ub can attach to seven internal lysines of the acceptor Ub via a peptide bond. Prolonged substrate ER-retention of the low density lipoprotein 6 (LRP6) has been shown to lead to extension on mono-Ub by E3 ligases forming PUCs and these PUCs are recognized by the ERAD system and connect it to the ERQC [135].

Retrotranslocation ensues as the third step of ERAD and is the most perplexing. ERAD substrates must be moved from the ER to the cytoplasm for ubiquitination and proteasomal destruction by a process called retrotranslocation. Many aspects of retrotranslocation are poorly understood, including its generality, the cellular components required, the energetics and the mechanism of transfer through the ER membrane [139-142]. Here, the protein can be removed through the retrotranslocon channel or by removal of the protein and the surrounding membrane by interaction with the small VCP/p97-interacting protein (SVIP) [8]. The latter is an AAA ATPase complex and uses ATP hydrolysis for possible mechanical removal of the misfolded protein especially since it is folded in the lumen or membrane spans in the lipid bilayer.

The presence of six-ATP sites in the assembled complex may reflect an extreme energy requirement for this process [140]. The AAA ATPAse complex binds multiubiquitin chains and has also been implicated in the energy-dependent movement of polyubiquitined proteins from non-covalent complexes in a wide variety of circumstances [143]. An intriguing question remains as to whether the AAA ATPase pulls the substrates across the membrane or alternatively, mediates removal of ubiquitinated substrates bound to the ERAD complex after retrotranslocation. The proteasome itself has been proposed to actively participate in the retrotranslocation or extraction of proteins from the ER membrane because of its resemblance structurally and functionally to VCP/p97 [144]. The proteasome utilizes ATP hydrolysis to undergo large conformational changes of the unfolding and/or movement of substrates out of the ER membrane [110, 135, 144, 145].

The last step of ERAD is “degradation”, as its name implies. Misfolded proteins are escorted to the 26S proteasome by a 19S cap. An enzyme named N-glycanase removes *N*-glycan residues and de-ubiquitinating enzymes remove ubiquitin tags within the cytosol or proteasome cap [146]. The 20S proteasome core contains enzymes with trypsin-like, chymotrypsin-like and caspase-like peptidases. These enzymes cleave the misfolded protein into short peptides for recycling back into the cell [6, 50, 110, 147].

## 2.3 Human disease and the involvement of ERAD

Mutations as modest as a single amino acid substitutions have been directly linked to protein misfolding with ER retention of misfolded proteins and the pathogenesis of multiple human genetic disorders [4]. ERAD is the underlying cause of many highly debilitating disorders ranging from Alzheimer's disease to cystic fibrosis (CF) [1, 18, 148, 149]. Disease-associated mutations often jeopardize acquisition of the native folding conformation of the affected protein and/or destabilize the native structure. Proteins which are unable to fold into their native

conformations have either full or partial loss-of-function. In some instances, for example in neurodegenerative diseases, inefficient removal of misfolded proteins results in aggregations with cytotoxic effects perturbing essential cellular functions and integrity.

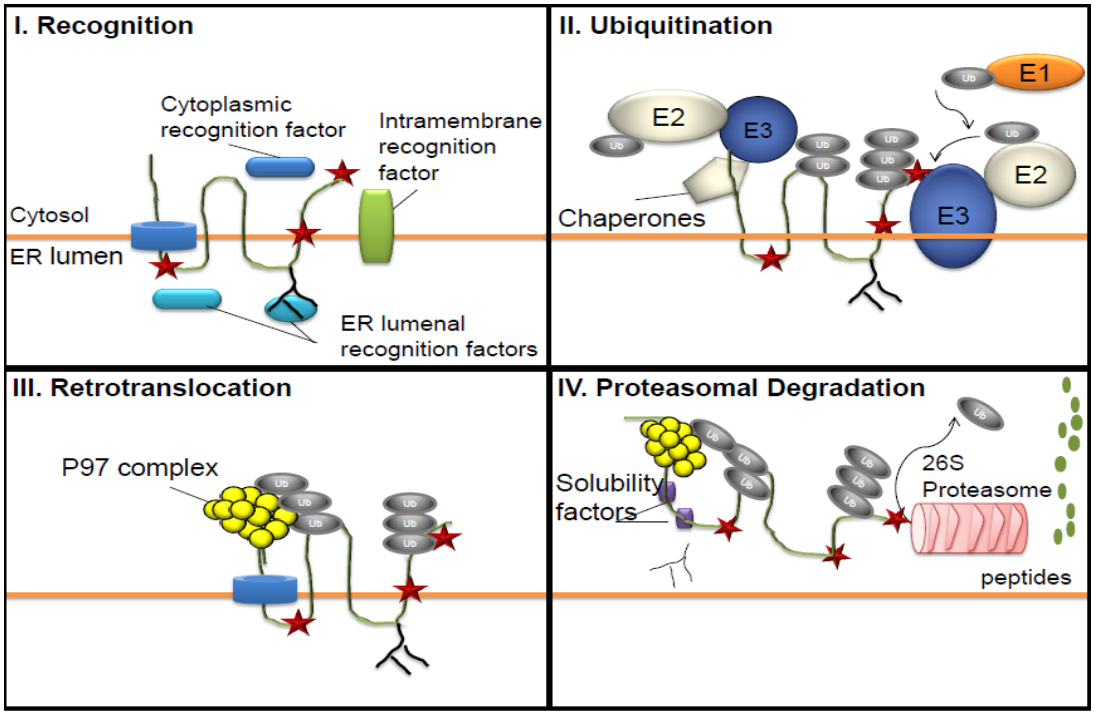


Figure 2.3.1. The four main steps for endoplasmic reticulum protein associated degradation (ERAD). Step 1 is recognition where a misfolded region (red stars) are recognized by cytoplasmic, ER luminal or transmembrane recognition factors depending on the site of lesion and occurs during protein synthesis. Ubiquitination is step 2. Chaperones and co-chaperones direct the misfolded substrate to the dislocation machinery. An ubiquitin activating enzyme (E1) transfers ubiquitin (Ub) (grey circles) to a cysteine residue in an active site of an ubiquitin conjugating enzyme (E2) using ATP as energy. Ubiquitin ligase then transfers Ub to a lysine residue on the substrate protein. The latter process occurs on either the ER or cytoplasmic side of the membrane. Retrotranslocation is step 3. The substrate protein is removed either by passing through the translocon or by complete removal of the misfolded protein and surrounding membrane. This is mainly done by the VCP/P97 AAA ATPase which interacts with Ub on the substrate and deubiquitinates the mutant protein and sends it off to the 26S proteasome for degradation. Degradation step 4 is the final step. Here, the polyubiquitinated substrates are escorted to the 26S proteasome to degrade the faulty proteins maintaining homeostasis in the ER lumen. *N*-glycans are cleaved off by an N-glycanase and Ub moieties are removed by de-ubuitinating enzymes found in the cytoplasm or in the proteasome cap to release small peptides shown in green. Redrawn from reference [8].

### 2.3.1 The link between ERAD and disease

One of the first diseases linked to the ERAD pathway was cystic fibrosis (CF). CF is caused by defects in the CFTR. The classic ΔF508-CFTR mutant protein is the cause of disease in 80% of Caucasian patients with CF. This mutation causes the CFTR protein to misfold in the ER or prevents folding altogether and/or alters membrane spanning domain folding. This leads to protein instability and a defect in the presentation of an ER exit motif, causing the ΔF508-CFTR to be retained in the ER. This retention causes the CFTR to be eradicated by ERAD and thus its expression at cellular apical plasma membranes in ducts and airway epithelia is drastically reduced. The outcome is the loss-of-function of the CFTR protein as a chloride channel i.e. its function is compromised and hydration of the mucosal layer lining the lungs' airways is reduced, leading to bacterial growth and lung fibrosis [1].

There are more than 100 diseased states currently identified in the literature, where ERAD is involved as the underlying cellular mechanism for disease [1, 8]. The retention and degradation of a mutant protein leads to the loss of its biological function which very often leads to a disease state [1, 18]. Given the high proportion (~30%) of cellular proteins that are targeted to the secretory pathway, it has been reasoned that ERAD is the cellular pathogenesis of more diseases relative to the ERAD-related diseases currently recognized in the literature [1, 14, 15]. These disorders include monogenic diseases, neurodegenerative disorders, metabolic diseases, serinopathies, viruses, toxins, ATP-binding cassette transporters and cancers among many others. A list of ER causative diseases can be accessed in the latest ERAD review by Guerriero and Brodsky (2012) alongside Aridor, et al. (2000, 2002 and 2007).

## 2.4 Data mining for disease causing ERAD candidate genes

### 2.4.1 Receptor tyrosine kinase-like orphan receptor 2 gene

Disease-associated alleles were sought after using bioinformatic algorithms and databases as previously described [18]. Candidates for initial analysis included the receptor tyrosine kinase-like orphan receptor 2 (*ROR2)* gene, an orphan receptor tyrosine kinase with alleles associated with Robinow and Brachydactyly type 1B syndromes [150]. Robinow syndrome is an autosomal recessive disorder. All but one of the missense mutations reported to traffic abnormally were found in the Fz-CRD. One mutation was found in the kringle domain close to Fz-CRD. Interestingly, it was determined that such alleles were responsible for misfolding of the ROR2 protein confirming ER-retention and therefore loss-of-function due to ERAD as the underlying mechanism in all Robinow syndrome-causing missense mutations [18, 148].

### 2.4.2 Natriuretic peptide receptor B

Hume et al., (2009) recently found that eleven out of the twelve known missense pathogenic mutations in the natriuretic peptide receptor B (*NPR-B)* gene found in Acromesomelic Dysplasia type Maroteaux (AMDM) patients resulted in the retention of the mutated proteins in the ER. Hence, this confirmed that loss-of-function in AMDM is indeed due to the trafficking defect of the receptor.

### 2.4.3 Discoidin domain receptor tyrosine kinase 2

ERAD is also responsible for most of the mutations causing Sponydylo-meta-epiphyseal Dysplasia with short limbs and abnormal calcifications caused by mutations in discoidin domain receptor tyrosine kinase 2 (*DDR2*) [149]. The finding that almost all the missense mutations in *ROR2*, *NPR-B* and *DDR2* resulted in the retention of mutant proteins in the ER and their degradation by ERAD provided support for the bioinformatic approach [18].

### 2.4.4 Endoglin and activin receptor-like kinase

More recently, Osler-Rendu-Weber syndrome or hereditary hemorrhagic telangiectasia (HHT), a genetically heterogeneous autosomal dominant vascular disorder was studied. Endoglin (*ENG*) and activin receptor-like kinase (ACVRL1) encode endoglin and ALK1 proteins, respectively, that modulate transforming growth factor (TGF)-β superfamily signaling in vascular endothelial cells are commonly mutated in hereditary hemorrhagic telangiectasia 1 and 2 (HHT1 and HHT2), respectively. Mutations lead to the development of fragile telangiectatic vessels and arteriovenous malformations. In addition, they are characterized by multi-organ vascular dysplasia, recurrent epistaxis and mucocutaneous telangiectasia.

Endoglin is a disulfide-linked homodimer integral membrane glycoprotein. Randomly selected missense mutants within the orphan domain known to cause HTT were examined and demonstrated that eight of eleven mutations were retained in the ER [151].

It has become evident that a large number of diseases with very different pathologies share a common framework of protein misfolding, accompanied by degradation and/or aggregation of these misfolded proteins. Inherited genetic diseases which harbor missense mutations affect the folding process and/or the stability of the folded structure of the proteins. By obstructing the folding process, increasing aggregation or de-stabilizing the native structure, disease-associated amino acid replacements may cause loss-of-function or gain-of-function pathologies.

## 2.5 The importance of the cysteine rich domain

Frizzleds (Fz) and Wnts have been identified in all major groups of metazoans. Extracellular amino terminus Fz-CRD serves as the Wnt binding domain and Fz-CRD is the key mediator [152] in the Wnt signalling pathway: considered vital during

embryogenesis. In adult tissue, disturbances in the Wnt pathway can lead to human degenerative disease and cancer.

A study on Wnt3-Fz 1 chimera was used as a model to look at canonical Wnt signaling [153]. A chimera of human Wnt3 and Fz1 receptor was developed that efficiently activated the T cell transcription factor (TCF)-luciferase reporter. As a result it was shown that the Fz-CRD was also critical for Wnt signaling, as a deletion of 29 amino acids in the 2nd cysteine loop resulted in the total loss of TCF-luciferase activation.

Wnt interacts with the soluble N-terminal CRD of frizzled, which relays signals to downstream effectors inside the cell to regulate a number of signaling events, e.g. β-catenin-dependent activation of target genes in the canonical Wnt pathway. Wnt11r binds MuSK through its Fz-CRD *in vitro*. In the embryo, wnt11r binds in a non-canonical dishevelled signaling manner in muscle fibers and this is required for MuSK function [154].

Fz-CRD is a mobile evolutionary unit that has been found in members of the seven-pass transmembrane proteins (Fz1-Fz8), certain receptor tyrosine kinases such as MuSK [19, 21] and ROR [25]. The majority of the Fz-CRD domains are named so because they possess 10 conserved cysteines that exhibit a general pattern of “C*C*CX8CX6C*CX3CX6,7C*C*C” (C: conserved cysteine; *: a variable number of residues, Xn: n residues, and Xm,n: m to n residues). The number of residues between the seventh and eighth conserved cysteines is usually six, while receptor-tyrosine kinase-associated CRDs have seven residues between them [24]. Structural studies of three CRDs, in mouse FZD, mouse secreted Frizzled-related proteins (SFRPs), SFRP3 [19] and rat MuSK [21] revealed a common alpha-helical fold mainly consisting of four core alpha-helices. They also contain the same two N-terminal beta strands (β1-β2). In all these structures, the disulfide connectivity

patterns among the 10 conserved cysteines are C1–C5 (between the first and fifth conserved cysteines), C2–C4, C3–C8, C6–C10, and C7–C9 [24, 155].

FZD4 crystal structure has not been reported however, it is structurally similar to the FZD8 and MuSK crystal structures placed on the PDB website: http://www.rcsb.org/pdb/home/home.do. Xenopus Wnt8 (XWnt8) has been seen as a complex with several Fz-CRD and this XWnt8/Fz-CRD complex has been observed as oligomeric forms with molecular weights ranging from ~50 kDa to ~200 kDa [22]. FZ-CRD has been shown to oligomerize in the ER [20] and the crystal structure of the Fz-CRD displays a conserved dimer interface that may be a feature of Wnt signalling [19]. MuSK's Fz-CRD forms an asymmetric dimer [21]. The Fz-CRD then goes on to form homo-and heterodimers in the ER and possible oligomerization [20-23]. Consequently, proteins harboring Fz-CRD must fold correctly and dimerize in the ER to function in the Wnt pathway.

## 2.6 The clinical value of targeting ERAD for therapeutic purposes

As previously mentioned, ERAD has been implicated in the mechanism of numerous human diseases. ER retention of possibly functional proteins has resulted in research for drug-induced rescue of their cell surface expression (misfolded protein and ER-targeted therapy). Therefore, understanding the underlying mechanism is of clinical value. New therapeutic approaches are aimed at either correcting the basic protein folding defect "protein repair" or at overcoming the intracellular retention of the mutant protein through the manipulation of the key interacting players "protein rescue". Targeting ERAD is complex as the proteostasis network for cell types is different and the folding properties of a variety of client proteins is regulated by cyclical interactions with a variety of different co-chaperones and/or chaperones.

Potential therapeutic intervention and manipulation of ΔF508-CFTR has been sought after for many years and has been successful. The ΔF508-CFTR trafficking and therapeutic manipulation has been considered a model for this group of genetically inherited diseases. A group of 10 academic laboratories came together and unified a hypothesis that the biogenesis of ΔF508-CFTR can be manipulated by understanding the intra-molecular fold alongside the rate-limiting inter-molecular interactions in the ER as compared to the cell surface and manipulate these factors accordingly [27].

### 2.6.1 Chemical compounds (chemical chaperones)

To alleviate misfolding or correct a mutant protein's ER-retention, a lot of research has been dedicated to the protein folding environment. The ΔF508-CFTR protein was tested for its ability to fold *in vivo* at 37° C and at temperatures below 30 °C and a comparison was made. It was observed that at higher temperatures, the synthesized protein was misfolded and consequently degraded by ERAD. In contrast, at lower temperatures the ΔF508-CFTR mutant protein was able to fold properly into its native state. These so called "thermosensitive" mutant proteins could then be manipulated or their environment modulated by chemical chaperones which may stabilize the mutant proteins or correct folding defects. These compounds have been collectively called "chemical chaperones" [30] and were named so because of their influence on protein conformation [156]. Brown et al. defined these chemical chaperones as "low molecular mass compounds known to stabilize protein conformation against thermal and chemical denaturation" [31].

Chemical chaperones have been observed to account for the rescue of several different classes of misfolded proteins. To name a few: CFTR [157], α1-antitrypsin [158], human Phenylalanine hydroxylase (hPAH), aquaporin-2 [159], vasopressin V2 receptor [160], ATP-binding cassette transporter proteins [35], α-galactosidase A [161], Fukutin protein [162], the prion protein PrP [156], the temperature-sensitive

mutants of the tumor suppressor protein p53, viral oncogene protein pp60, the ubiquitin-activating enzyme E1 [163] and P-glycoprotein [164] among many others.

Interestingly, the variant ΔF508-CFTR is mainly retained in the ER as a result of misfolding yet, when a minute amount of the ΔF508-CFTR protein is expressed on the cell surface, it exhibited significant chloride-channel conductance activity [29, 165]. Such results provide insight that the molecular machinery that directs folding and export could play an important role in both understanding the molecular basis for disease and achieving correction by promoting folding and transport of ΔF508-CFTR to the cell surface [29].

Following these observations on CFTR, several approaches have been attempted to overcome the retention of mutated proteins in the ER by stabilizing mutant protein conformation or by inducing a stress response, leading to up-regulation of molecular chaperones. Enhancing the cellular folding capacity by remodeling the proteostasis network promotes native folding. The approaches used consist of low temperature treatments.

### 2.6.2 Low temperature incubation

In recent years, there have been a growing number of reports on the use of reduced temperature cultivation of mammalian cells for the enhanced production and improved product quality of trafficking proteins. Low temperature incubation of affected cells and/or tissues has never been a feasible therapeutic option. However; this data shows how modulating kinetic i.e. speed of folding and/or thermodynamic aspects of any protein may possibly suffice when targeting the protein for ERAD.

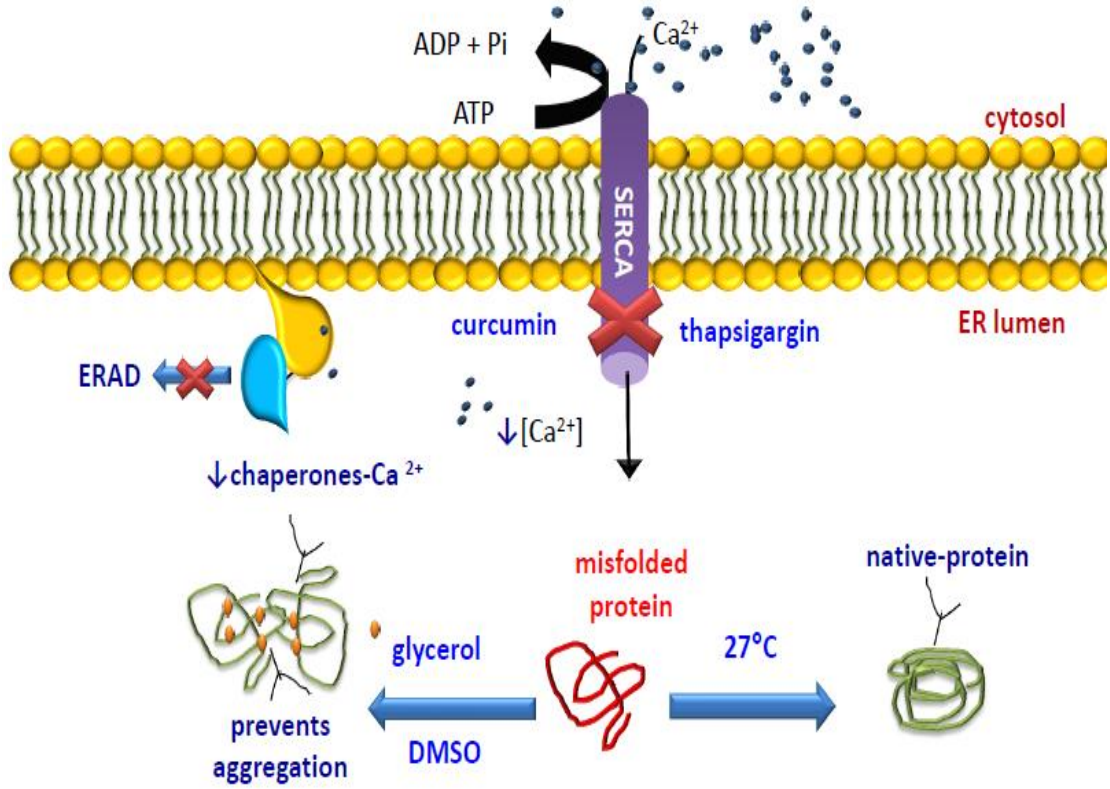


Figure 2.6.2. The effects of chemical chaperones. Glycerol increases the hydration layer, the strength of the intramolecular hydrophobic bonding of the protein, in the ER, which consequently allows the free movement of proteins, so as to prevent aggregation. Differing concentrations (0.1-1%) of DMSO probably act by increasing protein synthesis of the misfolded proteins or by overwhelming the quality control system [166]. Thapsigargin is an inhibitor of the ER sarco/endoplasmic reticulum $Ca^{2+}$-ATPase (SERCA) calcium pump, and has been shown to increase cytosolic calcium, resulting in an enhanced rescue of mutant proteins [160]. Curcumin, a nontoxic natural constituent of turmeric spice affects the calcium ($[Ca^{2+}]_{ER}$) ATPases [167] found on the ER plasma membrane, by inhibiting their ability to maintain a high ER calcium level. This in turn, affects the ability of ER molecular chaperones to target the misfolded protein for ERAD, hence, allowing the mutant protein to exit the ER.

The sub-physiological culture of mammalian cells (28-34 ºC) results in changes in gene expression and culture longevity [168]. Moderate hypothermia (16-20 ºC) for 24-48 hours has been used to enrich cultures. For example shifting HeLa cells from 37 ºC to 33 ºC doubles their generation time. These temperature shifts have been

used to prolong the cell cycle by up to 7-fold. Temperatures of 25-33 ºC results in temporal dilation of the G1 and S phases with G2 being the least sensitive [169].

Cell membrane expression of functional ΔF508-CFTR has been achieved by growing the expressing cells at lower temperatures [30, 32]. Processing of ΔF508-CFTR reverts towards that of wild-type as the incubation temperature is reduced. When the processing defect is corrected, cAMP-regulated chloride channels appear in the plasma membrane.

Recent studies show how a reduced temperature culture (e.g. 27 °C) treatment corrected the subcellular location of the Fukutin missense mutants in Fukuyama-type congenital muscular dystrophy (FCMD) [170]. The cellular localization of a pathogenic mutant of human glucagon receptor causing Mahvash disease was restored by culturing at 27 °C [171].

Another recent example was a study involving the human cardiac Kv1.5 (hKv1.5). The amount of protein expressed at a lower temperature increased the immature protein and this was shown not to be due to inhibition of proteolysis. The low temperature treatment markedly shifted the subcellular distribution of the mature hKv1.5, which showed considerable overlap with the trans-Golgi component. *N*-glycosylation of hKv1.5 was also shown to be more effective at 28 °C than at 37 °C. The hypothermic treatment also rescued the protein expression and current of trafficking-defective hKv1.5 mutants. These results indicate that low temperature exposure stabilizes the protein in the cellular organelles or on the plasma membrane, and modulates its maturation and trafficking, thus enhancing the current of hKv1.5 [172].

### 2.6.3 Glycerol

Glycerol acts as an osmolyte increasing the hydration layer, the strength of the intramolecular hydrophobic bonding of the protein in the ER, which consequently allows the free movement of proteins, so as to prevent aggregation [28].

Glycerol has three hydroxyl groups which makes it soluble in water. Glycerol can decrease the relative hydration of the mutant polypeptide. This tighter packing has an increased hydrophobic effect allowing the polypeptide more stability in the cellular environment [31, 173, 174]. Glycerol is an example of a chemical chaperone which stabilizes mutant protein native conformation [160]. This chemical compound improves the yield of the soluble human phenylalanine hydroxylase enzymes (hPAH) by 2-3 times. It was also able to increase the specificity of chaperones towards the mutant enzyme  Glycerol's effect has increased the rate of *in vitro* protein re-folding [175]. Another feature of glycerol is that it can improve the kinetics i.e. the rate of oligomeric assembly of proteins [176].

Others postulated that glycerol may rescue ER-retained mutants by increasing mutant expression or change the course of stress-sensitive molecular chaperones [177, 178]. Yeast ER membrane protein 3-hydroxy-3-methylglutaryl-CoA reductase (Hmg2p) [179] and the ΔF508 CFTR [28] temperature-sensitive trafficking mutant and a vasopressin mutant [160], among many others, were stabilized by the addition of glycerol to the expressing cells.

Addition of glycerol has been shown to affect the refolding parameters of recombinant human brain-type creatine kinase (rHBCK) [180]. It can affect refolding yield, reaction kinetics and aggregation. The results indicate that glycerol could alleviate the aggregation of rHBCK during refolding in both dilute solutions and macromolecular crowding systems, and increase refolding yields and reaction rates.

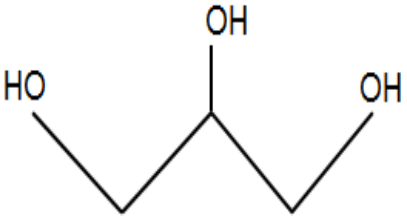


Figure 2.6.3. Glycerol is a simple polyol (sugar alcohol) compound. It is a colorless, odorless, viscous liquid that is widely used in pharmaceutical formulations. Glycerol has three hydroxyl groups that are responsible for its solubility in water and its hygroscopic nature.

### 2.6.4 Dimethyl sulfoxide

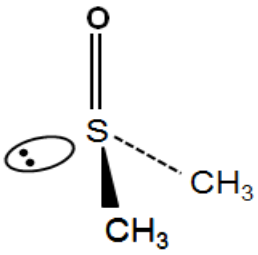


Figure 2.6.4. Dimethyl sulfoxide (DMSO) is an organosulfur compound with the formula $(CH_3)_2SO$. This colorless liquid is an important polar solvent that dissolves both polar and nonpolar compounds and is miscible in a wide range of organic solvents as well as water. DMSO is used as a mild oxidant. DMSO acts as a buffer in solution and has a structural effect on proteins.

Other chemical chaperones like dimethyl sulfoxide (DMSO) [181], trimethyl-amine-N-oxide [182], calcium pump inhibitors [167] and curcumin [183] have been tested to shift the folding equilibrium of mutant secretory proteins towards their native states, thus releasing them from the ER retention state. DMSO has been postulated to have the same action as glycerol [31, 160, 177-179]. It's solvation results in exposing the protein's hydrophobic residues by methyl groups in DMSO [184]. DMSO also acts to expose the protein's surface area: allowing chaperones to possibly interact with the protein to enhance protein processing. *In vitro* studies with DMSO show reduced cytotoxicity and cell death, therefore DMSO offers a possible therapeutic approach [185].

Missense mutants of transmembrane protein E-cadherin were shown to be rescued from ERAD by treatment of cells with the proteasomal inhibitor, MG132, or 2% dimethyl sulfoxide (DMSO) [186]. Retinol dehydrogenase 12 (RDH12) is a

microsomal enzyme that catalyzes the reduction of all-trans-retinaldehyde to all-trans-retinol when expressed in cells. Mutations in RDH12 cause severe retinal degeneration, albeit some of the disease-associated RDH12 mutants retain significant catalytic activity. T49M and I51N variants of RDH12 undergo accelerated degradation through the ubiquitin-proteasome system, which results in reduced levels of these proteins in cells. However chemical chaperones, namely 2% DMSO, were able to restore the mutant localization to the cell surface [187].

### 2.6.5 Curcumin

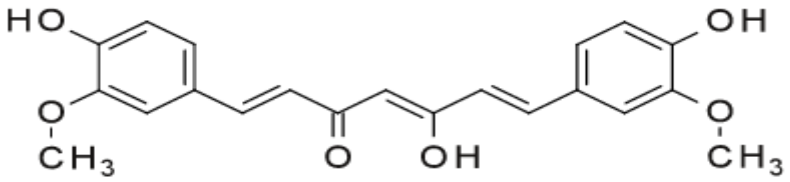


Figure 2.6.5. Curcumin is a diarylheptanoid, $C_{21}H_{20}O_6$. It is the principal curcuminoid of the popular South Asian spice turmeric, which is a member of the ginger family (Zingiberaceae). Curcumin appears to possess a spectrum of pharmacological properties, due primarily to its inhibitory effects on metabolic enzymes. It has been studied as a universal remedy for most diseases ranging from cancer and most inflammatory diseases. Image taken from http://pubchem.ncbi.nlm.nih.gov/

This chemical chaperone affects the internal cellular proteostasis within the cell. By acting in this way, curcumin allows an enhanced favorable fold for the protein and/or affects its trafficking environment. Curcumin may still be able to treat CF as it can function at different steps of CFTR biogenesis and it has been shown to help other types of CFTR mutants [188]. Reproducing some of the results on CF mouse models with curcumin treatments has been disputed [189].

Recent studies show that 10 µg/ml curcumin treatment at 37°C corrected the subcellular location of the Fukutin missense mutants in FCMD [170]. Curcumin affects the calcium ($[Ca^{2+}]_{ER}$) ATPases [167] found on the ER plasma membrane by inhibiting their ability to maintain a high ER calcium level. This in turn, affects the

ability of ER molecular chaperones to target the misfolded protein for ERAD, hence, allowing the mutant protein to exit the ER. Protective effects in two prominent diseases; Creutzfeldt-Jakob Disease [190] and Parkinson Disease [191] have been observed by a decrease in protein misfolding and therefore protein aggregation. Curcumin has therefore succeeded for treating misfolded proteins and their diseases.

### 2.6.6 Thapsigargin

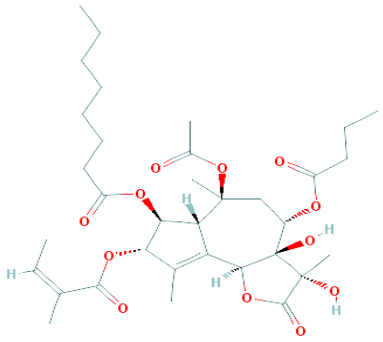

Figure 2.6.6. Thapsigargin. Thapsigargin is a sesquiterpene lactone found in roots of Thapsia. It inhibits $Ca^{2+}$-transporting-ATPase mediated uptake of calcium into the sarcoplasmic reticulum. Image taken from http://pubchem.ncbi.nlm.nih.gov/

Thapsigargin is the most widely used inhibitor of the ubiquitous sarco-endoplasmic reticulum $Ca^{2+}$-ATPases in mammalian cells. Over the past twenty years, this compound, of plant origin, has become a popular tool in a host of studies directed at elucidating the mechanisms of intracellular $Ca^{2+}$ signaling. Its remarkable potency and selectivity have been instrumental in expanding our understanding of the function of intracellular $Ca^{2+}$ stores to include such key aspects as store-operated $Ca^{2+}$ entry, or the involvement of the stores in protein synthesis and cell growth.

### 2.6.7 Pharmacological chaperones

Pharmacological chaperones are a particular type of chemical chaperone that directly binds to the misfolded proteins [1]. They are more specific to the protein in that they support folding, counteract formation of toxic aggregates and/or stabilize the native structure of mutant proteins. By lowering the protein's free energy state, they promote better protein folding [8]. Some pharmacological chaperones are

competitive inhibitors and have been used to help stabilize mutant proteins and rescue them from ER retention.

The F508 position is important for the folding and assembly of native CFTR. It participates in the formation of interdomain contacts that stabilize interactions between the domains of the protein. Yu et al., 2011 [192] demonstrated the use of a pharmacological chaperone, VRT-325, which resulted in partial correction of the nucleotide binding domain (NBD) of ΔF508-CFTR. The combined application of another drug known as a potentiator, VX-770, had an additive effect that restores both the folding and trafficking defects associated with ΔF508-CFTR and potentiated its reduced channel activity. It has been shown that the CFTR corrector, VX-809, allows the cell surface expression of functional ΔF508-CFTR. This cell surface expression results in partial restoration of chloride transport in cultured human bronchial epithelial cells derived from people with CF who are homozygous for ΔF508-CFTR [193]. VX-809 was chosen from a National Cancer Institute diversity set I (NCIDS) database through molecular docking screening [194].

*In vitro*, chloride transport can be enhanced by combining VX-809 with Corr-4a [195] or VRT-325 [196], or with CFTR potentiators, for example, VX-770 (also known as Ivacaftor) [196]. In clinical trials, VX-809 in combination with VX-770 improved clinical measures of CFTR function and lung function [196, 197].

Robben et al., [160] have shown how vasopressin V2 receptor mutants are rescued via pharmacological chaperones, and different chemical chaperones, such as osmolytes, namely 4% glycerol and 1% DMSO. Rescue of ER retained proteins is postulated to be due to an increased expression of changed functionality of stress-sensitive molecular chaperones. Calcium ($[Ca^{2+}]_{ER}$) ATPase inhibitors such as: 1 µM thapsigargin and 1 µM curcumin, showed an increase in cytosolic calcium, resulting in enhanced rescue of the receptor. They also show how the rescue activity of a pharmacological versus chemical chaperone is broader and stronger.

A well-established example is the use of the pharmacological chaperone 1-deoxygalactonojrimycin to rescue the trafficking of some missense α-galactosidase A (α-Gal A) mutants, from the ER to the lysosome, for the treatment of Fabry disease in patients. Fabry disease is a lysosomal storage disorder caused by α-Gal A enzyme deficiency. Fan et al., [198] have demonstrated the rescue of the enzyme activity in lymphoblasts for Fabry disease patients harbouring two missense mutations within the α-Gal A gene. This was achieved by cultivating the mutant expressing cell in a medium containing 1-deoxygalactonojrimycin, a potent competitive inhibitor of α-Gal A enzyme. The same group further confirmed that most of the disease-causing missense mutations are retained in the ER, albeit they are biologically functional and this loss-of-function trafficking defect can be corrected by the chemical chaperone approach [199].

## 2.7 Silencing of ERAD machinery components by siRNA

ERAD encompasses a number of different pathways, each responsible for the degradation of subsets of proteins that share common physical properties [116, 139, 145, 200]. A lot of research has gone into dismantling the components of the ERAD machinery [35].

siRNA has been used to dictate the difference between a deleterious mutation and a tolerated polymorphism as is seen with CF [201]. Partial silencing of the Hsp90 co-chaperone ATPase regulator (Aha1) [201] improved the trafficking of ΔF508-CFTR from the ER to the cell surface. *In vitro* [30] as well as *in vivo* [202] experiments have shown, however, that defective CFTR proteins are still functionally competent as chloride ion transporters [165].

The ability to control cell fate via the ER-folding, export and degradation pathways provides an exciting direction in future drug development within monogenic diseases. Identifying the cellular mechanism underlying genetic disease

has offered hope to CF and other patients. It remains to be determined if these disease causing mutations can be rescued, or if the ER milieu can be altered to allow these defective proteins to function as close as possible to their WT counterparts. This will provide the basis for designing specific drugs such as chemical and/or pharmacological chaperones that aid the transport of the diseased protein(s) to cellular membranes and eventually open up options for these patients. Likewise, tissue-specific chaperones can be therapeutic targets and have the capacity to be important tools in biotechnology.

One major hurdle for parsing mutated proteins by ER quality control is substrate recognition. Certain chaperones are shown to be substrate specific [158]. A detailed section on the silencing of ERAD components will be discussed in Chapter 4: Results; section 4: Gene silencing of ERAD components. The ERAD components chosen for this study were dependent on the substrate model chosen.

# Chapter 3: Materials and Research Methods

## 3.1 Resources

### 3.1.1 Reagents and chemicals

The following were purchased from Sigma-Aldrich Corp. (St. Louis, MO, USA): endoglycosidase H (Endo H) (A0810), protease inhibitors (S8830, SIGMAFAST protease inhibitor cocktail tablets), phosphatase inhibitor cocktail (P0044), phosphatase inhibitor cocktail 2 (P5726), β-mercaptoethanol (BME) (M7154), glycerol (G5516), thapsigargin (T9033), dimethyl sulfoxide (DMSO) (5879), curcumin (C7727), dithiothreitol (D9779), cycloheximide (C1988) and MG132 (C2211). Turbo *Pfu* DNA polymerase was obtained from Stratagene (La Jolla, CA USA). A bicinchoninic acid protein (BCA) assay kit (No. 23227) and Sepharose A/G beads (No. 20421) were obtained from Pierce (Rockford, IL, USA). Immunofluor mounting media were purchased from Dako (Carpinteria, CA, USA). A cell surface biotinylation kit (EZ-Link sulfo-NHS-SS-biotin, 89881 from Pierce, Rockford, IL, USA.

### 3.1.2 Antibodies

Antibodies, their dilution, sources and usage for immunofluorescence (IF) and western blot (WB) are as follows: mouse FLAG octapeptide epitope tag (DYKDDDDK) (anti-FLAG) monoclonal antibody (1:1000, IF and WB; Sigma-Aldrich Corp.), rabbit anti-FLAG antibody (1–2 µg/mL immunoprecipitation [IP], F7425; Sigma-Aldrich Corp.), rabbit anti-calnexin polyclonal antibodies (1:50, IF; Santa Cruz, Dallas, TX,), mouse monoclonal anti–ubiquitin (Ub) antibody (1:1000, WB, U0508; Sigma-Aldrich Corp.), insulin-like growth factor 2 receptor (IGF2R) was a gift from Dr. Suhail Al-Salam (1:1000, WB, Sc-25462m Santa Cruz, Dallas, TX), AlexaFluor 568 goat anti-mouse IgG (1:200; Molecular Probes, Grand Island, NY, USA), and AlexaFluor 488 goat anti-rabbit IgG (1:2000; Molecular Probes).

Thermoscientific, UK: Anti-SYVN1/HRD1 (PA1-46121; 1:1000), Abcam, USA: anti-SEL1L (ab78298; 1:400), anti-OS9 (ab19853; 1:400), anti-DER1 (ab93341: 1:500).

Secondary antibodies for WB were anti-rabbit IgG (whole molecule)-peroxidase antibody produced in goat (A0545, 1:30,000; Sigma-Aldrich Corp.), anti-mouse IgG (whole molecule)-peroxidase antibody produced in rabbit (A9044, 1:50,000; Sigma-Aldrich Corp.), and Pierce ECL plus WB substrate (32132; Thermo Scientific, Rockford, IL, USA).

### 3.1.3 Cell culture

Human embryonic kidney (HEK 293T), HeLa, and COS-7 cells were obtained from ATCC (Manassas, VA, USA). HEK293 was a gift from Dr. Rajesh Mohanraj (Department of Pharmacology and Therapeutics, CMHS, UAEU). Bovine serum albumin was obtained from Fisher Scientific (Loughborough, UK). Dulbecco's modified Eagle's medium (DMEM) and PBS were obtained from Invitrogen (Grand Island, NY, USA). Fetal bovine serum (FBS), L-glutamine, and penicillin-streptomycin were obtained from GIBCO (Grand Island, NY, USA). The liposomal transfection reagent FuGENE HD was purchased from Promega (Madison, WI, USA).

### 3.1.4 cDNA clones

*TEK* (NM_000459.1 ) Human cDNA open reading frame (ORF) clone construct was obtained from Origene (catalogue number SC119843, USA); Wild-type *MUSK* (NM_005592) Human cDNA ORF clone (Origene catalogue number: RC212253, USA). *FZD4* construct was a gift from Dr. Jeremy Nathans (The John Hopkins University, Baltimore, Maryland, United States).

### 3.1.5 Silencer select pre-designed siRNA

Silencer® Select Pre-designed siRNA (Life Technologies) were used for silencing. Three mers were chosen to cover the majority of transcriptional variants

for each gene in the study. Silencer® Select Negative controls (catalogue numbers 4390843 and 4390846) were used as scrambled sequences for every experiment. Glyceraldehyde-3-phosphate dehydrogenase GAPDH (catalogue number 4390849) was used as a positive control for siRNA transfection efficiency.

Table 3.1.1. The targeting sequences to knockdown SYVN1, SEL1L, OS9 and DER1.

| Gene | Sense strand (5'-3') | Antisense strand (3'-5') |
|---|---|---|
| SYVN1 mer 1 | CCAGCAUCCCUAGCUCAGAtt | UCUGAGCUAGGGAUGCUGGtg |
| SYVN1 mer 2 | CCUACUACCUCAAACACCAtt | UGGUGUUUGAGGUAGUAGGcg |
| SYVN1 mer 3 | GCAUUGUCUCUCUUAUGUUtt | AACAUAAGAGAGACAAUGCgg |
| SEL1L mer 1 | GCACCGAUGUAGAUUAUGAtt | UCAUAAUCUACAUCGGUGCca |
| SEL1L mer 2 | GGAUAUUCACCUUGCGAAAtt | UUUCGCAAGGUGAAUAUCCtg |
| OS-9 mer 1 | GUAUGGAGAUAAAAUCAUAtt | UAUGAUUUUAUCUCCAUACtg |
| OS-9 mer 2 | GGAUGACAGUAAGGACUCAtt | UGAGUCCUUACUGUCAUCCtt |
| OS-9 mer 3 | GGGAAAAUUGAGAUCAAAAtt | UUUUGAUCUCAAUUUUCCCtg |
| Der1 mer 1 | GAGGCUCGGUAAUCAAUGAtt | UCAUUGAUUACCGAGCCUCcg |
| Der1 mer 2 | GCUUAGCAAUGGAUAUGCAtt | UGCAUAUCCAUUGCUAAGCca |
| Der1 mer 3 | GGGUUAUCCUUGGAUUCAAtt | UUGAAUCCAAGGAUAACCCag |

## 3.2 Experimental Procedures

### 3.2.1 Tagging of the cDNA construct

In the first cycle four amino acids (DYKD) of the FLAG tag were introduced prior to the stop codon of the cDNA. In the second cycle, the resulting construct was used as a template and the remaining four amino acids (DDDK) were introduced. Similarly, the HA-tagged version of the wild-type FZD4 was generated by site-directed mutagenesis to introduce the nine amino acids of the HA tag (YPYDVPDYA) in two cycles as shown below:

Table 3.2.1. Introduction of the HA and FLAG tags before the stop codon of FZD4 cDNA gene. The sequences corresponding to the TAGs are highlighted in bold font.

| FZD4 | Forward 5'-3' | Reverse 5'-3' |
|---|---|---|
| FZN4 HA 1 | GACTGTGGTA**TACCCATACGATG TT**TAAGGCTAGTCAGCCTCCATG | CATGGAGGCTGACTAGCCTTA**AAC ATCGTATGGGTA**TACCACAGTC |
| FZN4 HA 2 | TACGATGTT**CCAGATTACGCT**TA AGGCTAGTCAGCCTCCATG | CATGGAGGCTGACTAGCCTTA**AGC GTAATCTGG**AACATCGTA |
| FZN4 FLAG 1 | GACTGTGGTA**GATTACAAGGAT**T AAGGCTAGTCAGCCTCCATG | CATGGAGGCTGACTAGCCTTA**ATC CTTGTAATC**TACCACAGTC |
| FZN4 FLAG 2 | TACAAGGAT**GACGACGATAAG**TA AGGCTAGTCAGCCTCCATG | CATGGAGGCTGACTAGCCTTA**CTT ATCGTCGTC**ATCCTTGTA |

### 3.2.2 Molecular cloning of TEK

TEK-WT cDNA; was amplified using primers which contain a C-terminal hemaglutinin (HA) tag and then restriction enzymes (RE), EcoRI and XhoI, were used to cut and clone into a pcDNA 3.1 /Zeo+ vector. The TEK cDNA-pcDNA 3.1/zeo construct was subjected to site-directed mutagenesis for introduction of the RE and HA tag as shown below:

Table 3.2.2. Molecular cloning of TEK. The sequences corresponding to the TAG and RE sites are highlighted in bold font.

| TEK HA Forward 5'-3' | TCGAATTCCCACCATG**GACTCTTTAGCCAGCT**TA |
|---|---|
| TEK HA Reverse 5'-3' | AGCTCGAGCTA**AGCGTAATCTGGAACATCGTATGG GTA**GGCCGCTTCTTCAGCAGAAC |

### 3.2.3 Generation of missense mutants

All missense mutants were introduced by QuickChange site-directed mutagenesis with Turbo *Pfu* DNA polymerase (Stratagene) with wild-type Human cDNA as a template. Primers were generated using Primer X (http://www.bioinformatics.org/primerx/ [in the public domain]) and are shown:

Table 3.2.3. FZD4 missense primers used to generate the reported missense mutations used in this project. The mismatched nucleotides are highlighted in bold font.

| | Forward 5'-3' | Reverse 5'-3' |
|---|---|---|
| P33S (Pro33Ser) | CTGCTGCTCCTGGGG**T**CGGCGC GGGGCTTC | GAAGCCCCGCGCCG**A**CCCCAGGA GCAGCAG |
| G36D (Gly36Asp) | CTGGGGCCGGCGCGGG**AC**TTCG GGGACGAG | CTCGTCCCCGAA**GT**CCCGCGCCG GCCCCAG |
| H69Y (His69Tyr) | CAACCTGGTTGGG**T**ACGAGCTGC AGAC | GTCTGCAGCTCGT**A**CCCAACCAG GTTG |
| C181R (Cys181Arg) | AGCCTGGGGAAGAG**C**GTCACTCT GTGGGAA | TTCCCACAGAGTGAC**G**CTCTTCCC CAGGCT |
| M105V (Met105Val) | GTTCTGTTTATGTGCCA**G**TGTGC ACAGAGAAGATC | GATCTTCTCTGTGCACA**C**TGGCAC ATAAACAGAAC |
| M105T (Met105Thr) | CTGTTTATGTGCCAA**C**GTGCACA GAGAAGATC | GATCTTCTCTGTGCAC**G**TTGGCAC ATAAACAG |
| C204R (Cys204Arg) | CTGTGTGCTCAAG**C**GTGGCTATG ATGC | GCATCATAGCCAC**G**CTTGAGCACA CAG |
| C204Y (Cys204Tyr) | CTGTGTGCTCAAGT**A**TGGCTATG ATGCTGG | CCAGCATCATAGCCA**T**ACTTGAGC ACACAG |
| G488D (Gly488Asp) | CTTTGTTGGTGG**A**CATCACTTCA GG | CCTGAAGTGATG**T**CCACCAACAAA G |
| W335C (Trp335Cys) | CAGCAGGACTCAAATG**C**GGTCAT GAAGCCATTG | CAATGGCTTCATGACC**G**CATTTGA GTCCTGCTG |
| R417P (Arg417Pro) | GGCCTTGTTCAAAATTC**C**GTCAAA TCTTCAAAAGG | CCTTTTGAAGATTTGAC**G**GAATTTT GAACAAGGCC |
| R417Q (Arg417Glu) | GGTGGCCTTGTTCAAAATTC**A**GT CAAATCTTCAAAAGGATGG | CCATCCTTTTGAAGATTTGAC**T**GA ATTTTGAACAAGGCCACC |
| T445P (Thr445Pro) | CTCAGTACTGTAC**C**CAGTTCCTG CAACG | CGTTGCAGGAACTG**G**GTACAGTA CTGAG |
| G492R (Gly492Arg) | GGGCATCACTTCA**C**GCATGTGGA TTTGG | CCAAATCCACATGC**G**TGAAGTGAT GCCC |
| S497P (Ser497Pro) | GCATGTGGAT**T**TGGTTTGCCAAA ACTCTTCAC | GTGAAGAGTTTTGGCA**A**ACCAAAT CCACATGC |

Table 3.2.4. MuSK missense primers used to generate the reported missense mutations used in this project. The mismatched nucleotides are highlighted in bold font.

| Mutation | Forward Primer 5'-3' | Reverse Primer 5'-3' |
|---|---|---|
| T114A (Asp38Glu) | CTCTTGAAACAGTGGA**A**GCCT TAGTTGAAGAAG | CTTCTTCAACTAAGGC**T**TCCA CTGTTTCAAGAG |
| C1031G (Pro344Arg) | CAACACCTCCTATGCGGAC**CG A**GAGGAGGCCCAAGAGCTAC | GTAGCTCTTGGGCCTCCTC**TC G**GTCCGCATAGGAGGTGTTG |
| G1815A (Met605Ile) | CTATGAACCTTTCACTAT**A**GT GGCAGTAAAGATGCTC | GAGCATCTTTACTGCCAC**T**AT AGTGAAAGGTTCATAG |
| C2180T (Ala727Val) | CACCGAGATTTAG**T**CACCAGG AACTGCC | GGCAGTTCCTGGTG**A**CTAAAT CTCGGTG |
| G2368A (Val790Met) | GATGTGTGGGCCTATGGC**A**T GGTCCTCTGGGAGATC | GATCTCCCAGAGGACCA**T**GCC ATAGGCCCACACATC |
| A2503G (Met835Val) | GAGCTGTACAATCTC**G**TGCGT CTATGTTGG | CCAACATAGACGCA**C**GAGATT GTACAGCTC |
| Dead kinase K609A (Lys609Arg) | CACTATGGTGGCAGTA**GCG**AT GCTCAAAGAAGAAG | CTTCTTCTTTGAGCAT**CGC**TA CTGCCACCATAGTG |

Table 3.2.5. TEK missense primers used to generate the reported missense mutations used in this project. The mismatched nucleotides are highlighted in bold font.

| Mutation | Forward Primer 5'-3' | Reverse Primer 5'-3' |
|---|---|---|
| R849W (C2545T) | GAAGGATGGGTTA**T**GGATGGA TGCTGCC | GGCAGCATCCATCC**A**TAACCC ATCCTTC |
| Y897C (A2690G) | GAACATCGAGGCT**G**CTTGTAC CTGGC | GCCAGGTACAAG**C**AGCCTCG ATGTTC |
| Y897S (A2690C) | GAACATCGAGGCT**C**CTTGTAC CTGGC | GCCAGGTACAAG**G**AGCCTCG ATGTTC |
| R915H (G2744A) | CTGGACTTCCTTC**A**CAAGAGC CGTGTG | CACACGGCTCTTG**T**GAAGGAA GTCCAG |
| R918C (C2752T) | CTTCGCAAGAGC**T**GTGTGCTG GAGAC | GTCTCCAGCACAC**A**GCTCTTG CGAAG |
| A925S (G2773T) | GGAGACGGACCCA**T**CATTTGC CATTGC | GCAATGGCAAATG**A**TGGGTCC GTCTCC |
| V919L (G2755T) | CTTCGCAAGAGCCGT**T**TGCTG GAGACGGAC | GTCCGTCTCCAGCA**A**ACGGCT CTTGCGAAG |
| K1100N (G3300C) | GTTAGAGGAGCGAAA**C**ACCTA CGTGAATAC | GTATTCACGTAGGT**G**TTTCGC TCCTCTAAC |

### 3.2.4 DNA sequencing

Deoxyribonucleic acid sequencing was performed using the dideoxy Sanger method with fluorescent automated sequencing on the ABI 3130xl Genetic Analyzer (Applied Biosystems, Foster City, CA, USA). Data were analyzed using sequencing analysis ABI software version 5.3 (Applied Biosystems). ClustalW2 (http://www.ebi.ac.uk/Tools/msa/clustalw2/ [in the public domain]) was used for sequence alignments.

### 3.2.5 Cell culture and transfection

HeLa, COS-7, and HEK293 cells were cultured in DMEM supplemented with 10% FBS, 2 mM L-glutamine, and 100 U/mL penicillin-streptomycin at 37 °C with 5% carbon dioxide. For immunofluorescence (IF), cells were grown on sterile coverslips in 24-well tissue culture plates. Transfection was performed after 24 hours of seeding using the liposomal transfection reagent FuGENE HD (Promega) according to the manufacturer's instructions. For each well, 1-2 µg of wild-type or mutant constructs were used. Forty-eight hours post transfection, the cells were fixed and processed for confocal fluorescence microscopy (CFM) as described in section 3.4.7. For WB, 1 day before transfection cells were seeded on six multiwells (35 mm in diameter) and grown to about 70% confluency. Transfection was performed using the FuGENE HD transfection reagent (Promega) according to the manufacturer's instructions.

### 3.2.6 siRNA transfection

Stable HEK293 cell lines of MuSK-WT, P344R-MuSK were cultured in reduced serum-free media (OptiMEM) at 37 °C with 5% carbon dioxide. Transfection was performed using the FuGENE HD transfection reagent according to the manufacturer's instructions. The cells were transfected with siRNA for 72 hours.

### 3.2.7 Immunofluorescence and confocal fluorescence microscopy

For immunofluorescence (IF), cover slips-grown HeLa, HEK293 or COS-7 cells were washed with PBS, fixed with cold methanol at -20 ˚C for 7 minutes. Then fixed cells were then washed in PBS three times and incubated in blocking solution (10% BSA in PBS) for 1 hour at room temperature. The fixed cells were then incubated for 1 hour at room temperature with the primary monoclonal antibodies (anti-FLAG) alone or co-incubated with anti-calnexin polyclonal antibodies. After washing with PBS, the cells were incubated with the appropriate fluorescently-labelled secondary antibodies for 1 hour at room temperature then washed several times with PBS and mounted in immunofluor medium. We used enhanced green fluorescent protein-Harvey rat sarcoma viral oncogene homolog (EGFP *HRAS*) as a marker for the plasma membrane [203]. In this case, the EGFP *HRAS* construct was co-transfected with *MUSK* constructs. Data were acquired using a Nikon confocal microscope (Tokyo, Japan). For presentation purposes, images were pseudo-colored as either red (protein of interest) or green (calnexin and EGFP-H-Ras), contrast enhanced and merged using ImageJ version 1.47 (http://rsbweb.nih.gov/ij [in the public domain]). All images presented are single sections in the *z* plane. Colocalizations were quantitated when required using ImageJ version 1.47 or fiji http://fiji.sc/Colocalization_Analysis [public domain] [204].

### 3.2.8 Protein extraction and immunoprecipitation

Immunoprecipitation (IP) was used to isolate the expressed proteins from whole cell lysates of HEK293 cells or HEK293T. Forty eight hours following transfection, the cultured media was removed and cells were gently washed twice with ice cold PBS. After washing, 200 µl of ice cold lysis “MuSK extraction buffer” containing: 10 mM HEPES, pH 7.9, 417 mM NaCl, 10mM KCL, 1% IGEPAL, 0.8mM EDTA and 2 mM dithiothreitol (DTT) or radioimmunoprecipitation assay buffer (RIPA) containing

protease inhibitors was added to the dishes and incubated on ice for 10-15 minutes. Immediately after lysis, the NaCl concentration was adjusted and maintained at 400 mM. The cell lysates were then centrifuged at 1000 xg for 15 minutes at 4 ˚C. The supernatants were then transferred to a new tube without disturbing the pellet. Proteins were quantified by a BCA kit according to the manufacturer's instructions. A "MuSK extraction buffer" containing 50 mM HEPES, pH 7.5, 150 mM NaCl, 1.5mM $MgCl_2$, 1 mM EGTA, 1% Triton-X 100 and 10% glycerol was added to 0.5mg of cell lysate to a final volume of 400 µl. Two micrograms of rabbit anti-FLAG antibodies were added to the solution and incubated at 4 ˚C on a rotator for 1-3 hours then 30 µl of pre-equilibrated protein Sepharose A/G with protease inhibitors was added and incubated at 4˚C for 2 hours to capture the immune complex. The tubes were centrifuged at 1000 xg for 1 minute at 4˚C and the supernatant was carefully removed. The Sepharose A/G beads were washed three times with PBS buffer, re-centrifuged and the supernatant removed.

### 3.2.9 Generation of HEK293 stable cell lines

HEK 293 cells were stably transfected with *MUSK-WT*, *P344R-MuSK* constructs and an empty vector using a PCMV6-entry vector with a neomycin resistance cassette. Stable clones were selected for use with 700 µg/µl Geneticin® antibiotic (G418) for 4 weeks. Single clones for MUSK-WT and P344R-MuSK and the empty vector, as a control, were maintained at the same concentration.

### 3.2.10 Deglycosylation assays

Approximately 20 µg of the IP eluates were added to 5 µl of denaturation solution (containing 2% sodium dodecyl sulphate (SDS) and 1 M β-mercaptoethanol (BME)) and heated to 100 °C before the addition of 5 µl of sodium phosphate buffer (250 mM, pH 5.5 for endo-β-N-acetylglucosaminidase H (Endo H) and buffer 7.4 for peptide-N(4)-(N-acetyl-beta-glucosaminyl) asparagine amidase (PNGase F). For Endo H; 2 µl of Endo H enzyme was added to each sample and incubated overnight

at 37 ˚C. For PNGase F, 2 units of enzyme were added and the samples incubated for 24 hours at 37 °C and then another 2 units of enzyme were added for a further 24 hours. The treated samples were then subjected to SDS-PAGE and western blotting using anti-FLAG antibodies as described below.

### 3.2.11 Western blot analysis

Eluates of immunoprecipitation or whole cell lysates were treated with 6X Laemmli buffer. 30 µg of protein from control (untransfected cells), WT and mutant preparations were subjected to 8-15% sodium dodecyl sulfate-polyacrylamide gel electrophoresis (SDS-PAGE) and transferred to nitrocellulose membranes. After 1 hour of blocking in 3% non-fat dry milk (NFM) in TRIS-buffered saline (TBS) PH 8; 0.05% (w/v) Tween 20 (T), nitrocellulose blots were incubated for 1 hour with the appropriate primary antibodies in 3% NFM-TBS-T. Following washing with TBS-T, membranes were then incubated with rabbit anti-mouse IgG-peroxidase antibody or goat anti-rabbit IgG-peroxidase antibody in TBS-T containing 3% NFM for 1 hour and developed by Pierce ECL plus WB reagents (Thermo Scientific). All blots were viewed with Typhoon FLA 9500 ImageQuant TL software (GE Healthcare Sciences, Uppsala, Sweden).

### 3.2.12 Glycine elution of immunoprecipitates

Following immunoprecipitation, proteins were eluted from the Sepharose beads using 0.2 M glycine buffer at PH 2.6. 50 µl of glycine buffer was added to the beads and incubated for 10 minutes with frequent agitation before centrifugation. The eluates were pooled and neutralized by adding equal volumes of Tris pH 8.0. The beads were then neutralized by washing 2 times with 150 µl lysis buffer (without detergent) and pooled with eluates.

### 3.2.13 Cell-surface biotinylation

HEK293 cells underwent cell surface biotinylation according to the manufacturer's instructions. Briefly, cells were grown to a monolayer, serum-starved for 4 hours and then treated with chemical chaperones for 7 hours. Surface proteins were biotinylated by applying 0.5 ml of NHS-S-S-biotin in PBS for 30 minutes at 4°C on the apical side. After quenching, filters were excised and cells were lysed with 0.5 ml lysis buffer containing protease and phosphatase inhibitors. Lysed samples were briefly sonicated, centrifuged at 13,000 rpm for 10 minutes at 4°C, and the supernatant was collected and used for protein assay and pull-down experiments. Biotinylated proteins were pulled down with streptavidin-agarose beads. Bound proteins were eluted by incubating the beads in a sample buffer containing urea, protease and phosphatase inhibitor cocktails at 100 °C for 5 minutes. The samples were centrifuged at 10,000 rpm for 5 minutes, and the supernatant was separated and mixed with 0.125 ml of trichloroacetic acid (TCA), incubated for 10 minutes on ice, and centrifuged at 14,000 rpm for 5 minutes. Supernatants were discarded and pellets washed three times with ice-cold acetone. The pellets were air-dried and protein quantified before it was processed for SDS-PAGE. For immunoblotting, proteins were separated by SDS-PAGE, followed by immunoblotting with anti-FLAG antibodies. The integrity of the plasma membrane and cell surface specific biotinylation and equal loading was confirmed using the IGF2R as a control. Blots were quantified as described above and normalized to the total plasma membrane receptor fraction.

### 3.2.14 Cylcoheximide protein synthesis inhibition

Half-life ($t_{1/2}$) experiments employing cycloheximide (CHX) inhibition of protein synthesis were performed as described previously [205]. Cultures were treated with CHX (final concentration of 50 µg/ml) for the time periods indicated. In some cases the cultures were treated with inhibitors (45–60 minutes for proteasome inhibitors)

prior to harvesting, or the addition of CHX. The cells were lysed in lysis buffer plus inhibitors and lysates were run on a 8% SDS-PAGE gel. All $t_{1/2}$ and MG132 plus CHX experiments were repeated three or more times. A 0.1% DMSO vehicle was used as a control.

### 3.2.15 Proteasome inhibition

Proteasome inhibitor MG132 at a concentration of 25 μM was added at the time periods indicated. The cell lysates were subjected to SDS-PAGE and immunoblotting with anti-FLAG antibodies. A 0.1% DMSO vehicle was used as a control.

### 3.2.16 Anti-ubiquitin western blotting

Following IP and SDS-fractionation on an 8% SDS-PAGE gel, the immunoblots were stripped by a stripping buffer, washed 3X with TBS-T and then autoclaved as previously described [206]. The blots were then blocked with 1% NFM in TBS-T (0.05% w/v Tween 20). TBS contained (per liter) 8g NaCl, 0.2g of KCL and 3g of Tris-base and was adjusted to a PH of 7.4. Anti-ubiquitin antibody was diluted 1:1000 in 1% NFM in TBS-T and incubated overnight at 4 ˚C. The blots were washed 3X with TBS-T and incubated with secondary antibodies for 1 hour in 1% NFM-TBST and processed as described above.

### 3.2.17 Colocalization analysis

Colocalization with calnexin and/or H-Ras was measured as a function using Fiji and then compared with WT on multiple CFM image sections of at least 30 cells in three independent experiments.

Example 1: Merged protein colocalizes well with calnexin

1. Merged images; split channels

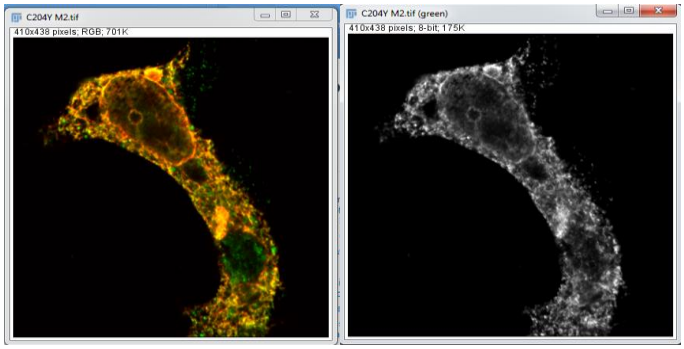


2. Choose parameters: e.g. Scatterplot with linear regression fit (white line) and correlation

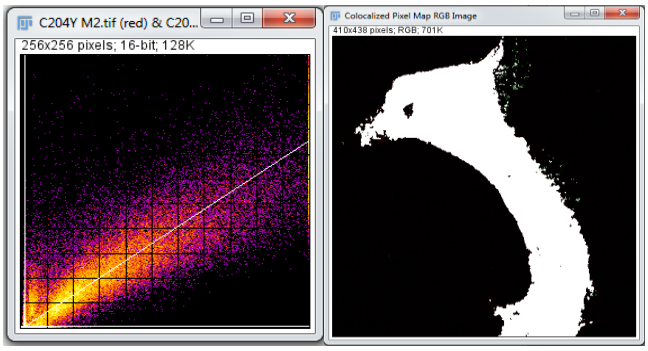


3. Results based on Pearsons coefficients (R) and Manders coefficients (M);

Results

File Edit Font Results

| Images | Mask | ZeroZero | Rtotal | m | b | Ch1 thresh | Ch2 thresh | Rcoloc | R<threshold | M1 | M2 | tM1 | tM2 |
|---|---|---|---|---|---|---|---|---|---|---|---|---|---|
| C204Y M2.tif (red) & C204Y M2.tif (green) | ROI0 | incl. | 0.928 | 0.691 | -0.9 | 3 | 1 | 0.8257 | -0.007 | 0.9307 | 1.0000 | 0.9307 | 0.9971 |

4. Interpret results for colocalization

Manders: 0 is no colocalization; 1 is perfect colocalization
Pearsons: Rcoloc for whole image close to 1; very good colocalization
R< threshold: <0
Linear regression line: gradient (m) close to 1; intercept (b) close to 0

Example 2: Merged protein does not colocalize well with HRAS

1. Merged images; split channels

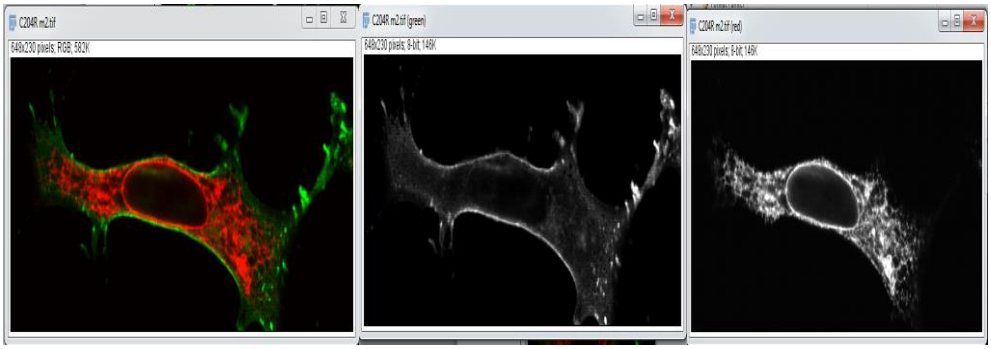

2. Choose parameters: e.g. Scatterplot with linear regression fit (white line) and correlation

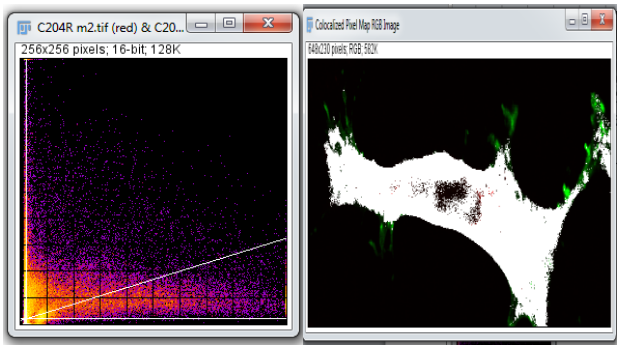


3. Results based on Pearsons coefficients (R) and Manders coefficients (M);

Results

File Edit Font Results

| Images | Mask | ZeroZero | Rtotal | m | b | Ch1 thresh | Ch2 thresh | Rcoloc | R<threshold | M1 | M2 | tM1 | tM2 |
|---|---|---|---|---|---|---|---|---|---|---|---|---|---|
| C204R m2.tif (red) & C204R m2.tif (green) | ROI0 | incl. | 0.333 | 0.310 | 3.7 | 5 | 5 | -0.0409 | 0.007 | 0.8517 | 1.0000 | 0.8384 | 0.8158 |

4. Interpret results for colocalization

Manders: 0 is no colocalization; 1 is perfect colocalization
Pearsons: Rcoloc for whole image close to 1; very good colocalization
R< threshold: <0
Linear regression line: gradient (m) close to 1; intercept (b) close to 0

### 3.2.18 Quantification

All blots were quatitified on both Typhoon FLA 9500 ImageQuant TL software and ImageJ version 1.47. An example of quantification using ImageJ version is shown below:

1. The region of choice to be quantified is selected

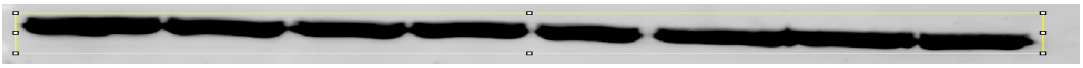

2. Calibration of the optical density (OD)

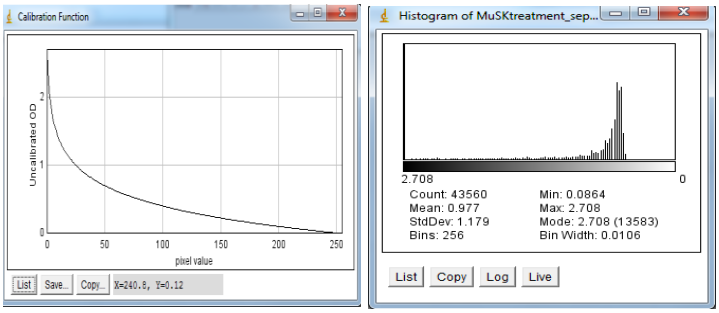


3. Each lane is highlighted

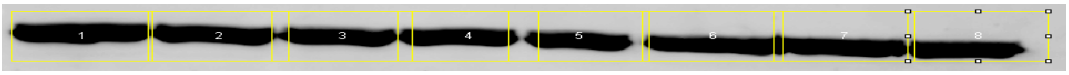


4. The protein is estimated in each lane and is plotted

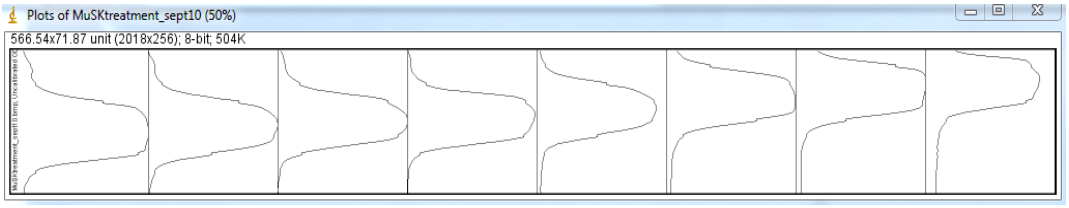


5. The output file can be used for normalization or expressed as a function

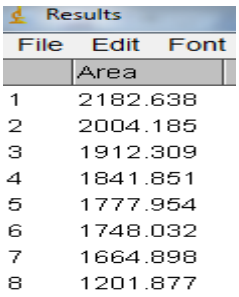


### 3.2.19 Statistical analysis

All statistical analyses were carried out on GraphPad (http://www.graphpad.com). Unpaired students *t* test was used for statistical comparisons. The mean ± standard error of each experiment with the N value.

# Chapter 4: Results and Findings

## 4.1 Frizzled Family Receptor 4 (FZD4) reported to cause Familial Exudative Vitreoretinopathy (FEVR)

### 4.1.1 Introduction

Familial Exudative Vitreoretinopathy (FEVR) (Online Mendelian Inheritance in Man 133780) is a developmental anomaly characterized by incomplete or no vascularization of the peripheral retina [207]. Patients with FEVR exhibit highly variable expressions of the disease, ranging from asymptomatic to complete blindness. FEVR is genetically heterogeneous and can be inherited in a dominant manner via frizzled class receptor 4 *(FZD4),* low-density lipoprotein receptor related protein 5 *(LRP5),* or tetraspanin 12 (*TSPAN12*) genes.

This condition can also be inherited in a recessive manner via mutations in the *LRP5* gene or in an X-linked fashion through mutations in the Norrin (*NDP*) gene [208]. However, the autosomal dominant inheritance is by far the most common cause of FEVR. Mutations in FZD4, a wingless-type mouse mammary tumor virus integration site family (Wnt) receptor, have been shown to cause premature arrest of retinal angiogenesis in patients with FEVR [209]. In addition, mutations in this protein have been linked to retinopathy of prematurity, a condition with phenotypic overlap with FEVR [210].

The seven-pass transmembrane FZD4 protein has a highly conserved extracellular frizzled cysteine-rich domain frizzled (Fz-CRD) (Figure 4.1.1). This N-terminal extracellular CRD is conserved among Fz family members and determines binding specificity for Wnt ligands. The intracellular domains contain threonine-X-valine PDZ-binding and lysine-threonine-X-X-X-tryptophan disheveled association sites [211]. The NDP/FZD4 proteins are involved in the wingless (Wnt) signaling

pathway controlling a transcriptional program that regulates endothelial growth and maturation throughout the course of retinal vascular development [212-214].

To date, 58 different FEVR pathogenic mutations have been reported for *FZD4,* of which 31 are missense changes scattered throughout the protein structure [215]. All the mutations except R417Q have been shown to cause the disease in the heterozygous state [216]. However, patients have been diagnosed as having more severe forms of FEVR when both alleles of *FZD4* gene are mutated [210].

Studies on the cellular localization of *FZD4* pathogenic mutations and their functional implications are scarce. A deletion of two nucleotides that led to a frameshift and created a stop codon at residue 533 (L501fsX533) resulted in a defective PDZ-binding motif and hence loss of FZD4 function in the calcium/calmodulin-dependent protein kinase II and protein kinase C signaling pathway [217]. A *FZD4* haploinsufficiency effect was postulated to be the causative defect underlying FEVR in a patient hemizygous for *FZD4* [218]. Due to the nature of the missense mutations and the importance of the CRD domains for proper protein folding [148]. It was hypothesized that some of the missense mutations in *FZD4* might lead to protein misfolding and failure to pass the stringent endoplasmic reticulum (ER) quality control machinery. Proteins that fail this machinery are targeted for degradation by ER-associated protein degradation (ERAD). As detailed in the literature review chapter (chapter 2), protein misfolding is the underlying cause of numerous highly debilitating disorders, ranging from Alzheimer Disease to Cystic Fibrosis [1, 18, 148, 149].

I examined the trafficking of 15 FZD4 missense mutations causing FEVR, shown in Figure 4.1.1. I characterized these mutations for their cellular processing, subcellular localization, and polyubiquitination profiles and compared them with wild-type (WT). I co-expressed the mutant constructs with WT construct to determine if a dominant-negative effect contributes to the disease pathology. I also evaluated

culturing the expressing cells at reduced temperatures or in the presence of chemical chaperones in an attempt to rescue trafficking defects of some mutants. My data suggest trafficking defects as the major disease mechanism underlying nine of the mutations studied, namely P33S [219], G36D [220], H69Y [221], M105V [210] M105T [220], C181R [221], C204Y [222], C204R [223], and G488D [210].

### 4.1.2 Results

#### 4.1.2.1 Nine of 15 *FZD4* mutants are predominantly localized to the ER

Fifteen FEVR-causing missense mutations shown in Figure 4.1.1 were generated by site-directed mutagenesis, and their localization was assessed in both HeLa and COS-7 cell lines using IF and CFM following transient expression. The data for the COS-7 cell line are not shown but were always consistent with the HeLa cell line results. In both cell lines, the ER lectin chaperone calnexin was stained to establish colocalization with the ER network. In contrast to the *WT-FZD4* construct, seven (P33S, G36D, H69Y, M105T, C204R, C204Y, and G488D) of the 15 tested mutants exhibited high degrees of colocalization with calnexin, suggesting mislocalization away from the plasma membrane in a perinuclear and reticular pattern, suggestive of the ER (Figure 4.1.2A [panels B–J are compared with panel A of WT-FZD4]).

In addition, two mutants (M105V and C181R) showed partial ER localization with some residual protein localizing to the PM (Figure 4.1.2A [compare with panels F, G]). Figure 4.1.2B shows quantification of the degree of colocalization of mutants with calnexin compared with WT. The localization of the other six FEVR-causing mutants (W335C, R417P, R417Q, T445P, G492R, and S497P) resembled WT-FZD4 on the plasma membrane (Figure 4.1.4).

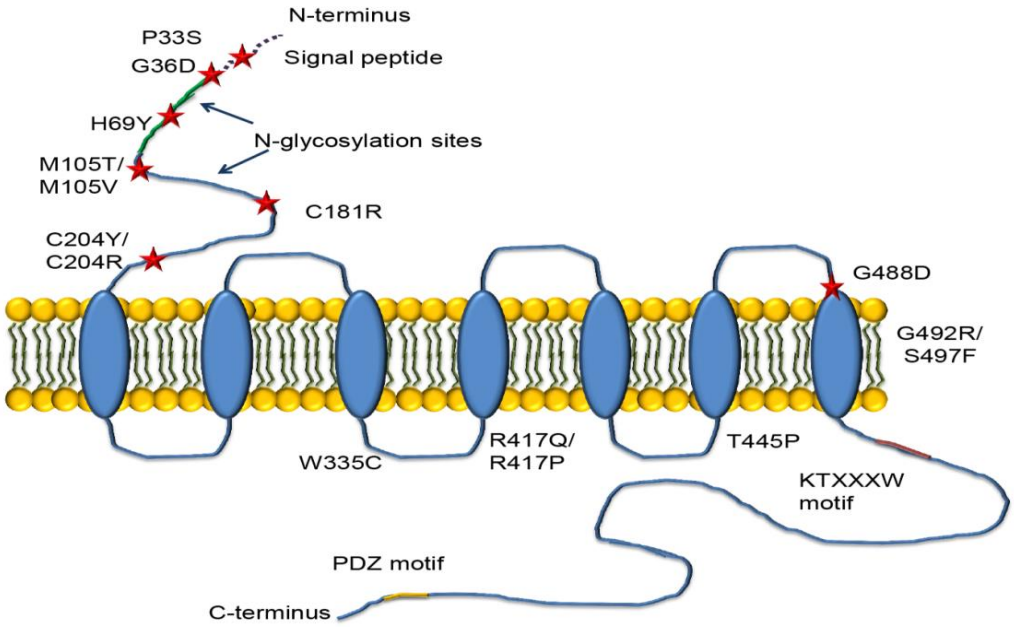


Figure 4.1.1. Illustration of FZD4 protein domain structure. Frizzled family receptor 4 is a seven-pass transmembrane protein with a signal peptide sequence found between amino acid positions 1 and 36/37, a Fz-CRD domain highlighted in green found at amino acid positions 42 through 167, a frizzled region spanning most of the protein within amino acid positions 210 through 514, a KTXXXW motif found at amino acid positions 499 through 504, and a PDZ motif located close to the C-terminal at amino acid positions 535 through 537. The two potential *N*-glycosylation sites are indicated by *arrows* at amino acid positions 59 and 144. Missense FEVR-causing mutations studied in this article are labeled across the protein. Missense mutations that traffic abnormally are shown with *red stars* (P33S, G36D, H69Y, M105T, M105V, C181R, C204R, C204Y, and G488D).

To further assess the subcellular localization, WT-FZD4 and the 15 *FZD4* FEVR-causing mutant constructs were cotransfected in HeLa cells with EGFP*HRAS* plasmid, the latter acting as a plasma membrane marker. The same seven mutants (P33S, G36D, H69Y, M105T, C204R, C204Y, and G488D) exhibited a distinct perinuclear reticular pattern that is clearly different from the EGFP-H-Ras, establishing mislocalization away from the plasma membrane (Figure 4.1.3B–E, H–J). A dual pattern of ER and PM localization for M105V and C181R mutants was once again observed (Figure 4.1.3F, 3G). The data in HeLa and COS-7 cell lines suggest that this mislocalization of the FEVR-causing FZD4 mutants is not cell-type specific.

A.

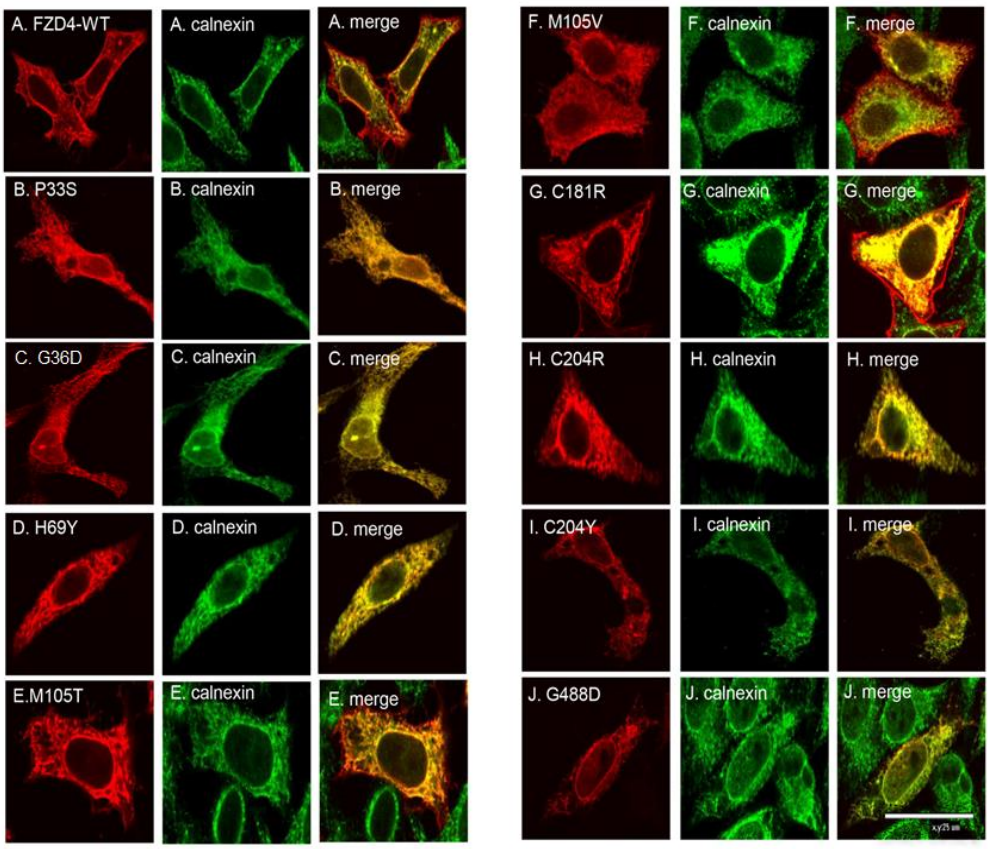
A. FZD4-WT
A. calnexin
A. merge
F. M105V
F. calnexin
F. merge
B. P33S
B. calnexin
B. merge
G. C181R
G. calnexin
G. merge
C. G36D
C. calnexin
C. merge
H. C204R
H. calnexin
H. merge
D. H69Y
D. calnexin
D. merge
I. C204Y
I. calnexin
I. merge
E.M105T
E. calnexin
E. merge
J. G488D
J. calnexin
J. merge

B.

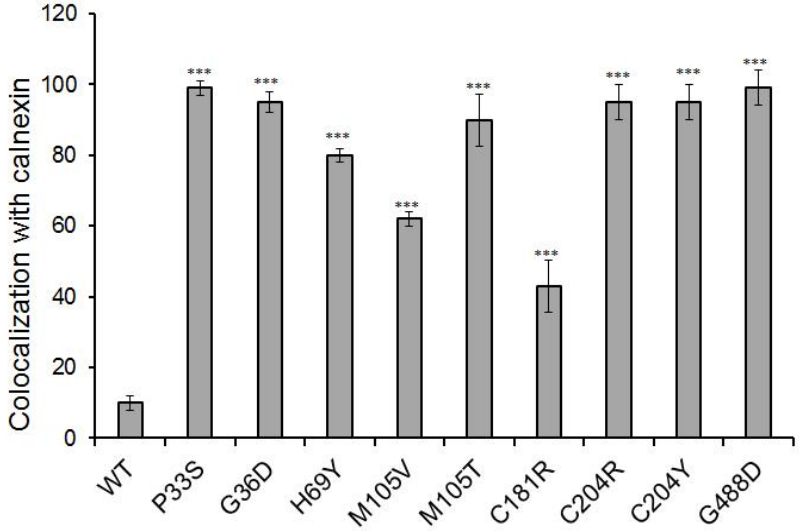
Colocalization with calnexin
120
100
80
60
40
20
0
***
WT
P33S
G36D
H69Y
M105V
M105T
C181R
C204R
C204Y
G488D

Figure 4.1.2. Colocalization of several FZD4 missense mutants with the ER marker in HeLa cells. CFM images of WT-FZD4 and FZD4 mutants (P33S, G36D, H69Y, M105T, M105V, C181R, C204R, C204Y, and G488D) show the colocalization of these mutants with calnexin, an ER marker. A FLAG epitope expressed WT-FZD4 protein, and mutants are seen in red on the left of each panel, and calnexin is shown in green in the middle image of each panel. The image on the right is the merging of the two signals. (A) Shown is WT-FZD4 localization to the plasma membrane, which is distinct from that of calnexin. In contrast, as shown in (B–J), these missense mutants are largely localized to an intracellular compartment that is perinuclear and reticular in nature and colocalizing with calnexin, suggestive of an ER localization. However, C181R and M105V seem to be partially localized to the ER, with some localization to the PM. Cells were transfected for 48 to 72 hours and then processed for IF as described in the Methods section. (B) Colocalization with calnexin was measured as a function and then compared with WT on multiple CFM image sections of at least 30 cells repeated for three independent experiments (mean [SE] of each experiment). Data (arbitrary units) are expressed as the mean (SE). ***$P <$ 0.001 compared with WT control. These images are representative images. No differences were found between the mutants' phenotype (localization patterns). *Scale bar:* 25 μm. Magnification: 100X.

#### 4.1.2.2 *N*-glycosylation profiling of the nine mutants is consistent with imaging data confirming ER retention

To further assess the subcellular localization of the ER-retained mutants, Endo H sensitivity and resistance *in vitro* assays on the expressed proteins were carried out. The FZD4 protein has two potential *N*-glycosylation sites in its extracellular domain (Figure 4.1.1, arrows). The principle of this assay is that the carbohydrate moieties of the ER-localized glycoproteins are cleavable by Endo H, whereas the post-ER species are resistant due to further remodeling of their *N*-glycans in the Golgi complex. Endo H cleaves after the first asparagine-linked *N*-acetylglucosamine (*N*-glycan) of high-mannose and hybrid polysaccharides.

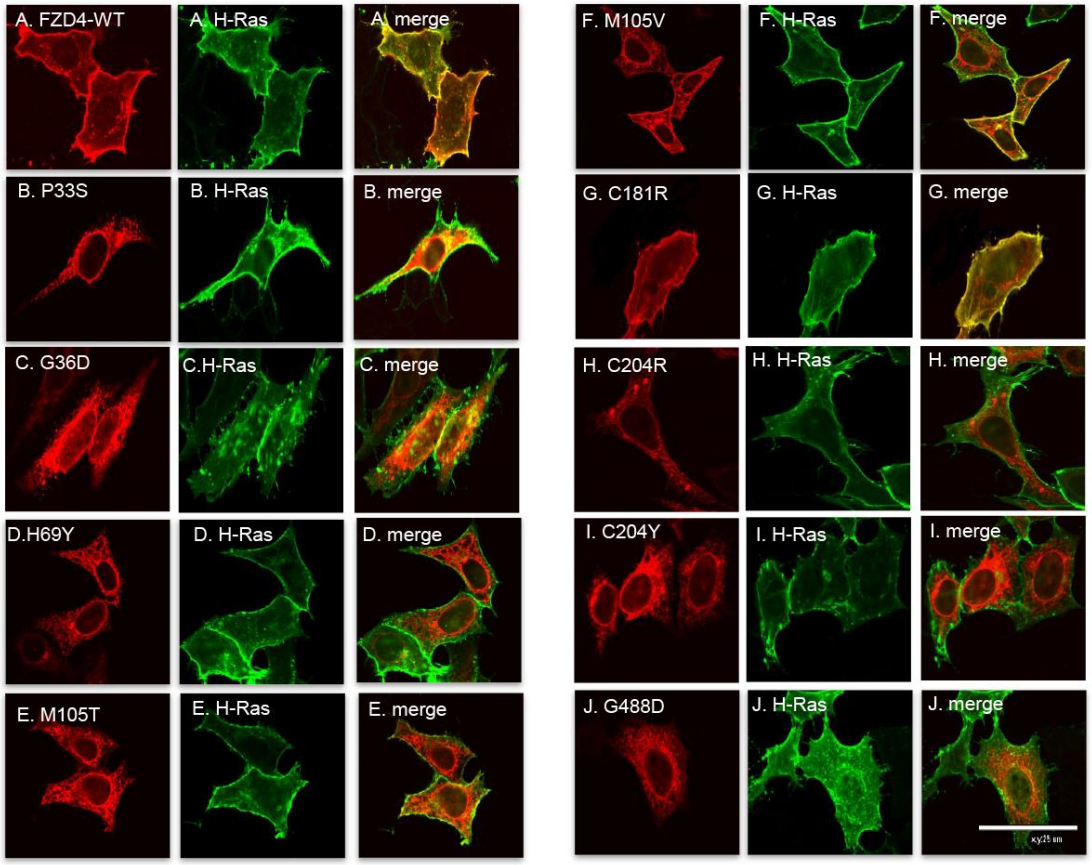


Figure 4.1.3. Exclusion of the seven missense FZD4 mutants from the plasma membrane in HeLa cells. The CFM images of WT-FZD4 and FZD4 mutants P33S, G36D, H69Y, M105T, M105V, C181R, C204R, C204Y, and G488D (red in the images on the left side of each panel) show their localization in HeLa cells relative to H-Ras, a plasma membrane marker (shown in the green image in the middle of each panel). The FLAG epitope-expressed WT-FZD4 protein in (A) indicates colocalization, with H-Ras indicating plasma membrane localization. However, (B–J) show that the mutants are largely excluded from the PM and localized to the perinuclear region, implying ER localization. C181R and M105V seem to be partially retained in the ER, with some PM localization, validating the data shown in Figure 2. Cells were transfected for 48 to 72 hours and then processed for IF. These images are representative images. No differences were found between the mutants' phenotype (localization patterns). Scale bar: 25 µm. Magnification: 100 X.

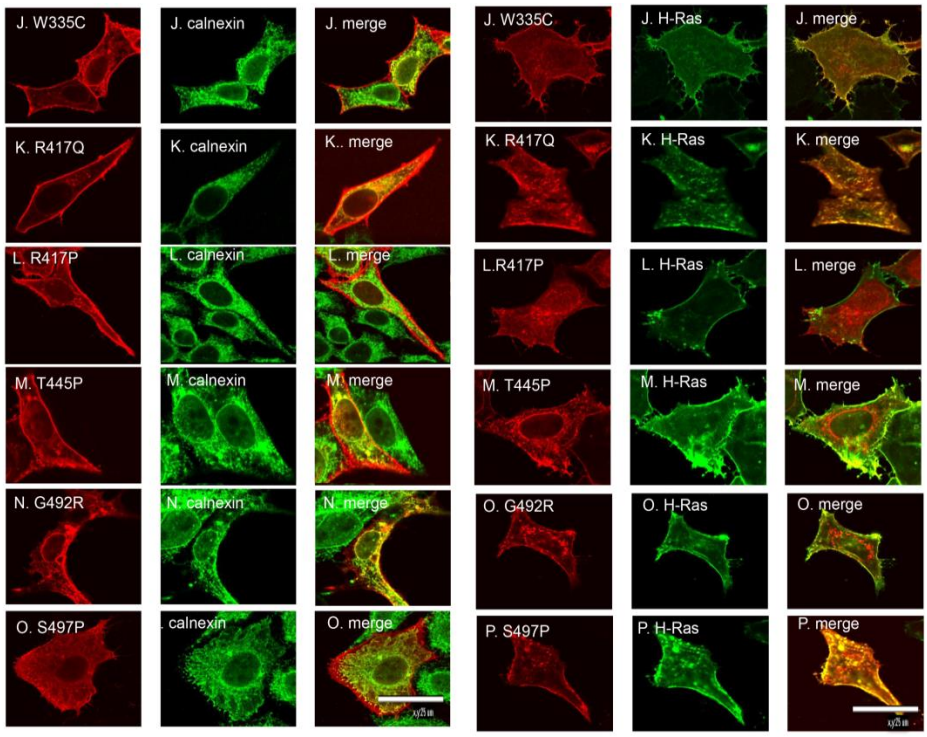


Figure 4.1.4. Six of the fifteen mutants localized to PM resembling the WT protein. Confocal images of the missense disease causing mutants in a HeLa cell line. Far left: confocal images of FZD4 mutants: W335C, R417Q, R417P, T445P, G492R and S497P showing their localization in HeLa cells alongside calnexin, an endoplasmic reticulum marker. Flag epitope expressed protein is seen as red fluorescence (far left) under the confocal microscope and the ER resident protein calnexin as green fluorescence (middle panel). When the two images are merged together, merge (far right) localization can be viewed clearly. Panels J-O clearly localize on the plasma membrane. Cells were transfected for 48 hours and then processed for IF. Scale bar = 25 µm; 100X objective lens. Far right: Confocal images of FZD4 mutants: W335C, R417Q, R417P, T445P, G492R and S497P showing their localization in HeLa cells alongside H-Ras, a plasma membrane marker. Flag epitope expressed protein is seen as red fluorescence (far left) under the confocal microscope and the PM resident protein as green fluorescence (middle panel). When the two images are merged together, merge (far right) localization can be viewed clearly. Panels J-O clearly localize on the plasma membrane. Cells were transfected for 48 hours and then processed for IF. These images are representative images. No differences were found between the mutants' phenotype (localization patterns). Scale bar = 25 µm; 100X objective lens.

Therefore, one can expect that the mutants retained in the ER will have their *N*-glycans cleaved when treated with Endo H. Proteins that have reached the Golgi complex would be resistant to Endo H treatment. Upon Endo H treatment, P33S, G36D, H69Y, M105V, M105T, C204Y, and C204R mutants showed complete conversion of the high-molecular-weight band into a lower-molecular-weight band, suggesting that these mutants are still in their immature states (Figure 4.1.5A). On the other hand, WT-FZD4 showed resistance to this treatment (Figure 4.1.5A). Interestingly, the C181R mutant gave two bands, one higher-molecular-weight band similar to the mature-form WT-FZD4 and a smaller-molecular-weight band that suggested incomplete ER retention of this protein (Figure 4.1.5A). Quantification of this is shown in Figure 4.1.5B. This observation may indicate that the change in amino acid may cause slow trafficking of this mutant to the PM. Interestingly, the M105V mutant, which previously appeared by IF to show a mixed localization between the ER and PM, resulted in one immature band. This may suggest that expression of the M105V mutant protein on the PM is somewhat minimal due to slow trafficking. It was notable that Endo H-treated and Endo H-untreated P33S and G488D samples showed a higher molecular weight band which was presumed to be due to dimerization and possibly oligomerization (Figure 4.1.5A). This behavior in FZD4 has been observed previously by other researchers [20, 224, 225] and is shown in Figure 4.1.7.

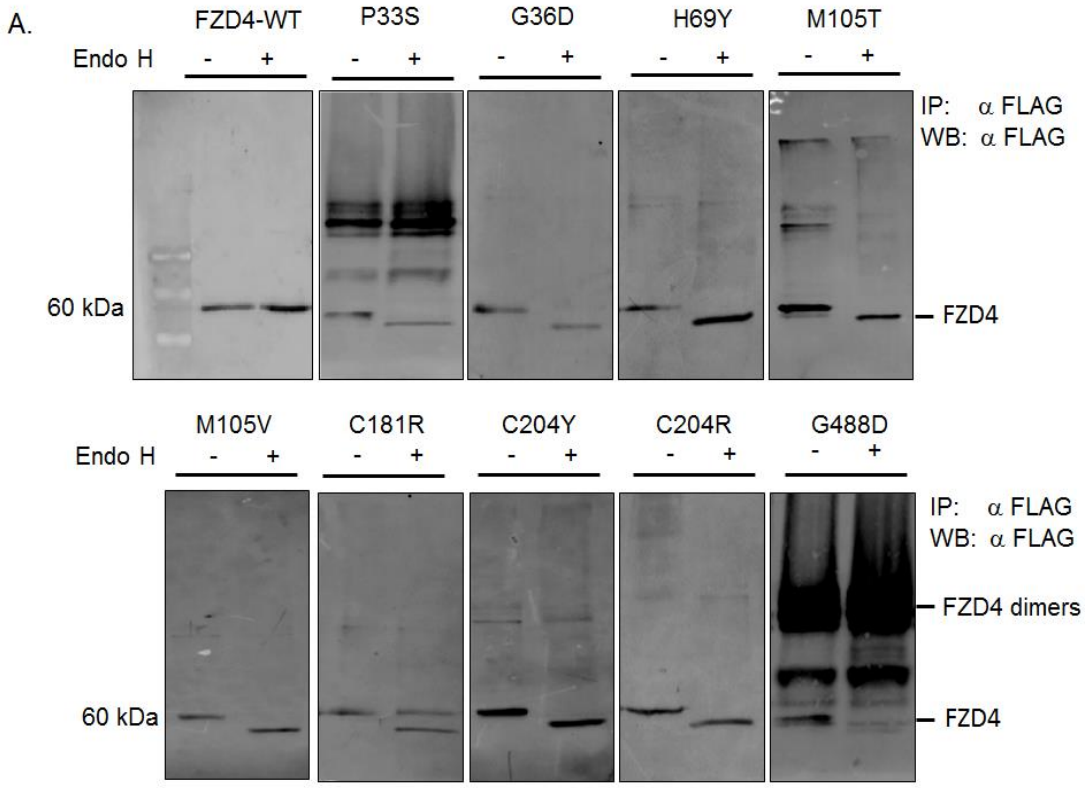


Figure 4.1.5. *N*-glycosylation profiles for the ER-retained mutants and WT-FZD4. In whole-cell lysates (WCL), WT-FZD4 expressed protein has been seen as a monomer, dimer, and multimers at the top of an SDS-PAGE gel ( Figure 4.1.6). Wild-type FZD4 and mutants were pulled down with mouse anti-FLAG antibodies, followed by sepharose A/G bead sedimentation as described in the Methods section. Upon elution, 20 µg protein was treated and then digested with Endo H for 5 hours with 60 mM DTT and 8 M urea (v/v) as described in the Methods section. P33S, M105T, and G488D mutants show an immature FZD4 protein, with lower-molecular-weight bands compared with WT-FZD4 and its treated counterpart, suggestive of possible folding defects. The monomer's molecular weight of FZD4 is approximately 60 kDa. Mutants P33S, G36D, H69Y, M105T, C204R, C204Y, and G488D were cleavable with Endo H, demonstrating their predominant localization in the ER. M105V and C181R were shown to have a dual pattern by CFM. However, when the M105V mutant was subjected to Endo H treatment, a single lower-molecular-weight band was observed. On the other hand, two bands, one mature and one immature, were observed for C181R. Furthermore, P33S and G448D formed dimers and probably multimers on Endo H treatment at a temperature of 37 ºC. Molecular mass standards are indicated in kDa. Quantification was carried out by Typhoon FLA 9500 ImageQuant TL software (GE Healthcare Life Sciences).

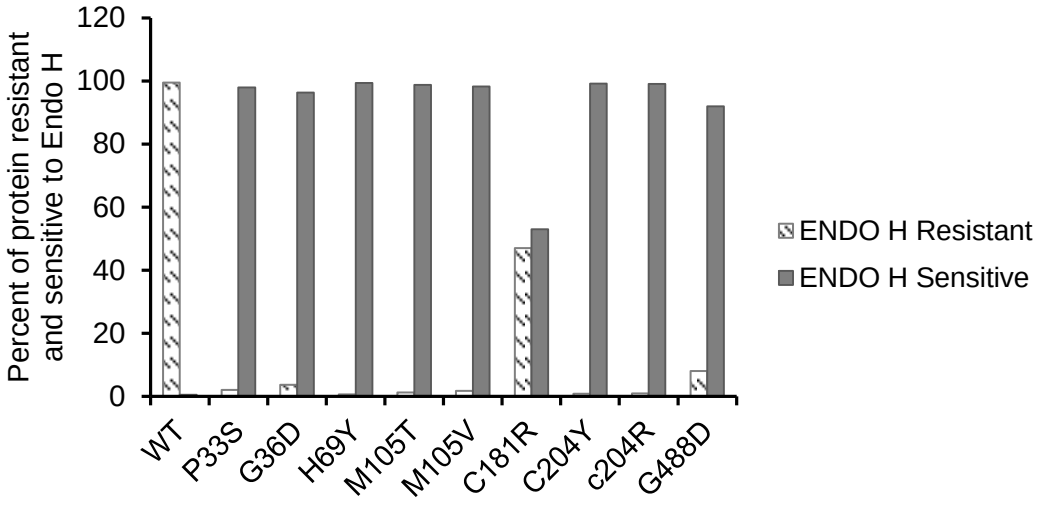


Figure 4.1.6. Percent of protein resistant and sensitive to Endo H. A bar chart in shows the percent of Endo H-resistant and Endo H-sensitive species for each sample in Figure 4.1.5. Wild-type is almost exclusively resistant to Endo H, whereas all the mutants (with the exception of C181R) are exclusively Endo H sensitive.


Figure 4.1.7. Western blot analysis of whole cell lysate from HEK293 cells transfected with FZD4 wild type construct. FZD4 homo and hetero-oligomerizes to form higher order dimers and oligomers on an 8% SDS-PAGE gel. The size of 130 kDa is consistent with the expected molecular mass of a Wnt dimer. A band at 78 kDa has previously been observed as HSPA5/BiP associating with Wnt receptors [226]. The higher order oligomers are possibly comprised of FZD4 with or without the BiP chaperone protein or aggreagates of FZD4 protein.

#### 4.1.2.3 The ER-retained mutants are highly polyubiquitinated

To determine if the ER-retained mutants are targeted for ERAD, HEK293T cells were transiently transfected with WT or mutant FZD4 plasmids. The expressed proteins underwent IP and were subjected to SDS-PAGE and probed with anti-FLAG antibodies (Figure 4.1.8B), stripped, and re-probed with anti-Ub antibodies. Immunostaining by anti-Ub antibodies showed a striking smear of presumably multiple Ub-moieties attached to FZD4-mutant conjugates at the top of the resolving gel (Figure 4.1.8A). Conjugates with multiple Ub moieties in the form of branched chains appear to be associated with the seven FZD4 mutants to a much greater extent compared with WT (Figure 4.1.8C). These data suggest that the seven ER-retained mutants are probably targeted for degradation by the proteasome via ERAD machinery.

#### 4.1.2.4 The effect of reducing temperature and incubation with different compounds directed at promoting folding and PM expression

Interestingly, ΔF508-CFTR mutants here shown to be mainly retained in the ER as a result of misfolding. However, when a small amount of the ΔF508-CFTR protein is expressed on the cell surface, it retains significant chloride channel conductance activity [29, 165]. Such results provided insight and proof of the principle that the molecular machinery directing folding and export could have an important role in both understanding the molecular basis for disease and developing novel therapeutic interventions [29, 227-229].

In addition, it has been shown that cell membrane expression of functional ΔF508-CFTR can be achieved by culturing the expressing cells at lower temperatures [30, 32]. Low-temperature incubation of affected tissues in CF is not a viable therapeutic option. However, incubation at lower temperatures may provide proof of the principle that the kinetic and/or thermodynamic aspects of secretory protein folding can be manipulated and therefore prevent targeting of the mutant

proteins to the ERAD machinery. Of the nine ER-retained mutants, M105T and C204Y showed partial rescue of trafficking to the PM by 57% and 46%, respectively, upon culturing the expressing cells at 27 °C (Figure 4.1.9).

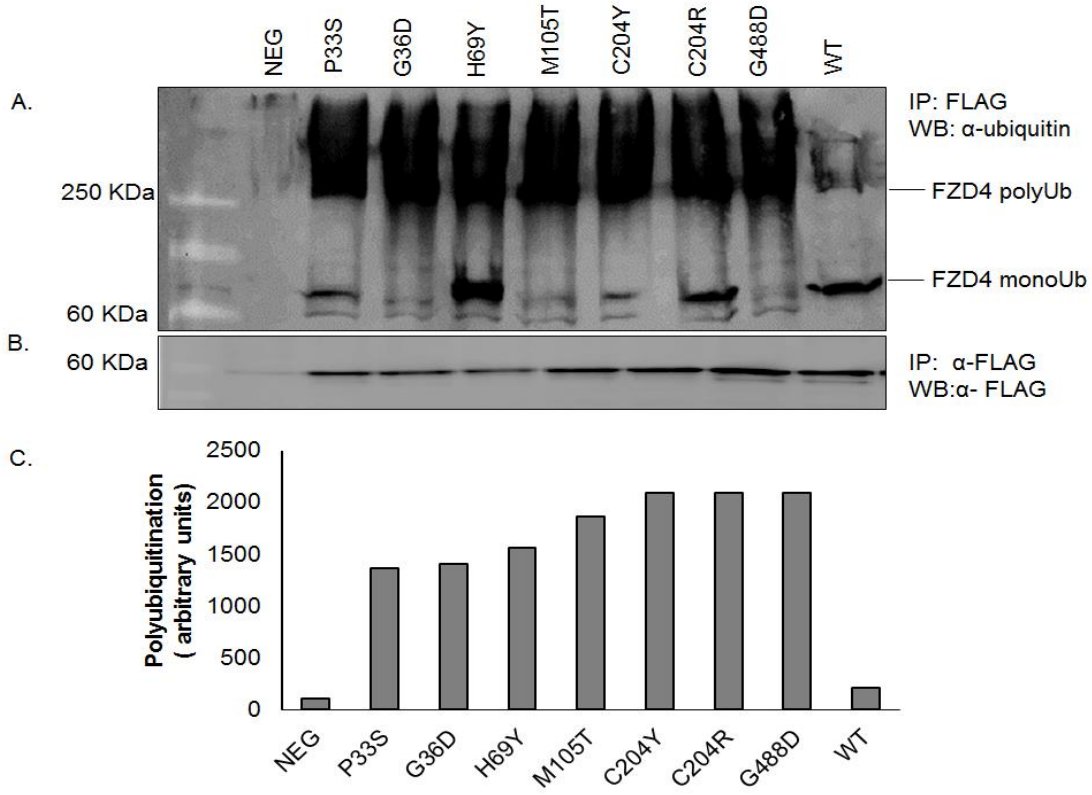


Figure 4.1.8. Polyubiquitination pattern of WT-FZD4 and ER-retained FZD4 mutants. (A) Immunoprecipitations of WT-FZD4, P33S, G36D, H69Y, M105T, C204Y, C204R, and G488D mutants were run on an 8% SDS-PAGE, blotted on nitrocellulose, and probed with anti-FLAG antibodies. The blots were then washed overnight with TBS-T, stripped, autoclaved [171], and then reprobed with anti-Ub monoclonal antibodies as described in the Methods section. The samples of the seven ER-retained mutants show very-high-molecular-weight smears, suggesting polyubiquitination. Wild-type FZD4 also seems to be ubiquitinated, albeit to a much lesser extent. (B) Shown is an immunoblot of IP WT-FZD4, P33S, G36D, H69Y, M105T, C204Y, C204R, and G488D with anti-FLAG antibody before stripping for polyubiquitination studies. (C) Quantification of the polyubiquitination blot presented above is shown. Considerably higher levels of ubiquitination are observed for the mutants compared with WT. A negative IP is presented for comparison. Quantification was carried out by Typhoon FLA 9500 ImageQuant TL software (GE Healthcare Life Sciences).

Different compounds have been shown to rescue folding of mutant proteins [35, 157, 162]. The IF pattern of M105T and C204R mutants when cultured in the presence of 7.5% glycerol showed escape from ER retention by approximately 50% and 32%, respectively (Figure 4.1.9B–E). This observation indicates that glycerol enhances protein processing and exits mutant protein from the ER to the cell surface, although its trafficking is expected to be slower than WT.

In addition, M105T and C204Y mutants were treated with 0.1% DMSO (Figure 4.1.9C), 10 µM thapsigargin, or 1 µM curcumin (data not shown). The M105T mutant showed partial PM distribution when treated with 0.1% DMSO by approximately 32% (Figure 4.1.9D, E). C204Y showed a lower pattern of rescue to the PM compared with M105T (Figure 4.1.9D, E). Both M105T and C204Y showed no rescue at differing concentrations with either thapsigargin or curcumin. The other ER-retained mutants showed no rescue to the PM with any of the treatments examined.

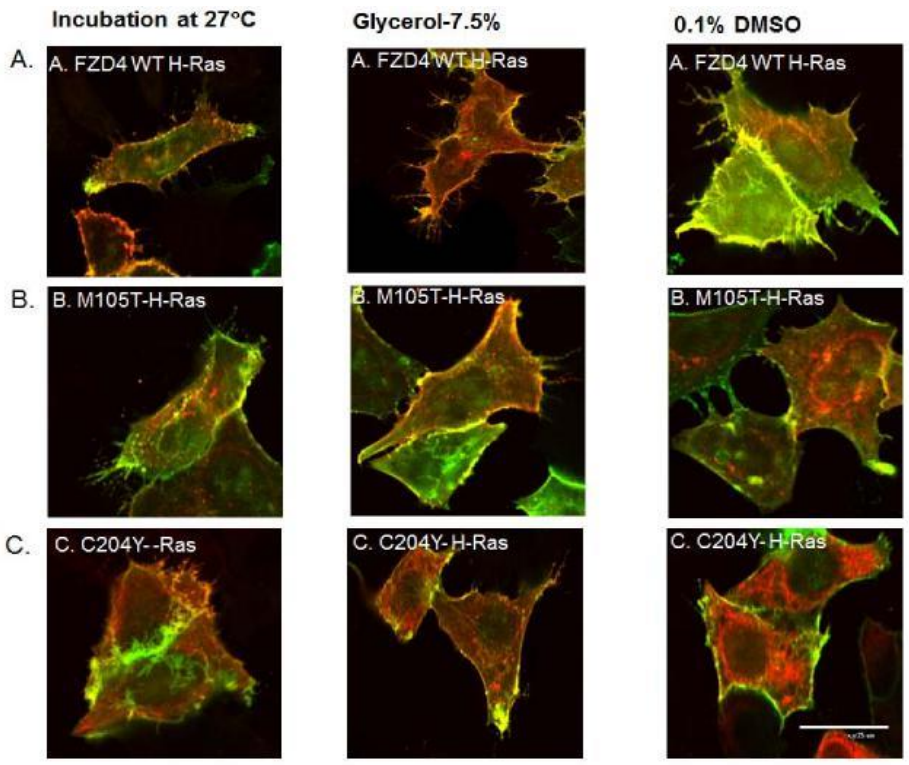


Figure 4.1.9. Effect of low-temperature incubation and chemical chaperones on M105T and C204Y localization. (A) Shown are CFM images of reduced temperature and chemical compound incubation of WT-FZD4 acting as a control. In panels (B) and (C), the presented CFM images are of M105T and C204Y mutants across the three treatments (culturing at 27 $^{o}$C, 7.5% glycerol, and 0.1% DMSO, respectively).

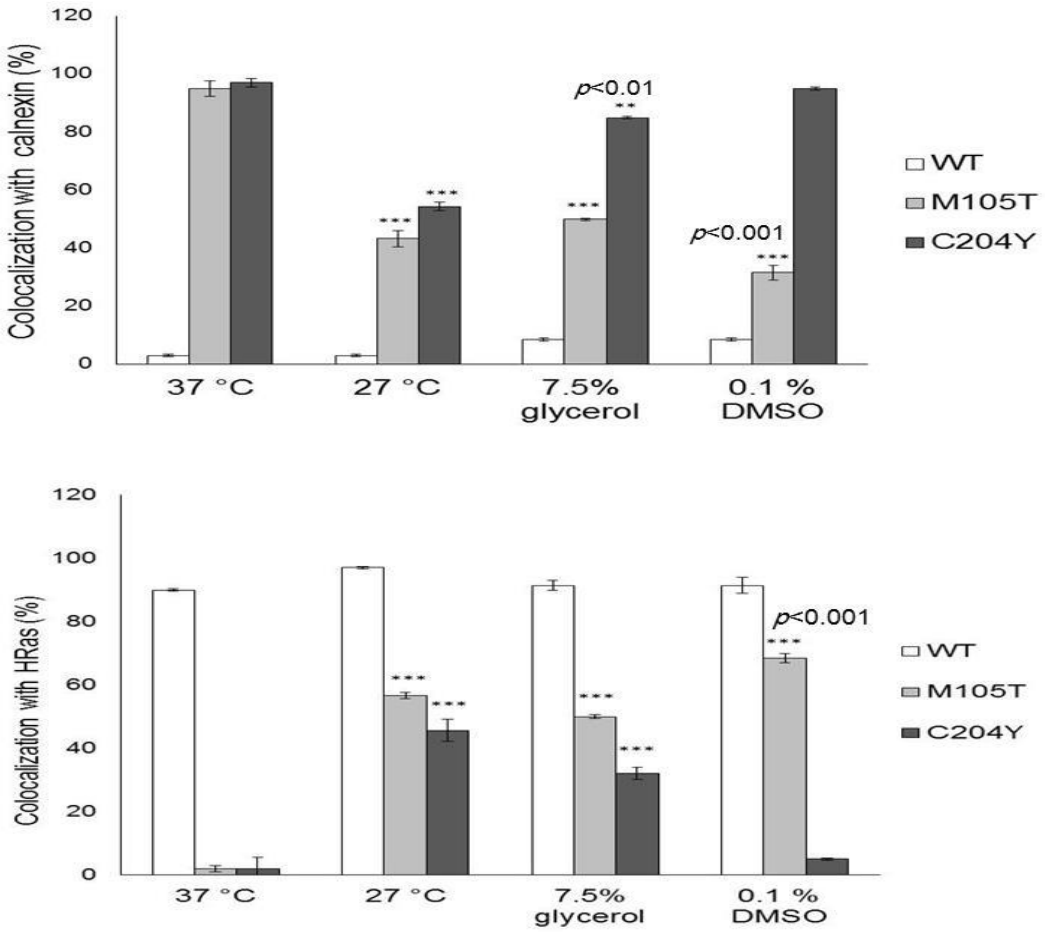


Figure 4.1.10. Quantification of colocalization, using ImageJ version 1.47, with the ER marker calnexin (above) and the PM marker H-Ras (below), expressed as a percent from the IF pattern of the expressed FZD4 proteins. At 27 $^{o}$C, WT colocalized with the ER marker by approximately 3% only, whereas M105T and C204Y colocalized by 43% and C204Y by 54%. With 7.5% glycerol, M105T colocalized by 50% and C204Y by 85%. With 0.1% DMSO, M105T colocalized with calnexin by 32% and C204Y by 95%. Colocalization with calnexin was measured as a function of and then compared with WT on multiple CFM image sections of at least 50 cells in three independent experiments (mean ± SE of each experiment). Shown is quantification of the amount of FZD4 proteins colocalizing with H-Ras, a PM marker. At 27 ºC, M105T and C204Y colocalized by 57% and 46%, respectively, whereas in the presence of 7.5% glycerol, M105T colocalized by 50% and C204Y by 32%. The M105T mutant showed partial plasma membrane distribution when treated with 0.1% DMSO by approximately 68% and C204Y by approximately 5%. One microgram WT-FZD4 or the mutant constructs was used for transfection experiments. For coexpression studies, 1 µg of each construct was cotransfected together. Colocalization with H-Ras was measured as a function of and then compared with WT on multiple CFM image sections of at least 50 cells in three independent experiments. Scale bar: 25 µm. Data (arbitrary units) are expressed as the mean (SE). ***P < 0.001.

#### 4.1.2.5 Dominant-negative effect of FZD4 ER-retained mutants negated

FZD4 proteins have been shown to homodimerize in the ER. The ER-retained disease-causing mutants could possibly dimerize with the WT-FZD4 protein and trap it in the ER and hence cause a dominant negative effect. The disease is inherited as an autosomal dominant manner and this could be the underlying cellular mechanism of disease for at least some of these mutants as the Kaykas group had suggested [20].

Therefore, I wanted to examine the possible dominant-negative effects of the mutant proteins on WT-FZD4. To be able to differentiate between the WT-FZD4 and the mutants, the WT-FZD4 was tagged with an HA epitope as described in the methodology section 3.3.1., whereas the different mutants are FLAG-tagged as described. The WT-FZD4 cDNA was co-expressed in 1:3 ratios with the following individual ER-retained mutants (P33S, G36D, H69Y, C181R, M105T, M105V, C204R, C204Y and G488D) and the localization of the WT-FZD4 was assessed by CFM.

Co-expression of WT-FZD4 with individual ER-retained mutants failed to show the retention of WT protein in the ER suggesting lack of dimerization with any of the mutants (Figure 4.1.11). Wild-type protein was expressed as usual on the plasma membrane when co-expressed with the mutants (Figure 4.1.11). Therefore, we can conclude that the ER-retained mutants studied do not trap WT within the ER and hence have no dominant-negative effects. In addition, IP of the mutant proteins failed to pull down WT-FZD4 (Figure 4.1.12). This implies that the mutant proteins may adopt conformations that do not allow dimerization with WT or that it is sequestered somehow away from WT. These data suggest that WT function might not be affected by the co-expression of the mutant alleles studied.

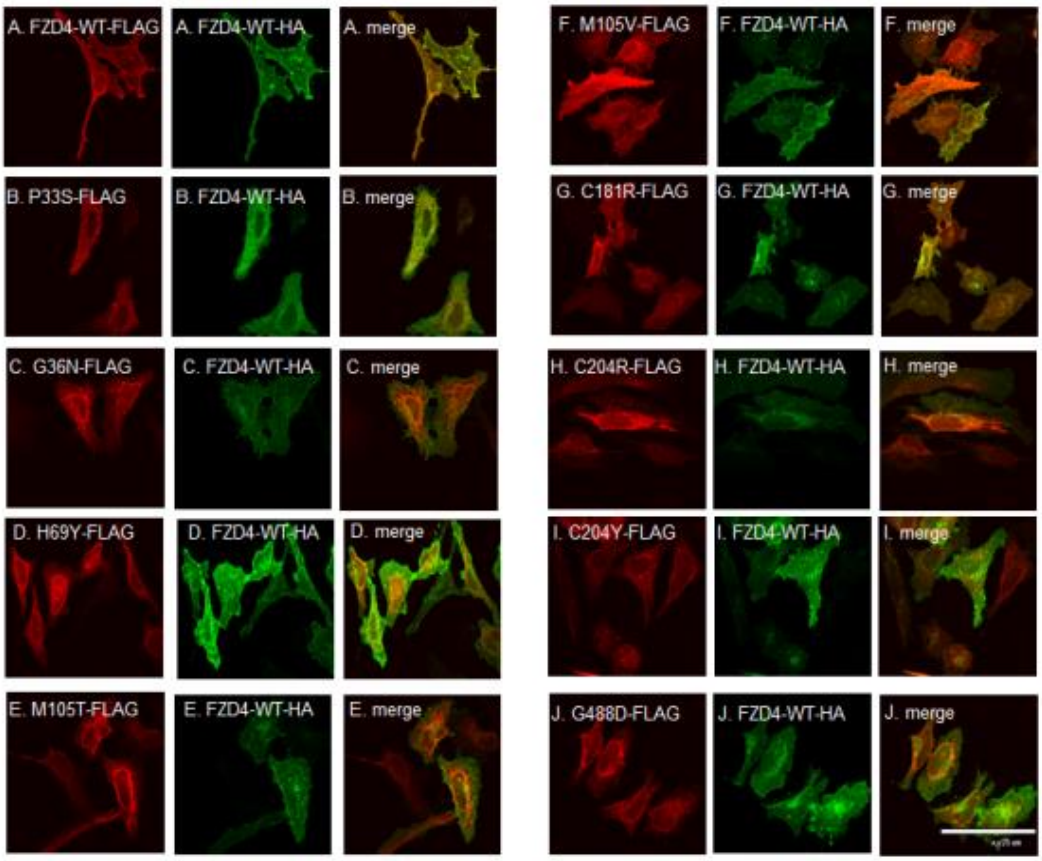


Figure 4.1.11. Absence of dominant negative effect of ER retained FZD4 mutants on WT-FZD4 protein. HeLa cells were co-transfected with WT-FZD4-HA and the individual ER retained FLAG-tagged mutants in a DNA amount ratio of 1:3 and cultured for 48 hours. The FZD4-WT was probed with polyclonal rabbit anti-HA antibodies (green) whereas the ER-retained mutants were probed with mouse anti-FLAG polyclonal antibodies (red). The FZD4-WT localized normally to the plasma membrane in all panels B-J in similar fashion to the wild-type FZD4 shown in panel A. Colocalization function on multiple confocal sections of at least 30 cells in three independent experiments revealed that approximately 3% of the wild-type co-localized with the mutants. All images were taken by a confocal microscope and overlayed using Image J 1.47v. All images presented are single sections in the z-plane. Scale bar = 25 µm; 100X objective lens.

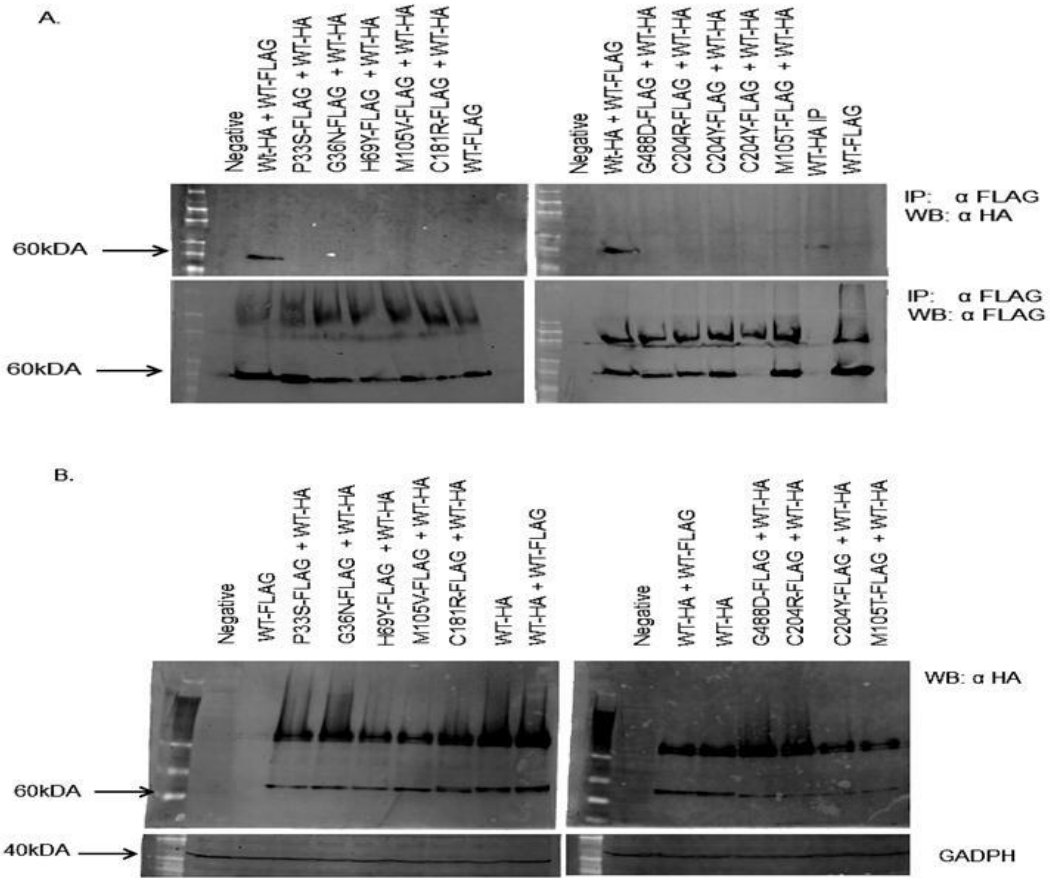


Figure 4.1.12. IP of the ER-retained mutants failed to co-IP the co-expressed WT protein. The wild-type FZD4 HA tagged and individually FLAG-tagged FZD4 mutants were co-expressed for 48 hours in HEK293T cells. The proteins were extracted and immunoprecipitated with anti-FLAG antibody. The samples were then run on an 8% SDS-PAGE gel and probed with anti-HA antibodies. Only the wild–type HA co-expressed with the wild-type FZD4 Flag tagged protein. This implies that they were able to homodimerize together and consequently precipitated together. The blots were stripped and re-probed with anti-FLAG antibodies. All IP proteins showed up on the blot. B. Whole cell lysates of the protein used for the IP experiments was run on an 8% SDS gel and stained with anti-HA as a control.

### 4.1.3 Discussion

Vascular diseases of the retina are a major cause of impaired vision and blindness. It has become evident that a large number of diseases with very different pathologies share a common framework of protein misfolding accompanied by degradation and/or aggregation of these misfolded proteins [1, 8]. Inherited diseases that harbor missense mutations may affect the folding or stability of proteins. For some of these types of mutant proteins, it might be possible to improve folding, stabilize the native structure, or suppress aggregation using chemical chaperones that mimic chaperone effects.

I have shown how several FEVR-causing mutations lead to the retention of the mutant proteins by stringent ER quality control machinery. The ER chaperones have been shown to detect misfolded proteins, unmodified or orphaned subunits of protein complexes and target them for degradation by ERAD [56, 105, 110, 112, 230]. My study shows that P33S, G36D, H69Y, M105T, C204R, C204Y, and G488D FZD4 mutants are exclusively retained in the ER. Interestingly, all these mutations are found in the extracellular portion of the protein except for the G488D mutation, which is found on the seventh transmembrane domain (Figure 4.1.1).

A closer look at each mutation's physicochemical properties and PolyPhen-2 (http://genetics.bwh.harvard.edu/pph2/ [in the public domain]) and SIFT (http://sift.jcvi.org/ [in the public domain]) server predictions sheds light on the predicted effects of some of the mutations on FZD4 protein (Table 4.1.1). For example, the P33S mutation is expected to cause inefficient or no cleavage of the signal peptide; therefore, the P33S mutant is likely to be stuck on the ER membrane. On the other hand, the C204R and C204Y mutations result in the disruption of a vital cysteine disulfide bonds. Smallwood et al. [214] have shown that the binding of Norrin to the CRD domain of FZD4 extends beyond the CRD's 114 amino acids to include residue C204. Any effect beyond the CRD on Norrin binding is likely to represent just an effect

on FZD4 folding and not direct contact with Norrin. Zhang et al. [211] demonstrated how the C204R mutation fails to bind Norrin. The retention of both of these proteins in the ER may explain the inability of the protein to bind to its ligand. The glycine at position 488 is also highly conserved in orthologs and paralogs [210], and the change to an aspartic acid is expected to be deleterious.

Table 4.1.1. Summary of the physicochemical properties of the FEVR-causing FZD4 mutations shown in this study to be mislocalized to the ER

| Mutation | PolyPhen2 | SIFT | Charge | Polarity | Hydrophobicity | Size | Score |
|---|---|---|---|---|---|---|---|
| P33S | None | 0.47, T | Equal | Increase | Increase | Decrease | 23 |
| G36D | 0.004, N | 0.62, T | Equal | Increase | Decrease | Increase | 32 |
| H69Y | 0.029, N | 0.08, T | Decrease | Equal | Increase | Equal | 49 |
| M105T | 0.997, D | 0.47, T | Equal | Increase | Decrease | Decrease | 32 |
| M105V | 0.66, T | 0.93, D | Equal | Equal | Equal | Decrease | 16 |
| C181R | 0.033, N | 0.52, T | Increase | Increase | Decrease | Increase | 77 |
| C204R | 1, D | 0.02, D | Increase | Increase | Decrease | Increase | 77 |
| C204Y | 1, D | 0.04, D | Equal | Increase | Equal | Increase | 85 |
| G488D | 0.06, T | 1, D | Increase | Increase | Decrease | Increase | 28 |

The modification score (INSTRUCT/CBI Knowledgebase; http://decrypthon.igbmc.fr/sm2ph/cgi-bin/home [in the public domain]) correlates with the severity of the change at the specified position. P33S is found within the signal peptide (SignalP 4.1 Server; http://www.cbs.dtu.dk/ services/SignalP/ [in the public domain]).[231] N, neutral; T, tolerated; D, deleterious change on the protein.

Interestingly, the M105V and C181R mutations showed dual patterns of localization (Figure 4.1.2F, G, Figure 4.1.3F, G). This partial ER retention behavior has been reported for other cysteine missense mutations [232]. The location of M105V and C181R is significant because they are within the CRD of the FZD4 extracellular domain and are highly conserved in other species.

P33S and G488D show mainly dimers, multimers, and oligomers on an SDS-PAGE gel, which has been previously observed with FZD4 protein (Figure 4.1.7 [20, 224, 225]). In addition, heating of FZD4 protein has been reported to cause the formation of aggregates [224], which was observed in the current experiments.

Interestingly, the mutations found to traffic abnormally are mainly found in the extracellular domain of FZD4, where the CRD region is located (Figure 4.1.1). The CRDs of frizzled proteins have been shown to form homo-oligomers and/or hetero-oligomers within the ER [19, 20]. ERAD results in loss of function of the mutant protein as a result of being degraded before reaching its final destination. Frizzled family receptor 4 proteins dimerize in the ER, and Norrin dimers have been shown to interact with FZD4 dimers [234].

Therefore, I wanted to examine the possible dominant-negative effects of the mutant proteins on WT-FZD4. However, coexpression of WT-FZD4 with individual ER-retained mutants failed to show the retention of WT protein in the ER or its dimerization with any of the mutants (Figure 4.1.11). Wild-type protein was expressed as usual on the plasma membrane when coexpressed with the mutants (Figure 4.1.11). Therefore, I can conclude that the studied ER-retained mutants do not trap WT within the ER and hence have no dominant-negative effects. In addition, IP of the mutant proteins failed to pull down WT-FZD4 (Figure 4.1.12). This implies that the mutant protein may adopt conformations that do not allow dimerization with WT. This may also be due to aggregation of these proteins. These data suggest that WT function might not be affected by the coexpression of a mutant allele. A reported hemizygous mutation has shown haploinsufficiency and therefore loss-of-function of FZD4 as the underlying disease mechanism [218]. My data support the haploinsufficiency theory for this disease [218].

All but one mutation are found in the heterozygous state. It is likely that the phenotypic variability observed in heterozygous individuals within the same family

may result from the effects of modifier genes alongside an alteration in the gene dosage, resulting in allelic insufficiency. The ER retention for reported compound heterozygote patients carrying two different mutations (H69Y and G488D [210]) can explain why a more severe phenotype is observed compared with single heterozygous mutations. This data further illustrate the complexity of FEVR and provide a better understanding of the genotype-phenotype correlations for some mutants.

M105V patients have been reported to show retinal folds, macular ectopia, peripheral non-perfusion, retinal exudates, retinal vascular tortuosity, retinal degeneration and holes [233]. Patients with the M105T had bilateral retinal detachment and partial and /or complete blindness at a very young age [220]. Therefore, the phenotype of the M105T mutation is more severe than the M105T and this may be due to the slow trafficking of the M105V to the cell surface. Interestingly, the M105T has an extreme phenotype at a young age. Our results also show this mutation to be rescued to the cell-surface. This data needs to be further investigated to allow for therapeutic options for patients harboring this mutation in FZD4. However, the exact effects of the studied mutants on retinal vascularization and angiogenesis remain to be fully established.

In addition, the non-ER-retained mutants could cause FEVR by forcing FZD4 to take up conformations that do not permit binding to its ligands or downstream targets. For example, Norrin, a cysteine knot protein and a ligand of FZD4, shows wide variation in the arrangement of monomers within the dimer and the surfaces that interact with receptors or other binding proteins [214, 234]. This may also affect ligand specificity. Interestingly, dimerization of frizzled is emerging as a possible mechanism for transduction specificity [235].

An essential outcome of ubiquitination is targeting to the 26S proteasome, a specific signal that is responsible for the degradation of many cellular proteins,

including numerous ER-retained proteins upon export from the ER to cytosol [110, 111]. Most proteasome substrates are tagged not by a single Ub (monoUb) but by a polyubiquitin (polyUb) chain (PUC). It is generally thought that PUC's longer than four Ub molecules are the preferred signal for efficient recognition and degradation by 26S proteasomes [236]. The FZD4 polyubiquitination pattern is that of a polyUb chain increasing the molecular weight of FZD4 to approximately 200 kDa (Figure 4.1.8). Once bound by proteasomes, substrate conjugates are deubiquitinated, unfolded, and subsequently degraded [8, 9]. Loss of function of FZD4 mutants caused by proteasomal degradation of the misfolded protein further reveals the mechanism of certain FZD4 mutations that cause retinal dysfunction.

Interestingly, incubation at lower temperatures of 27 to 28°C [30] rescued the M105T mutant and partially rescued the C204Y mutant, as is observed with previous studies on CFTR [30, 32]. Glycerol, a small synthetic chemical that acts as an osmolyte, increases the hydration layer and the strength of the intramolecular hydrophobic bonding of the protein in the ER, which consequently allows the free movement of proteins, so as to prevent aggregation [28]. DMSO acts by probably increasing protein synthesis of the mutant or by overwhelming the quality control system. Thapsigargin, an inhibitor of the ER sarco(endo)plasmic reticulum calcium adenosine triphosphatase calcium pump, has been shown to increase cytosolic calcium, resulting in enhanced rescue of mutant proteins [160]. Curcumin, a nontoxic natural constituent of turmeric spice affects the calcium adenosine triphosphatases [167] found on the ER plasma membrane by inhibiting their ability to maintain a high ER calcium level. This, in turn, affects the ability of ER molecular chaperones to target the misfolded protein for ERAD, hence allowing the mutant protein to exit the ER. It would be interesting to look into more compounds that will inevitably provide the groundwork for designing a pharmacological chaperone to further salvage these mutations from their trafficking defect.

The present work represents an initial step in delineating the cellular mechanisms underlying some FEVR-causing missense mutations. It supports efforts for rescuing trafficking of other missense mutations that cause human diseases. It will be of great interest to determine whether modulating this pathway could represent a therapeutic approach to human retinal vascular disease.

## 4.2 Muscle, Skeletal, Receptor Tyrosine Kinase (MuSK) gene causing Congenital Myasthenic Syndrome (CMS)

### 4.2.1 Introduction

Congenital Myasthenic Syndromes (CMSs), OMIM: 601296, is a group of heterogeneous hereditary diseases characterized by reduced acetylcholine receptor (AChR) clustering at the neuromuscular junction (NMJ). CMSs can be classified into pre-synaptic, synaptic and postsynaptic defects which can lead to a dysfunctional neuromuscular signal where altered phenotypes are observed with varying degrees of muscle weakness [237]. AChR clustering and postsynaptic differentiation is orchestrated by interactions of the proteoglycan agrin (AGRN), the co-receptor low density lipoprotein receptor-related protein 4 (LRP4), and the muscle, specific receptor tyrosine kinase (MuSK), docking protein 7 (DOK7) and rapsyn (RAPSN) as illustrated in Figure 4.2.1A.

Mutations in MUSK [238-241], among 18 known genes [242], have been identified to cause CMS. However, the cellular mechanism underlying MUSK-mediated CMS is not well understood [237]. Furthermore, heterozygous and/or homozygous mutations in MUSK result in varied levels of impaired neuromuscular transmission.

MuSK is a 97 kDA type 1, single pass tyrosine kinase receptor glycoprotein (Figure 4.2.1B) with an extracellular ectodomain containing three immunoglobulin (Ig)-like domains and a frizzled-like cysteine-rich domain (Fz-CRD) [243], a transmembrane-spanning region and an intracellular region including a juxtamembrane domain, a kinase domain and a short C-terminal tail [244]. The Fz-CRD in proteins shows a pattern of 10 cysteine residues forming a five disulphide-bridged domain and forms a well conserved and folded three dimensional structure [21, 245]. MuSK contains a Fz-like CRD (Fz-CRD) homologous to the domain on Fz receptors to which Wnt binds [246, 247]. In this regard, MuSK is related to orphan

receptor tyrosine kinase (RTK)-like proteins such as orphan receptor tyrosine kinases 1 and 2 [243, 245] and the Frizzled Family Wnt receptors [247].

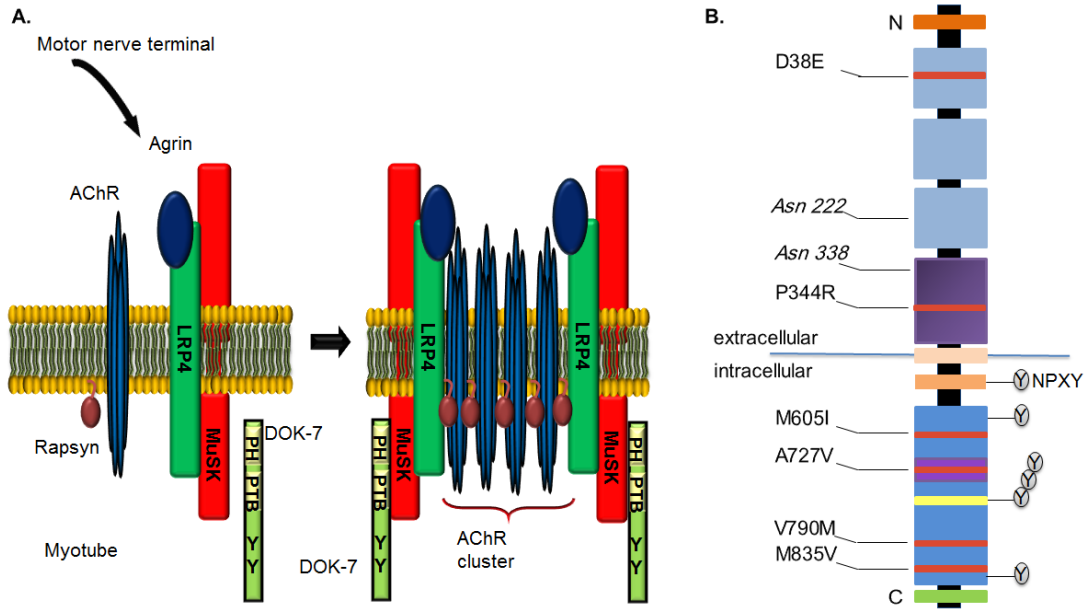


Figure 4.2.1 (A). MuSK is the key player in synaptic differentiation. Neural agrin stimulates synaptic differentiation by activating MuSK. LRP4 is a functional and obligate receptor for agrin, forms a complex with MuSK and mediates agrin-mediated MuSK activation. The N-terminal Ig-like domain in MuSK is essential for agrin to stimulate MuSK phosphorylation [21]. LRP4 self-associates and forms an agrin-independent complex with MuSK [248]. It has been proposed that agrin may alter the conformation of this preformed complex and MuSK is reoriented promoting trans-phosphorylation. However, the mechanism by which LRP4 transduces signals from neural agrin to MuSK remains unclear. DOK-7 binds to the intracellular portion of MuSK and AChR clustering at the NMJ. (B). Schematic representation of MuSK showing the position of missense mutations reported to date. Ig1-3, immunoglobulin-like domains highlighted in blue boxes extracellularly; CRD, cysteine-rich domain highlighted in purple; tyrosine kinase domain highlighted in blue intracellularly. The activation loop is highlighted in yellow attached to tyrosine residues. The NPXY domain is the PTB-domain binding motif; the PDZ domain binding motif is highlighted in green at the C terminal. The P344R mutation is found after the *N*-glycosylation sites: Asn222 and Asn338.

So far, six MuSK missense mutations have been reported in patients with CMS (Figure 4.2.1B) including D38E [249], P344R [240], M605I, A727V [239], V790M [238] and M835V [241]. The P344R mutation is found in the Fz-CRD domain and therefore we hypothesize that this mutation will result in the misfolding of the receptor and its handling by the ER quality control machinery. MuSK is a potential ERAD substrate because it has structural similarities with previously identified

ERAD substrates of the receptor tyrosine kinases family of proteins [18, 148, 149]. There is a high degree of conservation of the tyrosine kinase motifs and several mutations in the frizzled-related proteins have been shown to be retained in the ER [148, 250].

As detailed in the literature review chapter, the ER uses a stringent yet elaborate protein quality control system to ensure that only properly folded proteins are allowed to exit the ER to their final destinations [11, 126]. Remarkably, ER resident pro-molecular and molecular chaperones recognize misfolded polypeptides from their native counterparts [125]. A proportion of these ER-retained proteins are then targeted and dislodged from the ER, enter the cytosol where they get degraded by the ubiquitin/proteasome systems through ERAD [105].

For this study, I utilized subcellular localization, *N*-glycosylation profiling, and ubiquitination status to implicate ER retention as the major cellular mechanisms underlying the P344R-MuSK mutation. However, this intracellular mistrafficking is correctable when cells were grown at 27 ˚C instead of 37 ˚C and in the presence of glycerol, dimethyl sulfoxide (DMSO), curcumin and thapsigargin.

### 4.2.2 Results

#### 4.2.2.1 The P334R-MuSK mutant is largely localized within the ER in various cell lines

HeLa cells transiently transfected with the wild-type (WT) C-terminally FLAG-tagged MuSK cDNA show that the expressed protein is predominantly localized to the PM in contrast to calnexin, a well-established ER marker (Figure 4.2.2, panels A). Calnexin exhibits a typical perinuclear and reticular distribution suggestive of its ER distribution (Figure 4.2.2 middle Panels A). In contrast, the P344R-MuSK mutant was found to be predominantly localized to the ER as evidenced by its colocalization with calnexin (Figure 4.2.2, panels E). This mislocalization away from the plasma membrane in HeLa cells was further examined by its coexpression with EGFP-H-

Ras which localizes to the plasma membrane (Figure 4.2.2, compare panels B and F). The perinuclear and reticular distribution of the P344R-MuSK mutant is clearly distinct from that of EGFP H-Ras and thus further suggests its mislocalization to the ER. In addition, the localization of this mutant is clearly different from that of the wild type MuSK protein (compare panels A-B with E-F in Figure 4.2.2).

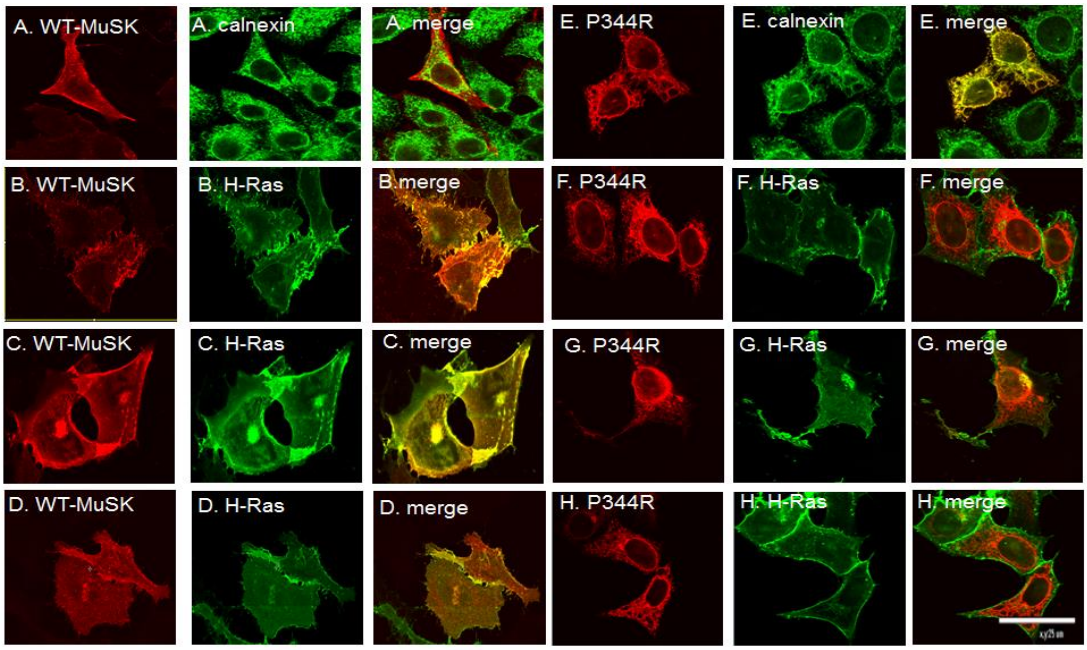


Figure 4.2.2. P344R-MuSK mutant localizes to the ER in HeLa, COS-7 and HEK293 cell lines. FLAG-tagged wild-type MuSK protein is seen as red fluorescence whereas calnexin and GFP-Ras as green signals as indicated. Panels A, B, C and D show WT-MuSK localizing to the plasma membrane away from calnexin (A) but with H-Ras (B, C and D) in HeLa (B), COS-7 (C) and HEK293T (D). On the other hand, the P344R-MuSK mutant localizes intracellularly with the ER marker (calnexin) in HeLa cells (F) and away from H-Ras in a HeLa cell line (F), COS-7 (G) and HEK293 (H) suggesting ER localization in all three cell lines. The scale bar represents 25µm and applies to all the panels.

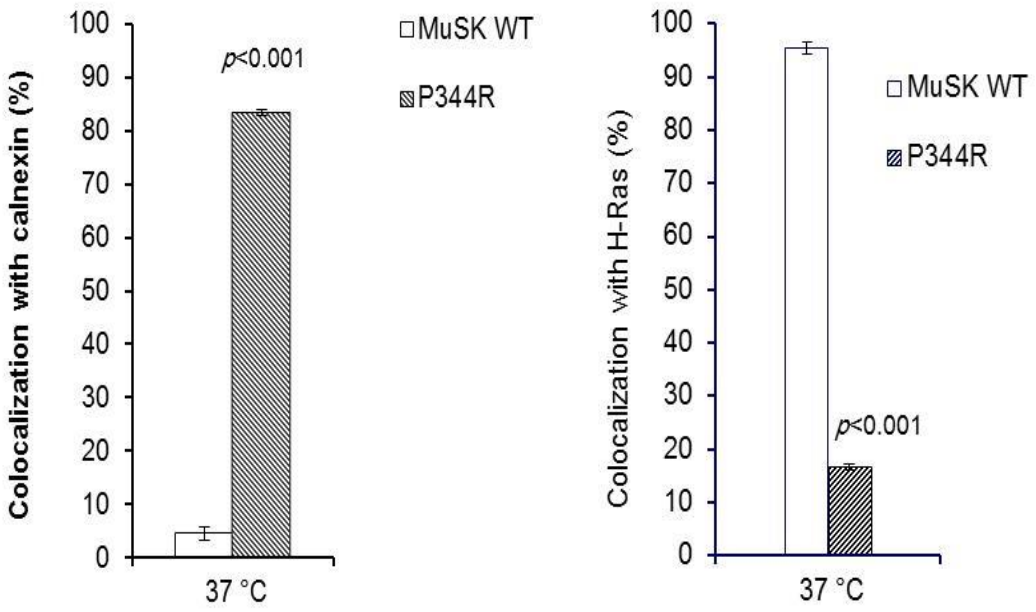


Figure 4.2.3. Colocalization with calnexin and with H-Ras was measured as a function using Fiji [204]. Colocalization was compared with WT on multiple image sections of at least 30 cells in three independent experiments. The p- values were determined by two-tailed Student's t-test when compared to the wild-type control. Statistical analysis by unpaired two-tailed Student's t-test analysis of Pearson correlation data for P344R-MuSK versus wild-type MuSK, confirms that a significant difference exists between the localization. Data (arbitrary units) are expressed as mean ± S.E. ***, Differences were considered statistically significant as follows: * = 0.01≤p<0.05; ** = 0.001≤p<0.01; *** = p<0.001 when compared to the wild-type control. Scale bar = 25 µm; 100X objective lens.

This mislocalization was verified in two other cell lines using EGFP H-Ras as a plasma membrane marker. In both COS-7 and HEK293 cells, WT MuSK colocalizes with this marker (Figure 4.2.2 panels C and D, respectively) whereas the P344R-MuSK mutant localized intracellularly away from EGFP H-Ras (Figure 4.2.2 panels G and H). These patterns of localization are suggestive of retention of the P344R-MuSK mutant within the ER and that this mislocalization is not cell line specific. The other five C-terminally FLAG-tagged missense CMS-causing mutants (D38E, M605I, A727V, V790M and M835V) were found to be largely localized to the PM, similar to wild type MuSK (Figure 4.2.4).

Quantification of the MuSK WT and / or the P344R-MuSK mutant colocalizing with either calnexin and or H-Ras in HeLa cells at 37 °C is shown in Figure 4.2.3.

This data shows that more than 85% of the mutant is colocalizing with the ER marker.

#### 4.2.2.2 Generation of HEK293 stable cell line for P344R-MuSK

The localization of P344R-MuSK prompted me to make a stable cell line of MuSK-WT, P344R-MuSK and the empty vector as described in the methodology section 3.2.9: Generation of HEK293 stable cell lines using the G418 selection marker. The MuSK-WT served as a positive control for all experiments and the empty vector as a negative control. Henceforth, all experiments were carried out on these stable cell lines which provided a genetically homogenous and single clonal population of P344R-MuSK expression. This would provide a more accurate assessment to chemical compound treatment and other applications. Figure 4.2.5; panels A-C shows a single clonal population for the protein expression of MuSK-WT stable cell line alongside P344R-MuSK and empty vector respectively using IF and panel D, shows the expression by western blot using GAPDH (E) as an internal control.

#### 4.2.2.3 The *N*-glycosylation profile of P344R-MuSK shows absence of the mature *N*-glycans and hence confirms ER retention

To further confirm the subcellular localization of P344R MuSK, PNGase and Endo H sensitivity and resistance *in vitro* assays of the expressed proteins were carried out. MuSK has two potential *N*-glycosylation sites in its extracellular domain [21] (Figure 4.2.1B). The principle of this assay is that the carbohydrate moieties of ER-localized glycoproteins are cleavable by Endo H whereas post-ER species are resistant due to further remodeling of their *N*-glycans in the Golgi complex. Endo H cleaves after the first asparagine-linked *N*-acetylglucosamine of high mannose and hybrid polysaccharides while PNGase removes both forms of the *N*-glycans. Therefore, one can expect that the ER-retained mutant will have its *N*-glycans cleavable when treated with the Endo H and PNGase enzymes suggesting its

presence within the ER. Upon this treatment, the P344R-MuSK mutant shows an exclusively Endo H susceptible protein with a lower molecular weight than the MuSK-WT and its untreated counterpart (Figure 4.2.6A) confirming its retention within the ER. It should be noted that the P344R-MuSK runs at a lower molecular weight compared to WT even before Endo H treatment implying an under-glycosylated and immature protein.

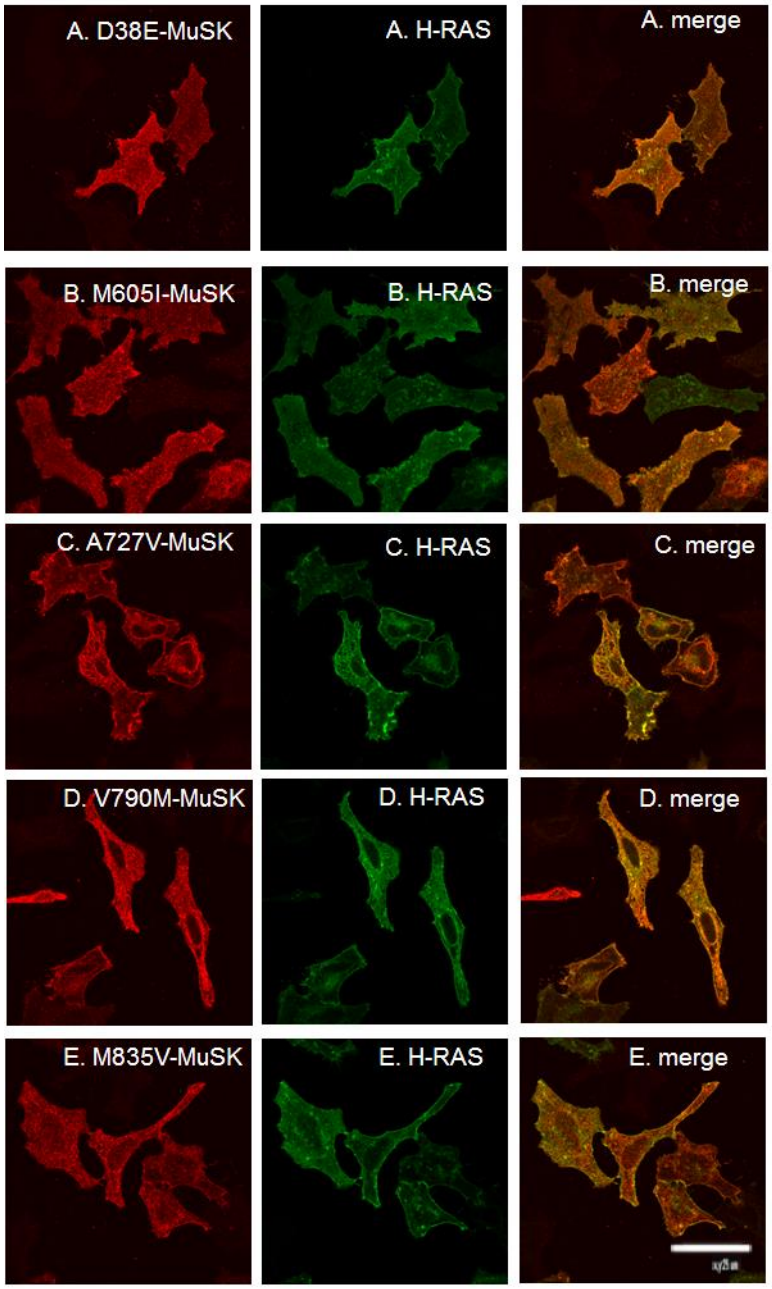


Figure 4.2.4. Confocal images of the missense disease causing mutants in a HeLa cell line. Confocal images of MuSK mutants: D38E, M605I, A727V, V790M and M835V showing their localization in HeLa cells alongside H-Ras, a plasma membrane marker. Flag epitope expressed protein is seen as red fluorescence (far left) under the confocal microscope and the plasma membrane resident protein H-Ras as green fluorescence (middle panel). When the two images are merged together, merge (far right) localization can be viewed clearly. Panels A-E clearly localize on the plasma membrane. Cells were transfected for 48 hours and then processed for IF. Scale bar = 25 μm; 40X objective lens.

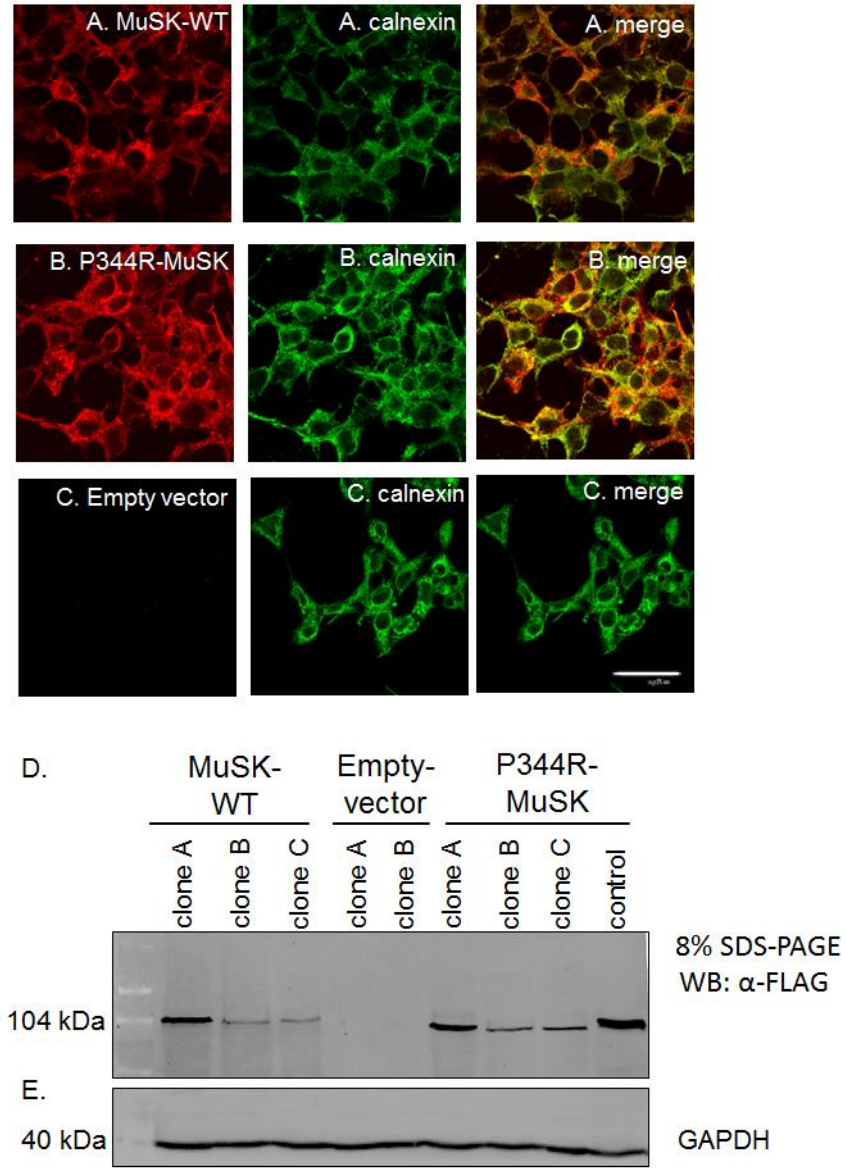


Figure 4.2.5. Stable cell lines of the MuSK-WT, P344R-MuSK and empty vector in HEK293 cell lines. HEK293 (A) MuSK-WT, (B) P344R-MuSK and (C) a negative empty vector control stable cell lines were generated as described in the methods and observed by CFM for protein expression. The (A) panel shows the single clonal protein expression stained with the FLAG epitope (red); the (B) panel shows the calnexin staining in green and the C panel shows the overlay of both the protein and the calnexin staining. (D) To verify protein expression, the clones were then run on an 8% SDS-PAGE to observe the strength of protein expression. (E) GAPDH was run as a loading control and to observe that the integrity of the ER was normal. The expression of clone A for both MuSK-WT and P344R-MuSK were chosen for subsequent experiments. Scale bar = 25 µm; 40X objective lens.

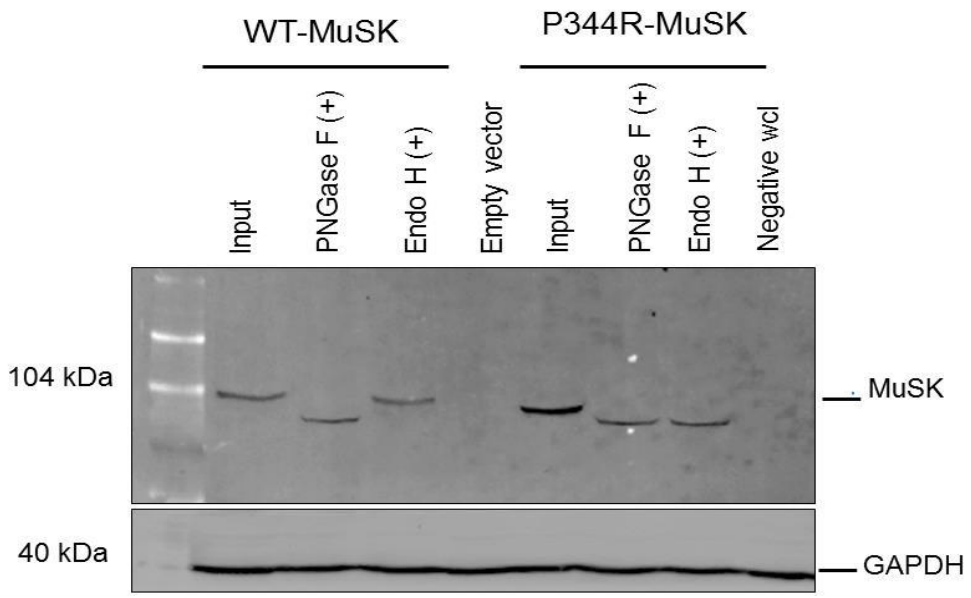


Figure 4.2.6. The *N*-glycosylation status of MuSK WT and P344R-MuSK mutant. (A) MuSK WT and P344R-MuSK stably expressing cell lines were subjected to Endo H and PNGase F sensitivity and resistance assays as described in the methods section. Untreated P344R-MuSK mutant was seen to migrate faster on an 8% SDS-PAGE gels compared to WT suggesting a folding defect or an immature protein (compare input in both cases). When treated with Endo H, the WT is resistant to this treatment whereas when treated with PNGase F, it migrated faster suggesting maturation of its *N*-glycans. In contrast the mutant migrated faster when treated with either Endo H or PNGase F suggesting immature *N*-glycans. (B). GAPDH blot was used as an internal loading control. This experiment was conducted in four times with similar results obtained in all instances.

#### 4.2.2.4 The P344R mutant retained its autophosphorylation activity

MuSK has an autoregulatory mechanism by which it can control its enzymatic activity through autophosphorylation of the kinase activation loop (A loop) [251]. Upon autophosphorylation, the kinase A loop adopts a conformation that is optimized for substrate binding. Autophosphorylation can also occur through the tyrosine kinase domain. Autophosphorylation of two tyrosines, Tyr-553 (NPXY) and A loop Tyr-754[251] shown in Figure 4.2.1; within the juxtamembrane segment relieves autoinhibition resulting in a fully active kinase. This autophosphorylation is important for further downstream signaling.

To examine the phosphorylation status, P344R-MuSK and MuSK-WT stably expressing cell lines were homogenized in a mild buffer to preserve cellular kinases. In addition, phosphatase inhibitors were added to preserve the phosphorylation status of the protein. The whole cell lysates were then immunopreciptated and run on an SDS page (Figure 4.2.7A). In Figure 4.2.7A, the proteins were stained with anti-phosphotyrosine (α PY) antibodies. In Figure 4.2.7B, the blot was stripped and re-probed with α FLAG antibody. Like the wild type MuSK, the P344R mutant is shown to be phosphorylated. The mutant protein may have retained about 50% of its enzymatic activity (Figure 4.2.7C). A kinase dead mutant (K609A) was used as a control for this experiment. This demonstrates that the phosphorylation is autophosphorylation in nature. This also implies that the mutation did not affect the kinase domain of the protein and therefore it may still retain significant biological function. Therefore, if the protein is restored to the plasma membrane upon exiting the ER, it may be able to interact in neuromuscular synaptogenesis.

#### 4.2.2.5 The trafficking defect of the P344R mutant is correctable by varying culturing conditions

Interestingly, ΔF508-CFTR has been shown to be exclusively retained in the ER as a result of misfolding and retention by ERAD. However, it has been demonstrated

that culturing cells expressing this mutant at reduced temperatures results in the restoration of some cell surface mutant expression, but crucially restoring the chloride-channel conductance activity of the CFTR [29, 30, 32, 165]. This data and others provides encouraging evidence that the ER retention and degradation machineries can be manipulated and therefore are potential therapeutic targets.

I therefore, examined the effect of reducing the culturing temperature on the trafficking of the P344R-MuSK mutant. The WT and P344R-MuSK constructs were co-transfected with the PM marker, EGFP-HRAS and cultured at 27 ˚C, and 37 ˚C for 24 hours and 48 hours. This was followed by confocal microscopy to establish the subcellular localization of the proteins. The subcellular localization of the wild type MuSK was not affected by culturing at the reduced temperature (Figure 4.2.8A). The P344R-MuSK mutant protein's localization to the plasma membrane was evident after 48 hours of culturing at 27 ºC (Figure 4.2.8B).

#### 4.2.2.6 Chemical chaperones rescued the trafficking defect of P344R-MuSK mutant

It has been established that some ER-retained temperature sensitive mutants can also be rescued when cells are cultured in the presence of chemical chaperones [28, 31]. Among these chemical chaperones are small synthetic chemicals such as glycerol, which act as osmolytes increasing the hydration layer, the strength of the intramolecular hydrophobic bonding of the protein, in the ER, which consequently allows the free movement of proteins, so as to prevent aggregation [28]. Quantification of the immunofluorescence pattern shows partial (~50%) rescue of the P344R mutant when treated with 2.5% glycerol (Figure 4.2.8; panels E and F). This observation indicates that glycerol allows the mutant to exit the ER and improves its appearance at the cell surface in a mature form (compare percent colocalization with calnexin compared to percent colocalization with H-Ras). P344R-MuSK mutant was also treated with 0.1% and 1% DMSO, 10 µm

thapsigargin or with 1 µM curcumin. P344R-MuSK mutant showed partial plasma membrane re-distribution when treated with these chemical chaperones especially with 10 µM thapsigargin (Figure 4.2.8A; MuSK WT and B; P344R). The MuSK WT was run as a control. Calnexin staining shown in Figure 4.2.8C with the vehicle alone and an empty vector with the vehicle is shown in Figure 4.2.8D.

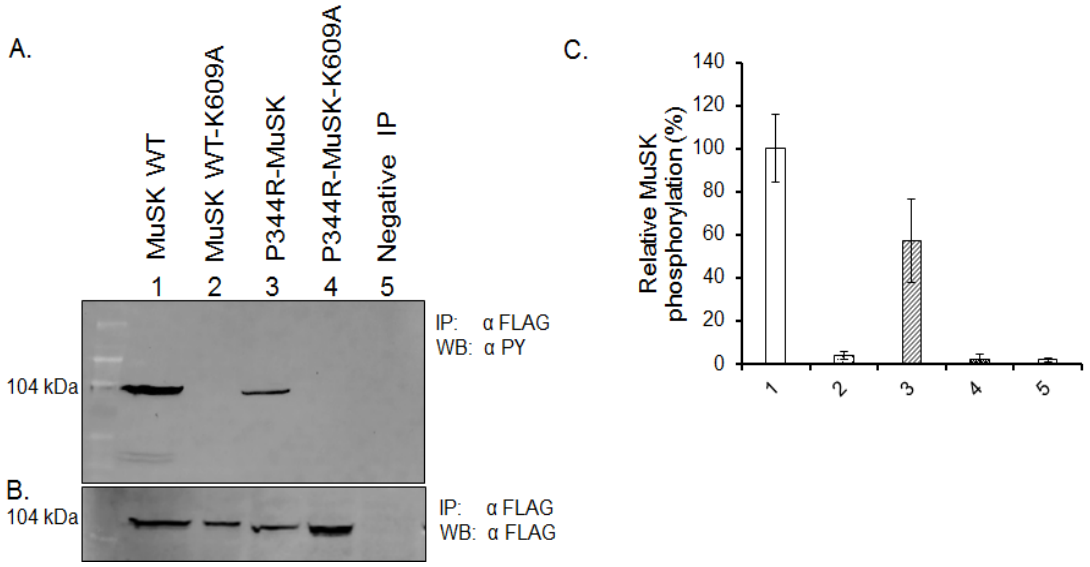


Figure 4.2.7. Effect of the P344R-MuSK mutation on MuSK autophosphorylation. HEK293 cells stably expressing WT MuSK or P344R-MuSK and empty vector constructs were subjected to IP and western blotting using anti-PY antibodies. Transiently transfected dead kinase K609A MuSK mutant (lane 2 and 4) and the empty vector construct (lane 5) were used as controls. Anti-PY antibodies were used for western blotting to detect the phosphorylated MUSK (A) then the blots were stripped and re-probed with anti-FLAG antibodies to determine levels of expression (B). Clearly, the MUSK WT (lane 1) is phosphorylated whereas the kinase dead mutants are not (lanes 2 and 4) suggesting autophosphorylation. The P344R seem to be also autophosphorylated by approximately 50% compared to the wild-type but not the double mutant P344R-K609A; lane 4. A representative experiment out of three realized is shown. MuSK amount and phosphorylation were then estimated with ImageQuantl J software. The introduction of the dead-kinase mutation in WT MuSK-K609A abolishes the autophosphorylation of MuSK WT and P344R seen in A (C) Phosphorylation is expressed as n-fold activation as compared to WT MuSK. Data are expressed as a percentage; and are the mean ± SE of three independent experiments.

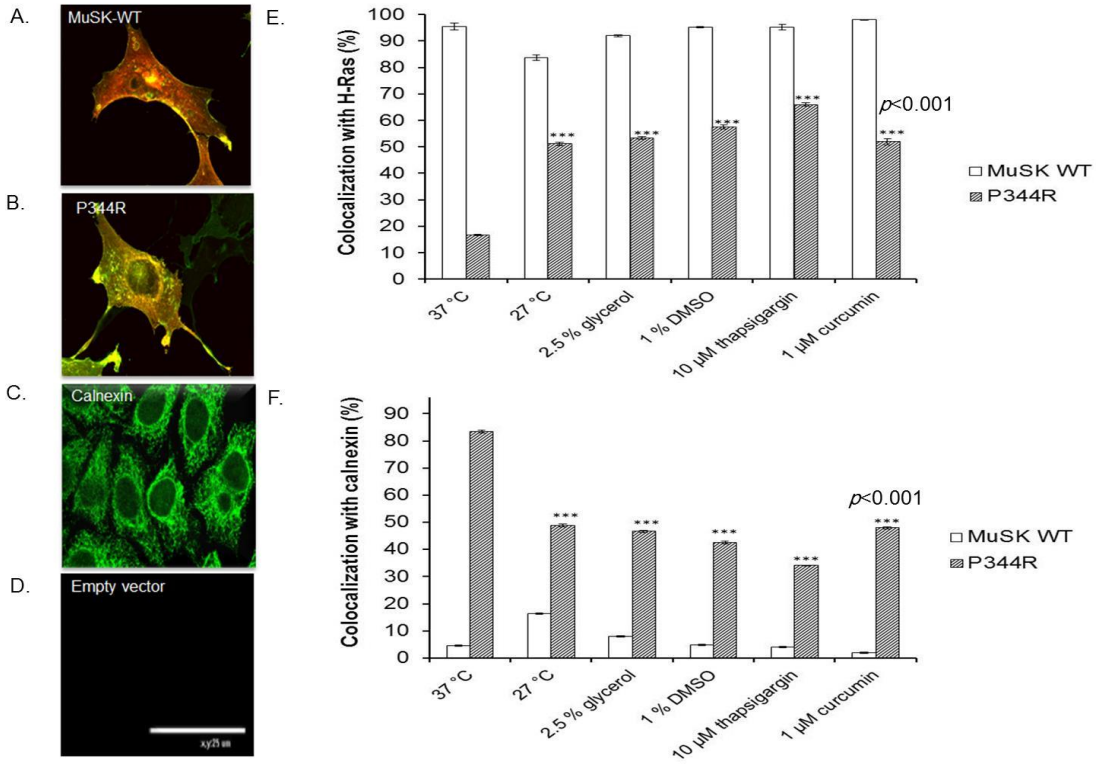


Figure 4.2.8. Different culturing temperatures for MuSK-WT and P344R-MuSK in HeLa cells using an EGFP-H-Ras PM marker. (A). Using merged MuSK WT with PM marker H-Ras as a control panel A, culturing conditions were varied with a reduced temperature of 27 ˚C for 48 hours; 2.5 % glycerol; 0.1-1 % DMSO and 1 µM-10 µM thapsigargin was not toxic to the cells and further modulated the P344R-MuSK mutant's rescue to the plasma membrane. (B). Merged P344R-MuSK with HRAS treated with 10 µM thapsigargin is represented. (C). P344R treated with 0.1% DMSO vehicle and (D). 0.1% DMSO with the empty vector. E. Colocalization with calnexin was measured as a function and then compared to the wild-type on multiple confocal images sections of at least 30 cells in three independent experiments. Data (arbitrary units) are expressed as mean ± S.E. when compared to the wild-type control. (F). Colocalization with H-Ras was measured as a function and then compared to the wild-type on multiple confocal images sections of at least 30 cells in three independent experiments (mean ± S.E.).Scale bar = 25 µm; 100X objective lens.

A western blot analysis pattern for the chemical chaperone treatment effect is seen in Figure 4.2.9. Stable transfected cell lines of P344R-MuSK were incubated for 4 hours with serum-free media. The concentration of chemical chaperone required was then added to a reduced serum-free medium and the cells were incubated for 7 hours. Proteins were then run on an 8% SDS-PAGE with GAPDH as an internal control. The P344R-MuSK mutant shows an increase in protein stability

compared to the non-treated P344R-MuSK. The wild-type was used as an experimental control and was seemingly unaffected by the chemical compound treatment (Figure 4.2.9A); with GAPDH as an internal control. Quantification of these blots is shown in Figure 4.2.9B indicating an increase in the mutant signals by about two fold with these treatments. Cell surface biotinylation shown in Figure 4.2.9 shows the amount of P344R-MuSK expressed on the cell surface compared to the untreated P344R-MuSK and MuSK-WT.

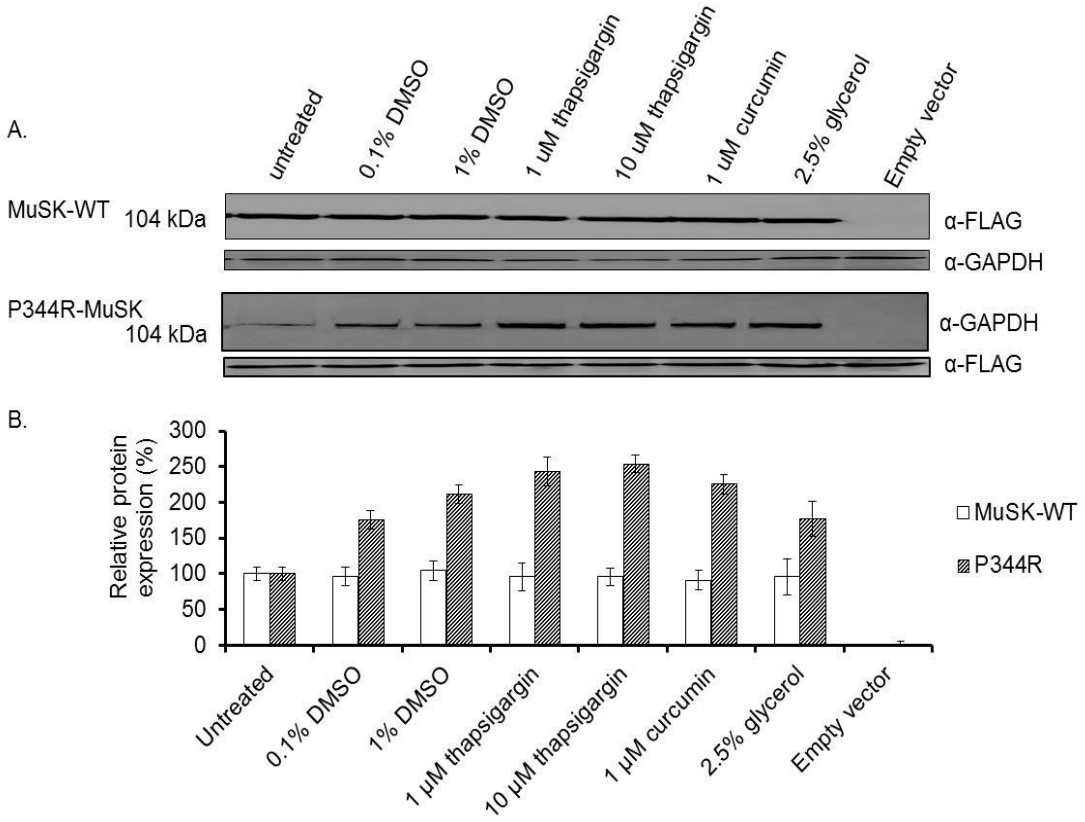


Figure 4.2.9. Effect of certain chemical chaperones on the maturation of P344R-MuSK mutation. Stable cell lines of HEK 293 cells expressing MuSK-WT and the P344R-MuSK mutant were incubated with serum-free media for 4 hours and then with the appropriate chemical compound for 7 hours in reduced serum-free media. The immunoblot (IB) was stained with anti-FLAG were antibody. (A) The wild-type MuSK seems unaffected by this treatment. The treated P344R-MuSK protein extracts show enhanced protein expression compared to the untreated P344R-MuSK counterpart. GAPDH is included as an internal control. 1% DMSO, 1 µM curcumin, 1 µM thapsigargin, 2.5% glycerol and 10 µM of thapsigargin show an enhanced protein processing compared to the untreated P344R-MuSK. (B) Quantification of the blots shows an increase in the stabilization of P344R-MuSK as compared to MuSK-WT under treatment.

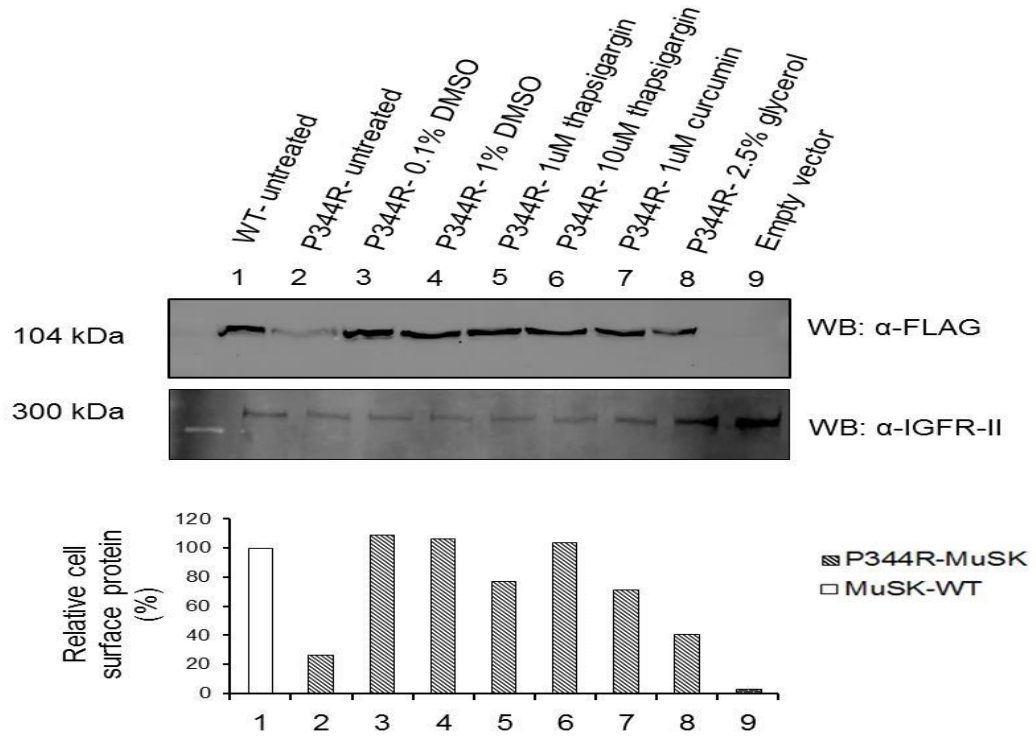


Figure 4.2.10. Western blot analysis of cell surface biotinylated fraction. The blot was then stripped and re-probed for IGF2R which served as a loading control. Relative MuSK protein levels were determined by ImageQuant TL and were normalized to IGF2R and displayed in a bar-chart. All samples with and without treatment were normalized to their own control. This experiment was conducted in duplicate with similar results obtained in both instances.

#### 4.2.2.7 MuSK protein degradation is mediated by the proteasome pathway

To test whether P344R-MuSK is actively degraded in cells, the stable cell lines were treated with cycloheximide (CHX), an inhibitor of protein synthesis. It has been previously shown that the MuSK is a short-lived protein [238]. As shown in Figure 4.2.11, MuSK-WT and P344R-MuSK levels declined quickly at short-interval time periods, and P344R-MuSK displayed a much shorter half-life than the MuSK-WT. Cells treated with the vehicle alone as a control (0.1% DMSO) were unaffected in both cell lines (Figure 4.2.14).

To determine whether P344R-MuSK degradation is mediated by the proteasomal pathway, the stable cell lines expressing P344R-MuSK mutant and MuSK-WT were treated with the proteasome inhibitor MG132. It was found that 90 minutes of treatment resulted in about a two-fold increase in P344R-MuSK protein (Figure 4.2.12). These data suggest that P344R-MuSK degradation is mediated through the proteasome-dependent pathway. Since the MuSK-WT protein is a short lived protein it was expected to increase in protein expression with MG132 treatment but not as drastically as the P344R-MuSK (Figure 4.2.12; MG132 graph).

It was then further investigated whether proteasome inhibition was indeed affecting the P344R-MuSK half-life. Stable cells were treated for different periods of time with CHX, in the presence of MG132 (Figure 4.2.13). In the presence of MG132, the P344R-MuSK mutant was as stabilized as the MuSK-WT (Figure 4.2.13; MG132 + CHX graph) confirming that P344R-MuSK is actively degraded by the proteasomal pathway in these cells.

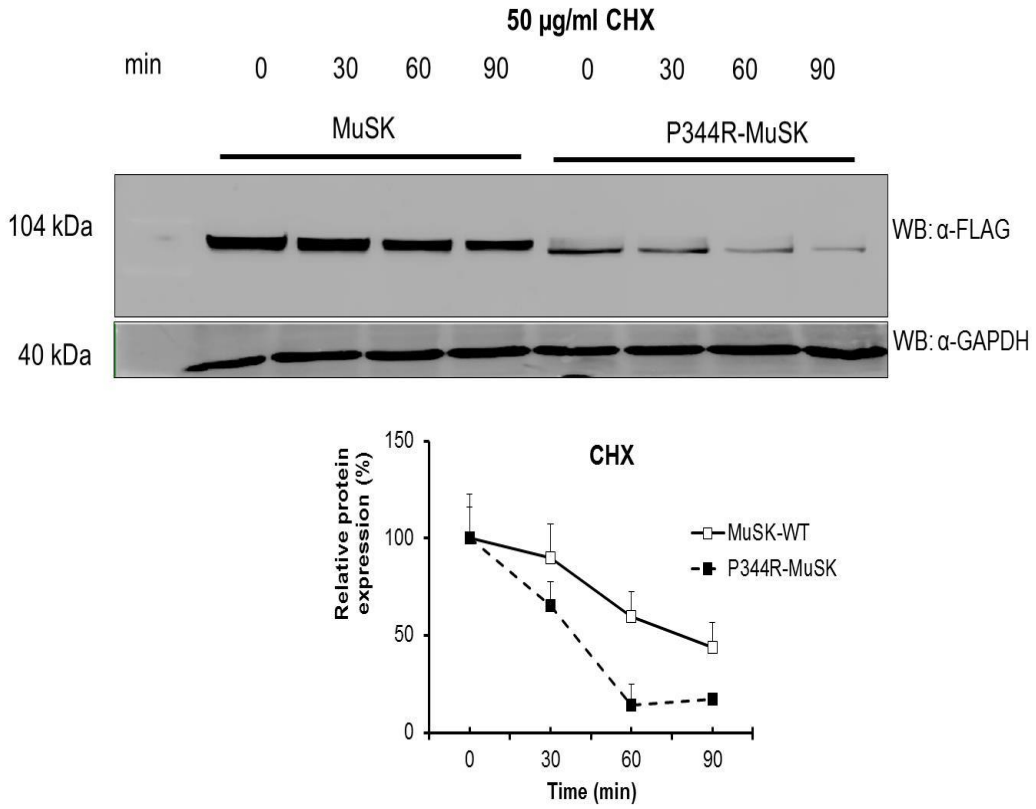


Figure 4.2.11. MuSK is a short-lived protein. MuSK and P344R-MuSK are rapidly degraded in the cell. Stably transfected MuSK-WT and P344R-MuSK HEK293 cells were incubated with 50 mg/ml cycloheximide (CHX) for the indicated periods. Western blots were performed on whole cell lysates using anti-FLAG. Relative MuSK protein levels were determined by ImageQuantl and were normalized to that obtained in nontreated samples (0 h control, no CHX). In the graph, samples with and without treatment were normalized to their own control (0 h, 100%) at the indicated time points. The mean ± SE of three independent experiments is shown.

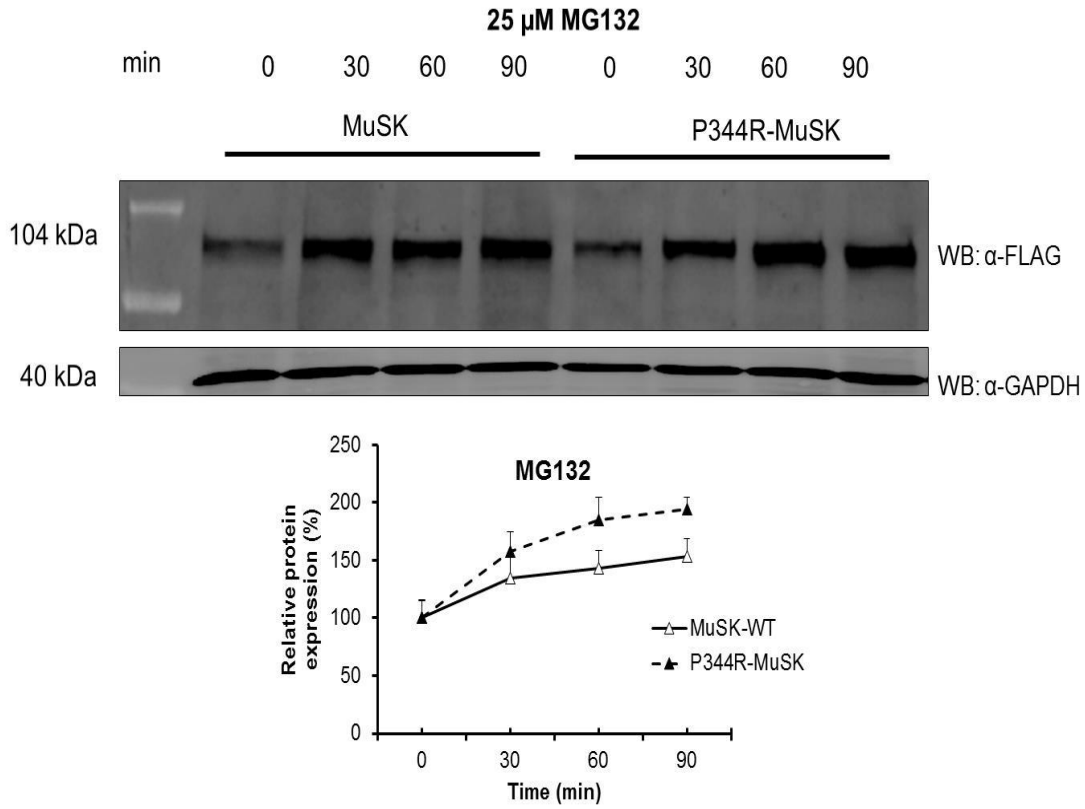


Figure 4.2.12. To observe the effects of the proteasomal inhibitor MG132 on MuSK and P344R-MuSK protein expression. Stably transfected MuSK-WT and P344R-MuSK HEK293 cells were incubated with 25 μM MG132 for the indicated periods. Western blots were performed on whole cell lysates using anti-FLAG. Relative MuSK protein levels were determined by ImageQuantl and were normalized to that obtained in nontreated samples (0 h control, no MG132). In the graph, samples with and without treatment were normalized to their own control (0 h, 100%) at the indicated time points. The mean ± SE of three independent experiments is shown.

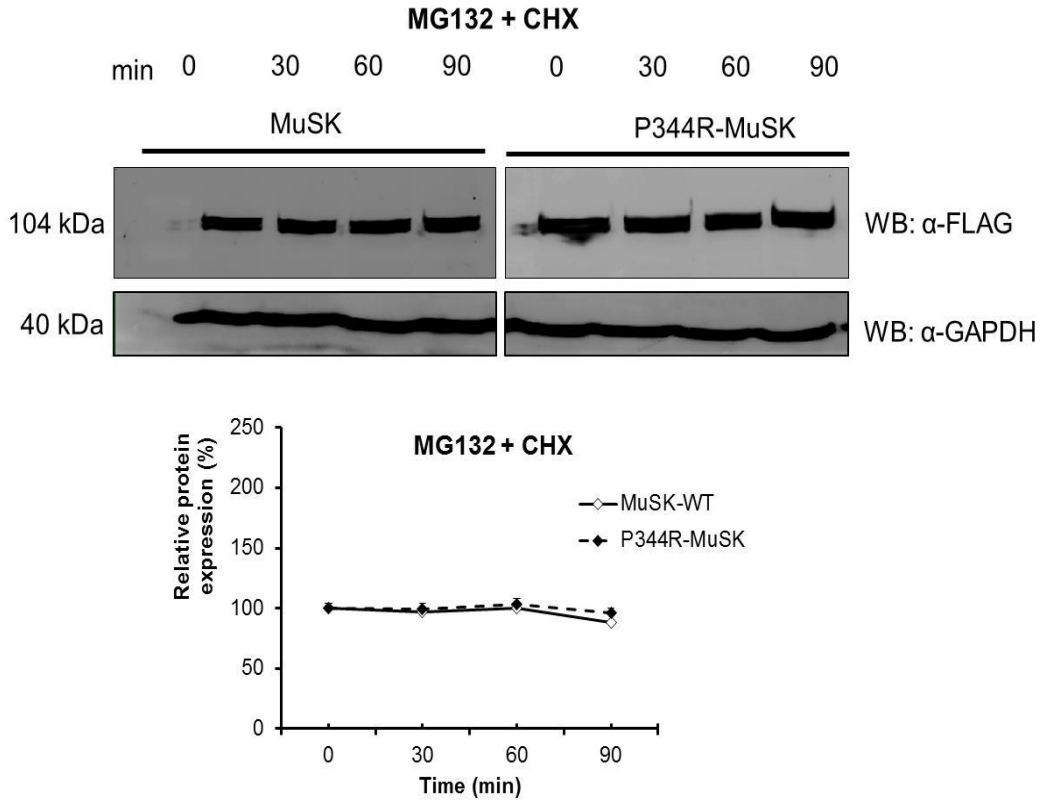


Figure 4.2.13. To observe the effects of both the proteasomal inhibitor MG132 and cycloheximide on MuSK and P344R-MuSK protein expression. Stably transfected MuSK-WT and P344R-MuSK HEK293 cells were incubated with 25 µM MG132 for one hour. CHX was then added at the indicated time points. Western blots were performed on whole cell lysates using anti-FLAG. Relative MuSK protein levels were determined by ImageQuantl and were normalized to that obtained in nontreated samples (0 h control, no MG132 + CHX). In the graph, samples with and without treatment were normalized to their own control (0 h, 100%) at the indicated time points. The mean ± SE of three independent experiments is shown.

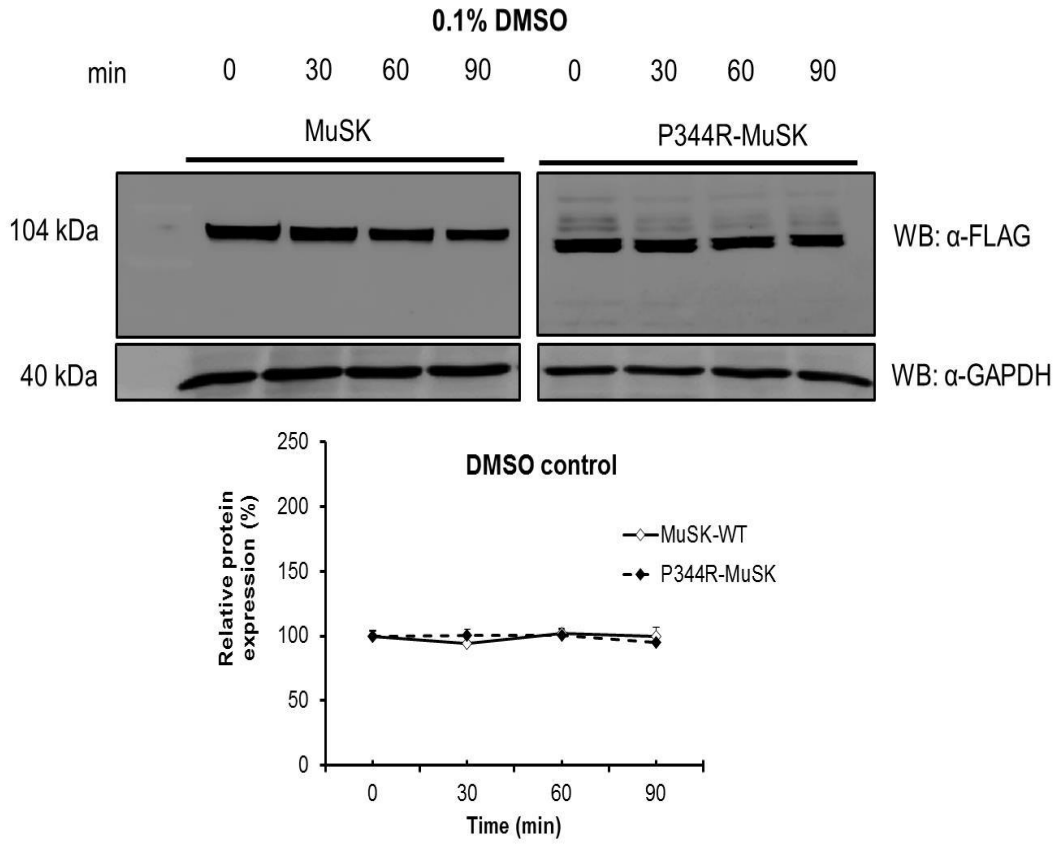


Figure 4.2.14. Incubation with DMSO control vehicle had no effect on MuSK and P344R-MuSK protein expression. Stably transfected MuSK-WT and P344R-MuSK HEK293 cells were incubated with 0.1% DMSO for the indicated time points. Western blots were performed on whole cell lysates using anti-FLAG. Relative MuSK protein levels were determined by ImageQuantl and were normalized to that obtained in nontreated samples (0 h control, no DMSO). In the graph, samples with and without treatment were normalized to their own control (0 h, 100%) at the indicated time points. The mean ± SE of three independent experiments is shown.

#### 4.2.2.8 The ER retained P344R-MuSK mutant is polyubiquitinated

To further verify if P344R-Musk is degraded by the proteasomal pathway. Stable cells of P344R-MuSK and MuSK-WT underwent separate treatments with MG132 and CHX at the various time periods highlighted earlier. The proteins were subjected to IP, run on an 8% SDS-PAGE gels and probed with anti-FLAG antibodies (Figure 4.2.15 and Figure 4.2.16 respectively), stripped and re-probed for anti-ubiquitin (Ub) as described in the methodology. Immunostaining by an anti-Ub antibody produced a striking accumulation of smears of multi-Ub-P344R-MuSK conjugates at the top of the resolving gel, in the presence of CHX (Figure 4.2.16) that was lower compared to MG132 treated samples (Figure 4.2.15).

These conjugates with multiple Ub moieties in the form of branched chains appear to be associated with the P344R-MuSK mutant very strongly compared to MuSK-WT. This is suggestive that the P344R-MuSK mutant is a target for degradation by the ERAD. To assess if the chemical compound treatments affected the ubiquitination of this mutant, the stable cell lines were treated with chemical chaperones and the proteins underwent IP (Figure 4.2.17), then were stripped and re-probed with anti-Ub. The blot shows higher level of conjugates of Ub-P344R-MuSK with anti-Ubiquitin antibodies staining for the P344R-MuSK mutant compared to the wild-type. The Ub moieties have a lower intensity smear pattern under treatment with chemical chaperones compared to the non-treated P344R-MuSK mutant.

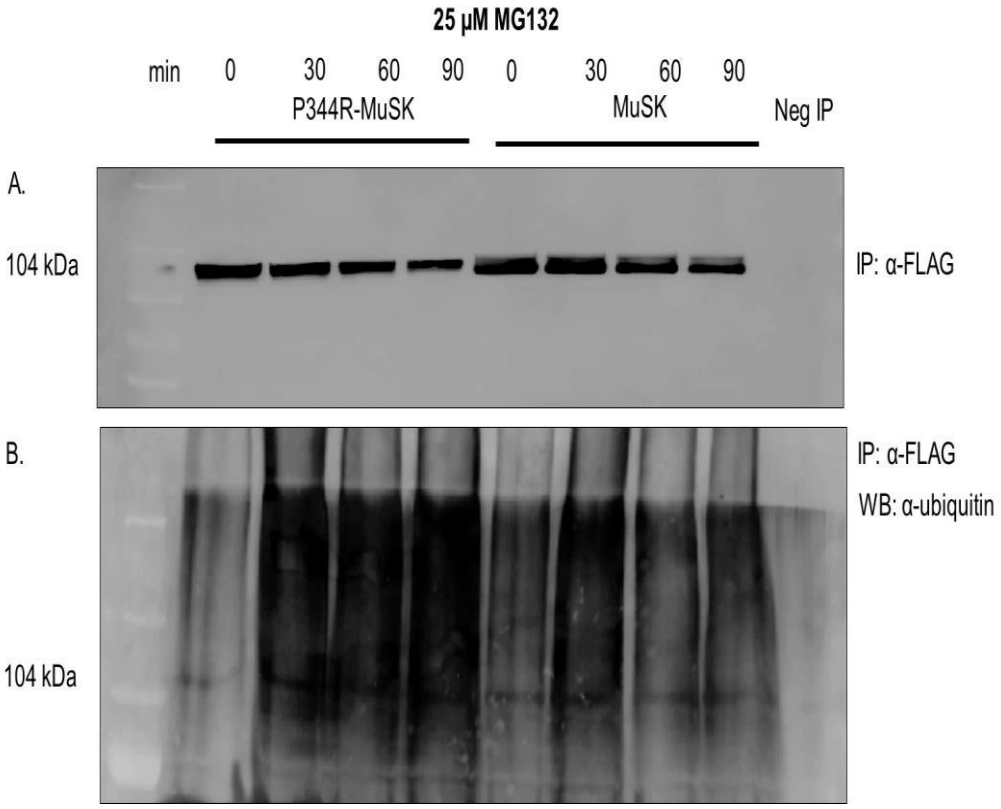


Figure 4.2.15. Polyubiquitination status of P344R MuSK mutant and MuSK wild-type under treatment. As a control for cycloheximide and MG132 treatment, MuSK-WT and P344R-MuSK were treated with 25 µM MG132 and then immunoprecipitated. The nitrocellulose blot was washed overnight with TBS-T, then stripped and autoclaved. The blot was then re-probed for anti-ubiquitin monoclonal antibody staining as described in the methods. The polyubiquitin smear is higher in P344R-MuSK compared to MuSK-WT under 25 µM MG132 proteasomal inhibition.

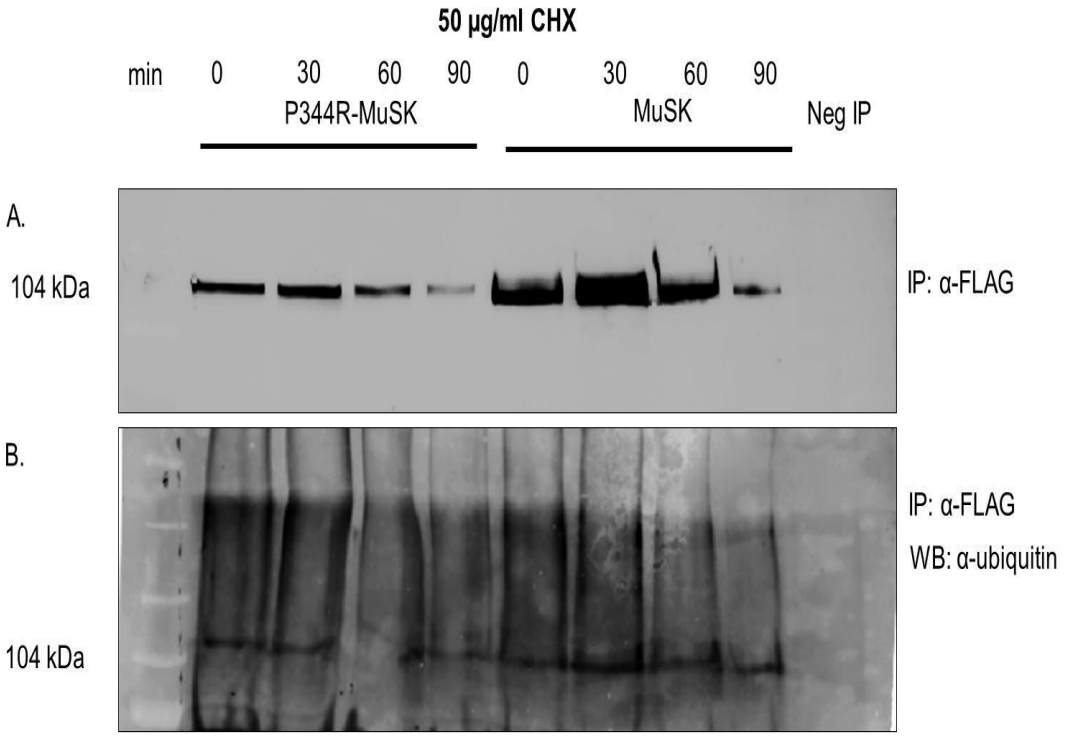


Figure 4.2.16. Polyubiquitination status of P344R MuSK mutant and MuSK wild-type under treatment. As a control for cycloheximide, MuSK-WT and P344R-MuSK were treated with 50 µg/ml CHX and then immunoprecipitated. The nitrocellulose blot was washed overnight with TBS-T, then stripped and autoclaved. The blot was then re-probed for anti-ubiquitin monoclonal antibody staining as described in the methods. The polyubiquitin status shows a decreasing smear compared in both MuSK-WT and P344R-MuSK indicating loss of protein translation.

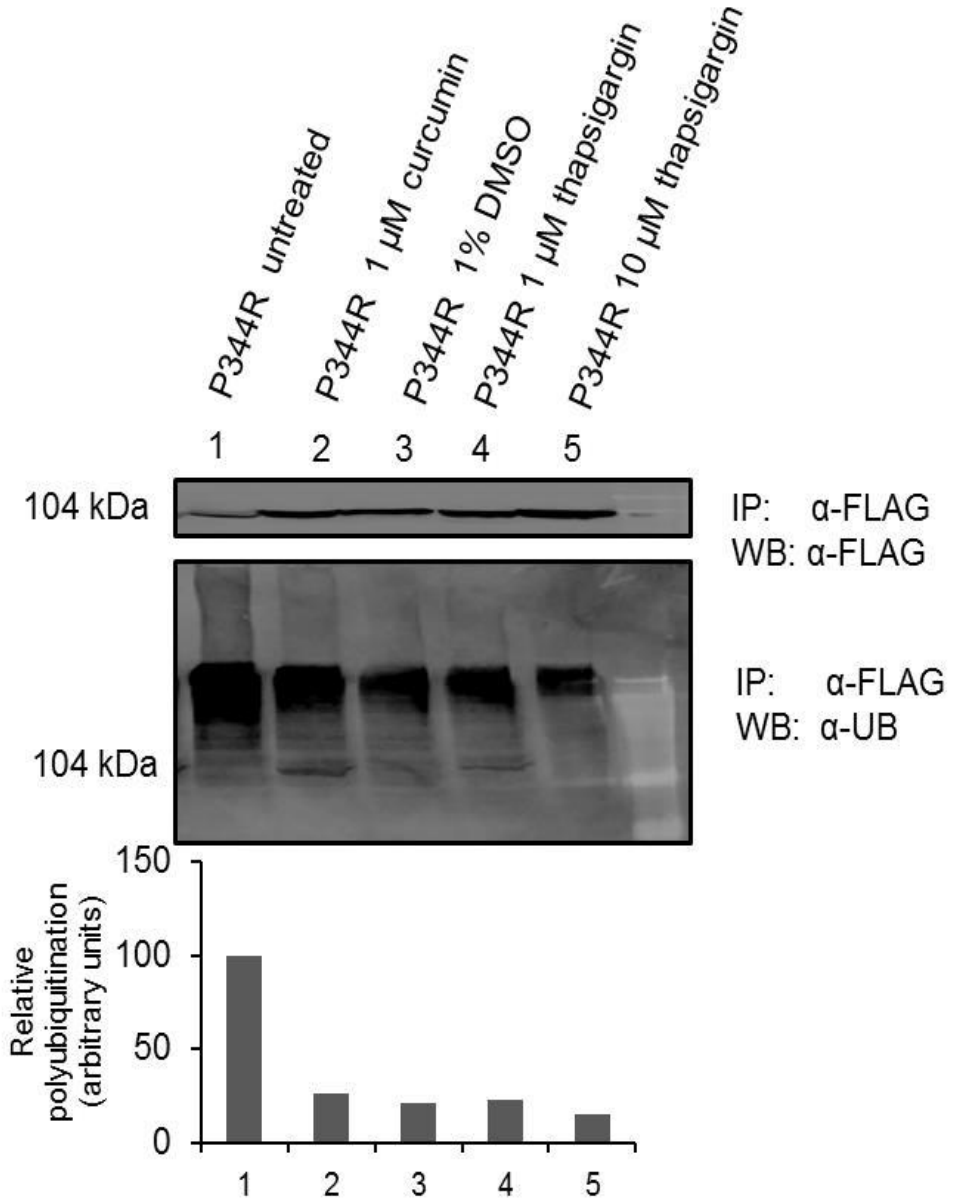


Figure 4.2.17. P334R-MuSK mutant was treated with chemical compounds and without chemical compounds run on an SDS-PAGE and blotted. The nitrocellulose blot was washed overnight with TBS-T, then stripped and autoclaved. The blot was then re-probed for anti-ubiquitin monoclonal antibody staining as described in the methods. Formation of ubiquitin (Ub) conjugates of the untreated P344R-MuSK mutant are of very high molecular weights, greater than the 280kDa top marker, in fact just resting at the top of the 8% resolving gel and at the end of the stacking gel. However, with 10 μm thapsigargin treatment, 1 μM curcumin and 1% DMSO (lanes 2-5), the poly-Ub conjugate “tree” smear is much less than the untreated P344R mutant counterpart. Quantification shows relative polyubiquitination of the polyubiquitin smear.

### 4.2.3 Discussion

Single point missense mutations in secretory proteins often produce molecules that are incapable of folding properly. These misfolded proteins may expose hydrophobic patches that are recognized by ER chaperones and so are deemed unsuitable to transit through the secretory pathway in this misfolded state. As a result they are initially retained in the ER then retrotranslocated back into the cytosol by the conserved ERAD machinery and passed on to the proteasome for disposal by degradation [8, 200, 252]. This ultimately results in the loss-of-function of the protein function at the cell surface and constitutes a cellular mechanism for many human monogenic diseases [148, 149, 151, 250].

The M605I, A727V, V790M and M835V mutations in CMS patients are all found in the kinase domain of MuSK and their cellular pathogenesis has previously been partially characterized. A recently identified D38E is located in the extracellular domain of the protein and the affected aspartate residue at position 38, which is part of a beta-strand of Ig-like domain 1 (Ig1) of MuSK extracellular region, it is known to form an asymmetric homodimer mediated by a hydrophobic face [253] (Figure 4.2.18).

Thus, the missense mutation D38E-MuSK might interfere with the proper dimerization of MuSK and the subsequent association with LRP4 to form a functional LRP4-MuSK complex, or it may interfere with Wnt ligand binding. The M605I-MuSK mutation has been shown to result in moderate impairment of both phosphorylation and binding to Dok-7 while the A727V-MuSK mutation results in drastic impairment of phosphorylation and MuSK-Dok-7 interaction due to its location in the catalytic loop of the MuSK protein. The V790M-MuSK mutation impairs the binding of MuSK to Dok-7 thus preventing the interaction necessary for synaptogenesis [254] but it does not appear to alter MuSK autophosphorylation. The

M835V-MuSK mutation results in a constitutively active MuSK receptor with a decreased agrin and Dok-7-dependent phosphorylation.

The ER retention of P344R-MuSK, a possible result of misfolding due to a small conserved cyclic non-polar, proline (Pro) being replaced by arginine (Arg), a positively charged polar amino acid with a larger size within the well conserved CRD of MuSK is plausible. Prolines are particularly well conserved in these RTK-like proteins [245] and prolines often introduce a kink into the helical structure of proteins (Figure 4.2.18). Deleting proline residues can interfere with the *cis-trans* isomerization causing the folding polypeptide forcing a *cis*-conformation of peptide bonds affecting the rate of folding and the folding pathway itself [50]. Interestingly, the P344R-MuSK mutation is found between a negatively charged, conserved Aspartate (D) and Glutamate (E) following a disordered region in the MuSK-CRD. It has been shown that X-Pro *cis* to *trans* changes in prolines completely disrupt conformational folding in Ribonuclease A [255]. It is therefore, conceivable how a proline to arginine change in the CRD may disrupt conformational folding by altering a critical pattern of peptide-peptide hydrogen bonds responsible for the local secondary structure of MuSK, which is essential for the subsequent folding of the protein [50].

Interestingly, the CRD is glycosylated and the P344R mutation is found after the two N-linked glycosylation sites, Asn222 and Asn338 [21] (Figure 4.2.1). PolyPhen-2, http://genetics.bwh.harvard.edu/pph2/ and SIFT, http://sift.jcvi.org/, have classified this mutation as probably damaging (0.985) and deleterious (0.05), respectively. Several strategies have been proposed to rescue the traffic of misfolded mutant proteins. The first approach is to manipulate the culturing temperature with the aim of observing if the misfolded protein is susceptible to therapeutic manipulation. Interestingly, the P344R-MuSK mutation trafficking defect is rescued upon culturing the cells at reduced culturing conditions of 27˚C, as was

also seen with the ΔF508-CFTR [256]. This suggests that the P344R-MuSK mutant might be a suitable ERAD candidate for therapeutic studies.

Chemical chaperones facilitate the escape of the P344R-MuSK mutation from the ER quality control system. They presumably shift the folding equilibrium of the mutant protein towards its native state, thus releasing it from its ER retention state. These chemical chaperones act more globally affecting the cellular proteostasis network, thereby leading to a more favorable folding and/or trafficking environment.

An essential outcome of ubiquitination is targeting to the 26S proteasome, a specific signal, which is responsible for the degradation of ER retained proteins [257]. The majority of proteasome substrates are tagged not by a single ubiquitin (monoUb), but by a polyubiquitin (polyUb) chain. It is generally thought that polyUb chains longer than four ubiquitin molecules are the preferred signal for efficient recognition and degradation by 26S proteasomes [236, 258]. The P344R-MuSK pattern is that of a polyUb chain increasing the molecular weight of P344R-MuSK to much more than 300 kDa. Once bound by proteasomes, substrate-conjugates are deubiquitinated, unfolded and subsequently degraded.

Taken together, my experiments demonstrate the potential for trafficking and the function of the P344R-MuSK mutant, to be rescued to the plasma membrane of HeLa, COS-7 and HEK293 cell lines. These findings suggest that extending the investigation to a larger number of chemical chaperones may identify chemicals that could potentially rescue trafficking and the function of this mutant. Although prescription of acetylcholinesterase inhibitors such as pyridostigmine, is so far the most cost effective therapeutic treatment for CMS, our study highlights that prospective alternative personalized treatments for patients suffering from the P344R-MuSK mutation causing CMS, can be developed to target the source of the disease, rather than its consequences. These findings also support efforts for rescuing trafficking of other missense mutations that cause disease. Treatments

suggest that the folding defect in P344R-MuSK can be improved. As a result, the P344R-MuSK mutant may be rescued however, a folding corrector or pharmacological chaperone has yet to be identified.

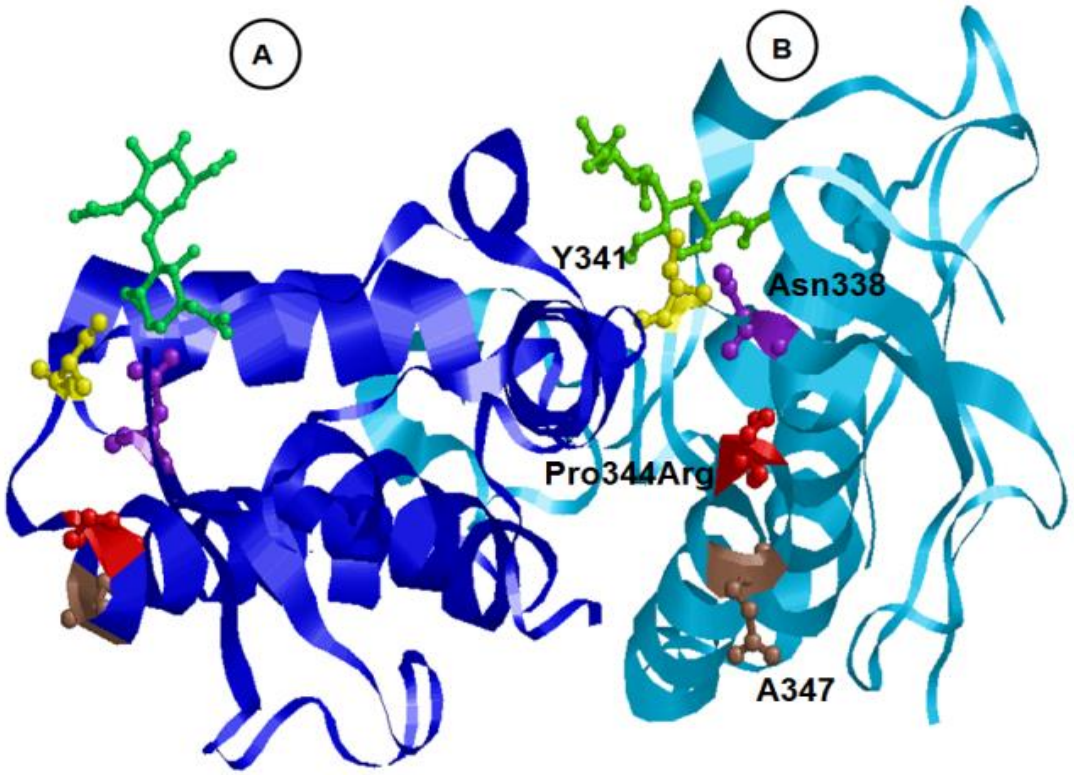


Figure 4.2.18. Crystal Structure of the asymmetric frizzled-like cysteine-rich domain dimer of MuSK. The FZ-CRD of MuSK is shown as an asymmetric dimer taken from PDB: 3HKL and then was manipulated using RasMol 2.7 (www.RasMol.org) [21]. An Asymmetric dimer formation of the two copies of MuSK-CRD in the asymmetric unit are colored blue (copy A) and cyan blue (copy B). The CRD *N*-glycosylation site (Asn338) is shown in purple ball and stick representation. The N-glycan is shown as a green ball and stick representation above the Asn338. The P344R mutation highlighted in red ball and stick representation is found as the first amino acid of the alpha-helix sheet (a.a: 344-359) after the beta-strand (a.a: 335-338); http://www.rcsb.org/pdb. A proline (Pro); a small non-polar amino acid interacts with the protein backbone twice forming a five-membered ring, is substituted to an arginine (Arg); a basic larger amino acid with an electrically charged side chain that is hydrophilic. The positively charged arginine may interact with the negatively charged asparagine (Asn) forming salt bridges. Due to its position, it may mask the Asn from the N-glycan resulting in an immature under glycosylated protein. The P344R mutation is also in close proximity with Y341 shown as a yellow ball and stick representation, found at the dimer interface [21]. The Y341 is found to form hydrogen bonds with the Asn338 [21]. The P344R mutation is also close to A347 (brown ball and stick representation) which is also involved in the dimer interface.

## 4.3 TEK Tyrosine Kinase, Endothelial (TEK) and autosomal dominantly inherited Cutaneomucosal Venous Malformation (VMCM)

### 4.3.1 Introduction

Autosomal dominantly inherited Cutaneomucosal Venous Malformation (VMCM; OMIM 600195)] has been shown to be caused by mutations in the genes encoding for the angiopoietin receptor TEK Tyrosine Kinase, Endothelial (TEK), OMIM: 600221 [259-261]. The vascular endothelial cell (EC)-specific receptor tyrosine kinase TEK plays a crucial role in angiogenesis and cardiovascular development [262, 263]. Germline substitutions in TEK cause a rare inherited form of venous anomalies where heterozygous TEK substitutions induce *in vitro* ligand-independent hyperphosphorylation [264, 265]. The lesions are characterized by multifocal small bluish cutaneous and mucosal lesions, composed of disorganized thin-walled vascular channels [260, 264]. VMCM is a rare disease that exhibits variable expressivity and high penetrance [266, 267].

TEK can associate with p85, the regulatory subunit of phosphatidylinositol-4, 5-bisphosphate 3-kinase, catalytic subunit alpha (PI3K), leading to activation of both PI3K and v-akt murine thymoma viral oncogene homolog 1 (Akt1) [268]. Tyrosine 1101 of TEK is the major site of association of p85 and is required for activation of PI3K and Akt. This pathway is involved in cell survival and anti-apoptosis, which helps to explain the role of TEK in normal vascular maintenance. The details of the TEK signaling pathway are just beginning to emerge.

There has been some controversy regarding the hyperphosphorylation status of the TEK receptor. Research has shown that overexpression of the mutants result in ligand-independent hyperphosphorylation of the receptor. However, Wouters et al., suggest this is a general feature of VMCM-causative TEK mutations [264]. Moreover, it has been shown that there is variation in the level of activation demonstrated by widely differing levels of chronic TEK hyperphosphorylation and

these are tolerated in the heterozygous state. This hyperphosphorylation is only observed in localized areas of lesions excised from the patients and is not found in the normal endothelial cells.

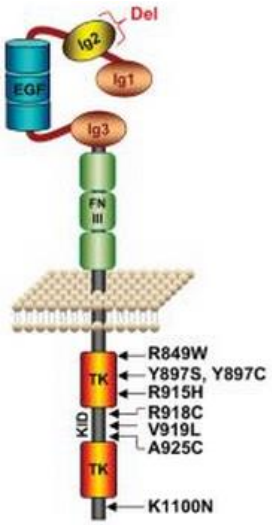


Figure 4.3.1. Schematic representation of TEK. TEK is made up of an extracellular region. The latter of which is made up of three immunoglobulin-like loops (Ig1, 2, 3), three epidermal growth factor-like repeats (EGF), and three fibronectin type III-like repeats (FNIII). TEK also has an intracellular region made up of 2 tyrosine kinase domains (TK) separated by kinase insert domain (KID). Locations of missense substitutions identified in inherited VMCM are shown. A somatic mutation “Del” deletes part of the Ig2 found in the extracellular domain in the TEK-WT allele of one VMCM patient carrying the inherited R849W mutation. Taken from reference [260]

Interestingly, Limaye et.al., identified a somatic, lesion-associated TIE2 “2nd-hit” alteration in one resected VMCM, from a patient carrying the germline R849W-TEK mutation. A cDNA screen revealed an in-frame deletion of 129-bp, corresponding to a loss of exon 3 and part of exon 4 (amino acids 122-165 of the extracellular Ig2 ligand-binding domain; “Del” of TEK (Figure 4.3.1). They also showed that the “Del” allele is occurs on the wild-type and the deletion is part of an intragenic somatic DNA deletion. The lack of 43 amino acids resulted in the wild-type being retained in the ER and therefore loss of cell surface expression of the receptor, as well as its inability to bind Ang1, in contrast to WT [260].

Another somatic 2nd hit causing loss of function of the receptor in resected VMCM lesions showed a frequent L914F mutation and a series of double-mutations that occur in cis (on the same allele). The L914F mutation also resulted in retention of the TEK protein within the ER lumen.

As a result, it was speculated that some of the eight reported inherited TEK missense mutations (R849W, Y897C, Y897S, R915H, R918C, V919L, A925S and K1100N) might traffic abnormally and get retained in the ER and eventually get degraded by the proteasome. I tested this hypothesis experimentally and it was shown to be incorrect as highlighted below.

### 4.3.2 Results

R849W, Y897C, Y897S, R915H, R918C, V919L, A925S and K1100N mutations in TEK failed to affect the trafficking of the protein to PM. All the generated TEK missense mutants (R849W, Y897C, Y897S, R915H, R918C, V919L, A925S and K1100N) [264] were found to be largely localized to the plasma membrane in HeLa cells (Figure 4.3.2). HeLa cells transiently transfected with the wild-type C-terminally HA-tagged TEK cDNA show that the expressed protein is predominantly localized to the plasma membrane (PM) in contrast to calnexin, a well-established ER marker (middle panels). Calnexin exhibits a typical perinuclear and reticular distribution due to its well-established ER distribution (middle panels). In contrast, the TEK-WT and TEK mutants were found to be predominantly localized to the PM (merged panels). This localization on the plasma membrane in HeLa cells excluded the examined TEK missense mutants from being ERAD substrates and therefore the underlying cellular mechanisms of these disease-causing mutations remain unresolved. Further functional studies are recommended to elucidate their disease-causing mechanisms.

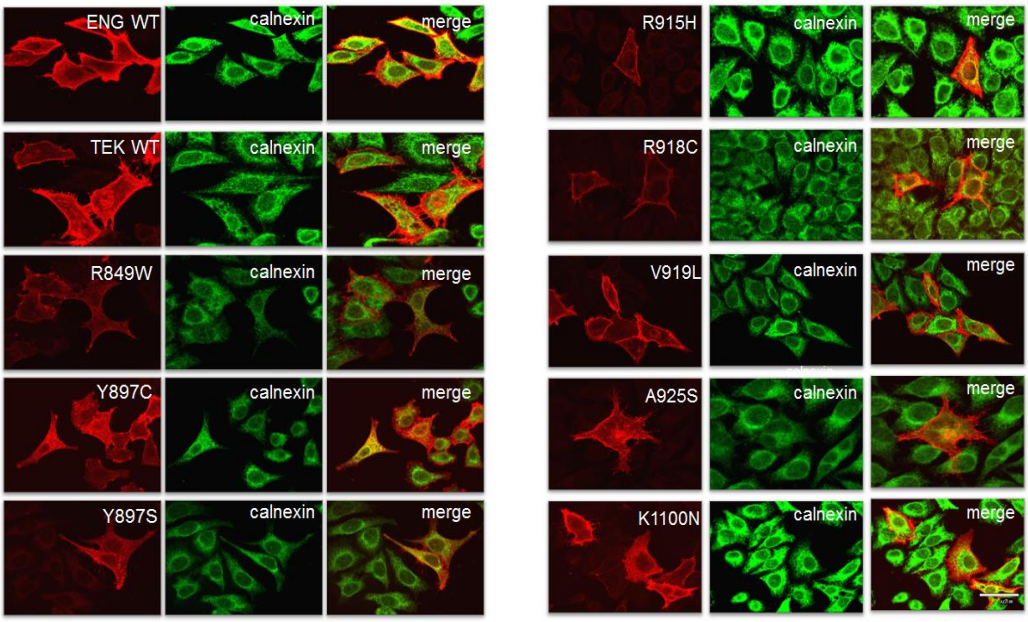


Figure 4.3.2. The localization of TEK-WT and the eight missense TEK disease-causing mutants. The eight missense mutants clearly do not localize with the ER calnexin marker and localize in a similar pattern to the TEK-WT when the expressed HA epitope for each corresponding mutant is merged with the calnexin marker. ENG-WT is a positive control for HA epitope.

### 4.3.3 Discussion

ER-retention and abnormal trafficking does not contribute to the cellular mechanism of inherited cutaneomucosal venous malformation disease for the eight reported inherited TEK missense mutations (R849W, Y897C, Y897S, R915H, R918C, V919L, A925S and K1100N). Therefore, the question remains open as to how these mutations cause disease. Elucidation of the presence of double mutants in cis and 2$^{nd}$ hit somatic mutation effects may aid our understanding of how these hyperphosphorylating mutations lead to the development of the vascular lesions observed in VMCM.

## 4.4 Attempts on silencing ERAD components in a cell line stably expressing an ERAD substrate

### 4.4.1 ERAD pathways

Recent evidence suggests that ERAD is composed of multiple pathways, is substrate specific and consequently caters for a range of different classes of substrates. The location of the misfolded lesion on a substrate relative to the ER membrane classifies the substrates into three types known as ERAD-cytoplasmic (ERAD-C); ERAD-luminal (ERAD-L) or ERAD-intramembrane (ERAD-M) substrates [7, 15, 16].

In ERAD-C, the misfolded domain lies at the cytoplasmic side of the membrane and are degraded by the ubiquitin ligase Doa10 complex. Proteins with luminal (ERAD-L) have the misfolded domain within the ER lumen are degraded by the SYVN1 complex alongside other proteins such as Derlin1, 2, 3 [17] which form a scaffold. This pathway also degrades soluble misfolded proteins of the ER lumen [18]. Since P344R-MuSK mutant is a type I integral protein, it is proposed that it has its lesion on the luminal side and I therefore assume that it follows the ERAD-L pathway.

OS-9 releases misfolded polypeptides with luminal or transmembrane folding defects (ERAD-L and ERAD-M substrates) to retro-translocation complexes built around the membrane-embedded E3 ubiquitin ligase, SYVN1. Misfolded polypeptides with cytosolic folding defects (ERAD-C substrates) also engage retrotranslocation complexes around E3 ubiquitin ligases. It has been observed that the location of misfolded domains(s) on ERAD substrates may determine which ERAD machinery complex is used for their degradation. This correlation between substrate class and choice of pathway is strongest in yeast and is found in mammalian cells to a much lesser extent [18].

Several resident ER proteins on the ER membrane have been proposed to form retrotranslocation channels for the dislocation of misfolded proteins out of the ER for degradation by the proteasome system [140]. These proteins are briefly described in the following sub-sections.

### 4.4.2 Synovial apoptosis inhibitor 1, synoviolin (SYVN1)

SYVN1 is an ER-localized membrane E3 ubiquitin ligase that polyubiquitinates ERAD substrates on the cytoplasmic face of the ER membrane (Figure 4.4.1). Ubiquitination of the protein substrate provides a critical step in protein dislocation [138]. The RING family constitutes the largest family of E3 ligases, with over 600 human genes, including those involved in ERAD [132, 269]. The cytosolic RING-H2 finger E3 domain creates a binding platform for the E2 conjugase and also interacts with the AAA ATPase [270]. Most ERAD E3 ligases are integral membrane proteins with a proportion of hydrophilic residues that result in a peptide-transporting pore [139, 140, 145, 271]. They form the core of the ERAD machinery, bringing together functionally distinct ERAD complexes. E3 ligases have been shown to ubiquitinate and deubiquitinate and also interact with deubuitinating enzymes before disposal [269]. SYVN1 has six transmembrane segments and is a very unstable protein, stabilized by the formation of a stoichiometric complex with SEL1L [272].

### 4.4.3 Sel-1 suppressor of lin-12-like (*C. elegans*) (SEL1L)

SEL1L is a type-I transmembrane protein with a large luminal domain containing SEL1 repeats [230]. SEL1L is an adapter membrane-associated glycoprotein that interacts with an assortment of ERAD regulators, including OS-9, ERLEC1/XTP3-B, EDEM1 and EDEM3, which facilitate substrate transfer from the protein-folding components to the ERAD complex [273]. SYVN1-SEL1L proteins interact with many proteins for example; OS9 [274], the Derlins, valosine-containing protein (VCP)/p97-interacting membrane protein (VIMP) (VCP/p97), and Herp forming a large scaffold within the ER membrane [131, 275].

### 4.4.4 Osteosarcoma amplified 9, endoplasmic reticulum lectin (OS-9)

OS-9 is found within the ER lumen and is an ER-resident glycosylated protein (Figure 4.4.1). It has a glucosidase type II domain involved in binding to misfolded proteins. OS-9 like ERLEC1/XTP3-B, another ER luminal protein, contain mannose-6-phosphate receptor homology (MRH) domain. MRH domains specifically bind to terminal α-1,6-mannose residues to facilitate transfer of terminally misfolded glycoproteins to the scaffolded ERAD complex [130, 274, 276]. They can bind to glycosylated and non-glycosylated misfolded proteins.

### 4.4.5 Derlin 1 (DERL1/DER1)

Derlin contains four transmembrane regions. Mammals have three such homologues known as Derlin1, 2, and 3 [277]. These proteins may be part of the ER membrane retrotranslocation channel. VIMP is a small connecting protein for VCP/p97 to Derlins. As previously mentioned, VCP/p97, is an AAA ATPase involved in the extraction of ERAD clients. Der1 has been shown to initiate the export of misfolded polypeptides from the ER lumen by moving the substrates through the ER membrane and passing them on to SYVN1 for ubiquitination [278]. Der1 has also been shown to be important for the dislocation of other substrates, as part of other ERAD complexes [140, 141].

In the ER of *S. cerevisiae*, a large complex made up Hrd1p-Hrd3p (SYVN1 and SEL1L in humans) alongside Der1p (DER1) has been observed. On the luminal side, Yos9p (OS9/OS-9) with other ER chaperones has been described.

The importance of these proteins in ERAD-L prompted me to choose these members of the ERAD dislocation machinery as candidates for possible interactions with the P344R-MuSK mutant. siRNA knockdown of these candidates in isolation or in pairs, could rescue or stabilize the P344R-MuSK mutant from its ERAD fate.

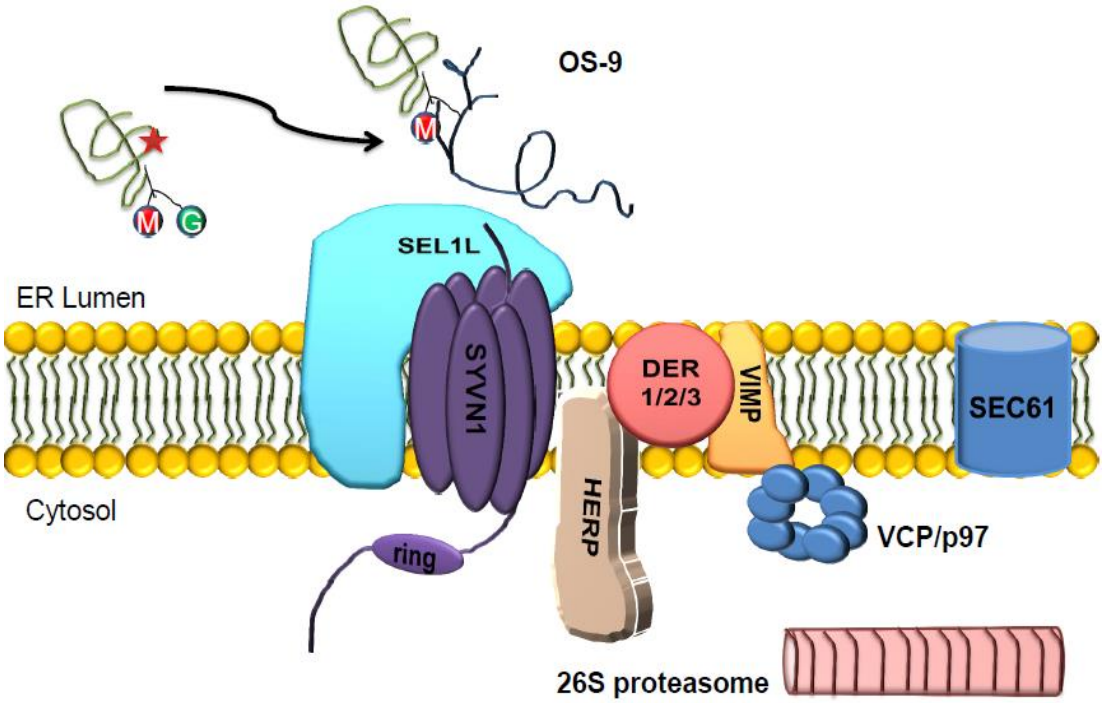


Figure 4.4.1. The SYVN1/SEL1L complex of the mammalian ERAD machinery. OS-9 is an ER lectin which recognizes misfolded substrates and passes them on to SYVN1, an E3-ligase. The SYVN1 ubiquitin ligase and SEL1L protein network and form a large scaffold embedded at the ER membrane. Other members of this scaffold include Derlin-1/2/3, VCP/p97, and Herp. The small membrane protein VIMP connects VCP/p97 to Derlins. SEL1L is a membrane-associated adapter glycoprotein which interacts with SYVN1 stabilizing it. SYVN1 is a very unstable protein with a short half-life. This E3 ligase polyubiquitinates the misfolded substrate on the cytoplasmic face of the ER membrane, while interacting with other components of the ERAD machinery forming this scaffold. Eventually the misfolded protein may or may not be unfolded before it reaches the VCP/P97 AAA ATPase which deubiquitinates the substrate and sends it off to the 26S proteasome for degradation. Redrawn from reference [272].

### 4.4.6 Silencing of ERAD components by siRNA

Small interfering RNA **(**siRNA) silencing has been used to dictate the difference between a deleterious mutation and a tolerated polymorphism as is seen with CF. As previously mentioned, partial siRNA silencing of the Hsp90 co-chaperone ATPase regulator (Aha1) [201] was able to rescue ΔF508-CFTR which has been shown to be functionally competent as a chloride ion transporter. Therefore, the goal of the majority of CF therapeutic treatments is overcoming folding and trafficking defects in the ER.

The ability to control cell fate via the ER-folding, export and degradation pathways provides an exciting direction in future drug development within monogenic diseases. Identifying the cellular mechanism underlying genetic disease has offered hope to CF and other diseased patients. It remains to be determined if these disease causing mutations can be rescued or the ER milieu can be altered to allow these defective proteins to function as close as possible to their wild-type counterparts. This will provide the basis for designing specific drugs such as chemical and/or pharmacological chaperones that aid the transport of the disease-causing mutant protein(s) to cellular membranes and eventually provide options for these patients. Likewise, tissue-specific chaperones can be therapeutic targets and have the capacity to provide important tools in biotechnology.

As mentioned earlier, SEL1L and SYVN1 form a large ubiquitin ligase complex that interacts with SVIP. Silencing of this SYVN1-SEL1L complex has been shown to downregulate the degradation kinetics of some ERAD substrates [272] providing yet another ERAD target for rescuing misfolded proteins. OS-9 has been characterized extensively in yeast and it has been shown that *N*-glycans lacking the terminal mannose from the C branch are recognized by OS-9 and targeted for degradation [275]. Der1 was considered to provide the missing link between events on the lumenal side of the ER and the cytosolic extraction catalysed by p97 [277].

## 4.4.7 Results

### 4.4.7.1 Optimization of SYVN1, SEL1L, OS-9 and DER1 siRNA-mediated knockdown

To assess the roles of SYVN1, SEL1L, OS-9 and DER1 in P344R-MuSK degradation they were knocked-down in HEK 293 cell line stably expressing this mutant. The siRNA transfection efficiency was optimized in non-expressing HEK cells to determine the optimal conditions that result in maximum gene silencing with minimal cytotoxicity. Proteins were extracted, run on SDS-PAGE gels and probed with the appropriate antibodies (Figure 4.4.2 and Figure 4.4.3). The four proteins (SYVN1, SEL1L, OS-9 and DER1) were effectively knocked down by a range of 85-99% (Figure 4.4.3 line graph) when 200 pmol of the relevant siRNAs were used. The positive internal control, GAPDH, allowed the integrity of the cell line to be monitored and acts as a loading control. The scrambled sequence was used as a negative control for all experiments.

### 4.4.7.2 Silencing of SYVN1, SEL1L, OS-9 and DER1 has no effect on the ER mislocalization of P344R-MuSK mutant

Endogenous SYVN1, SEL1L, OS-9 and DER1 were knocked down in HEK293 cells stably expressing the P344R-MuSK mutant. The effect of this down regulation was assessed by confocal microscopy and biochemically by deglycosylation assays. The ERAD components were knocked down individually and in-paired combinations (e.g. SYVN1 and SEL1L) to observe any synergistic effect of combined silencing. The results are shown in Figure 4.4.4. In short, the silencing of the above proteins did not have a profound effect on P344R-MuSK mislocalization to the ER and no rescue to the PM was observed. This may be due to a limitation in the efficiency of silencing. Final concentrations of siRNA in culture media beyond 200 pmol resulted in massive cell death when silencing SEL1L, SYVN1, OS-9 and DER1. This could be due to the cells not being able to withstand complete silencing of these ERAD components which leads to apoptosis of the stable cell lines. It might be that this

residual amount of silencing may be needed for complete silencing of the ERAD machinery components and to rescue P344R-MuSK to the cell surface.

The effect of siRNA mers of DER1 and OS-9 together had a lesser effect on silencing of these proteins than when they were silenced on their own. This could be due to saturation of the Argoraute proteins found in the RNA-induced silencing complex (RISC). siRNA scrambled sequences and siRNA of GAPDH, used as a controls for the siRNA transfections, did not show any effect on the localization of P344R-MuSK mutant nor the integrity of the cell as seen with calnexin staining. For confirmation, I also examined the *N*-glycosylation profiles of the mutant protein under these silencing conditions as shown in Figure 4.4.6.

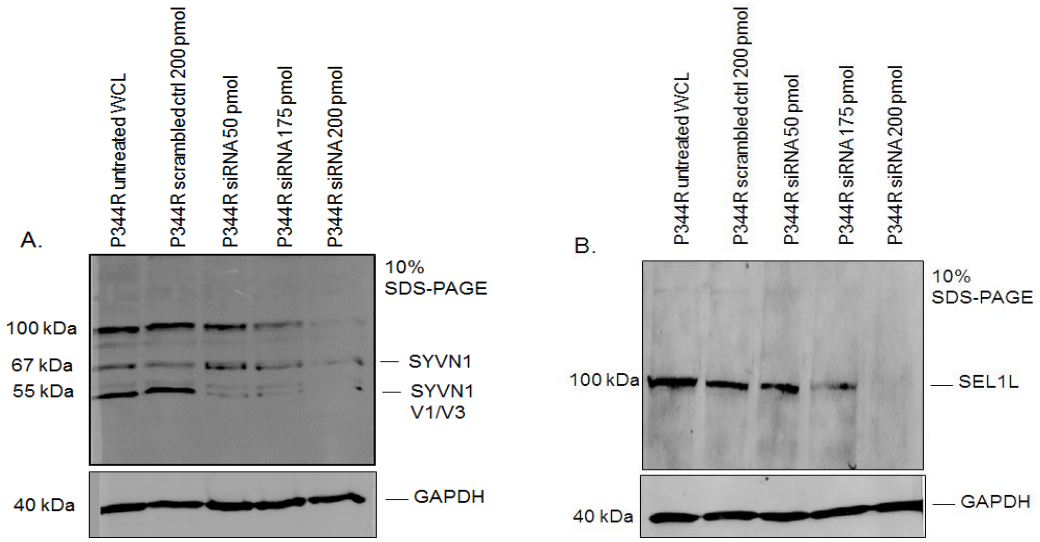


Figure 4.4.2. The effect of silencing of SYVN1 and SEL1L in HEK293 cells treated with targeted siRNA. The P344R-MuSK mutant HEK293 cell line was treated with increasing concentrations of silencing mers in triplicate. P344R-MuSK WCL untreated was taken as a control alongside scrambled mers at the highest concentration. The quantity of mers used ranged from 50-200 pmol. (A). WCL were run on a 10% SDS-PAGE and probed with anti-SYVN1 antibody. An untreated P344R-MuSK mutant stable cell line was used and the endogenous C terminus of the SYVN1 protein is shown. The 55 kDa is the expected size. The WCL was heated at 50 ºC to prevent aggregation and the upper bands may be smaller proteins still in complex with SYVN1 or the larger SYVN1 protein. (B) The blot was probed with anti-SEL1L and a band of approximately 100 kDa was detected. Scrambled siRNA was used as a non-specifc control alongside GAPDH as a loading control. Knockdown was most effective at 200 pmol.

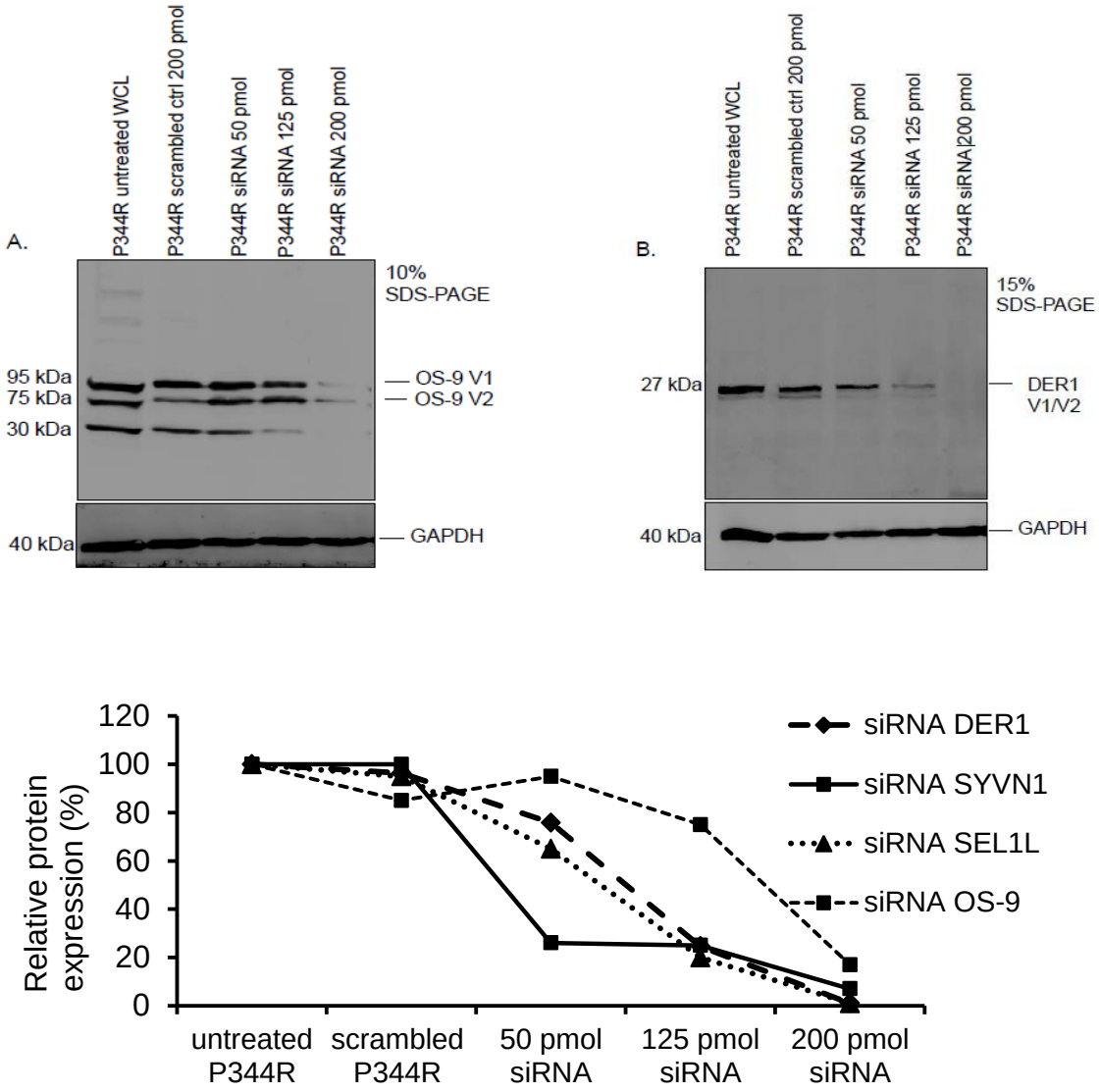


Figure 4.4.3. The effect of silencing of OS-9 and DER1 in HEK293 cells treated with targeted siRNA. The P344R-MuSK mutant HEK293 cell line was treated with increasing concentrations of silencing mers in triplicate. P344R-MuSK WCL untreated was taken as a control alongside scrambled mers at the highest concentration. The quantity of mers used ranged from 50-200 pmol. (A). WCL were run on a 10% SDS-PAGE and probed with anti-OS-9. An untreated P344R-MuSK mutant stable cell line was used and the endogenous protein expression of OS-9 is shown as 3 bands. OS-9 has eight reported transcriptional variants with two main variants V1 at 95 kDa and V2 at 60 kDa. A band of 30 kDa has also been shown to probe with anti-OS-9 (www.abcam.com). Knockdown was effective at 200 pmol. (B) DER1 protein of 27 KDa was also knocked down at 200 pmol. The effect of silencing is shown in a line graph. The silencing of OS-9 and SEL1L was around 99%; SYVN1 band 55 kDa was silenced at around 90% and OS-9 V2, reported to interact with the SYVN1 and SEL1L complex [272] was at around 85%.

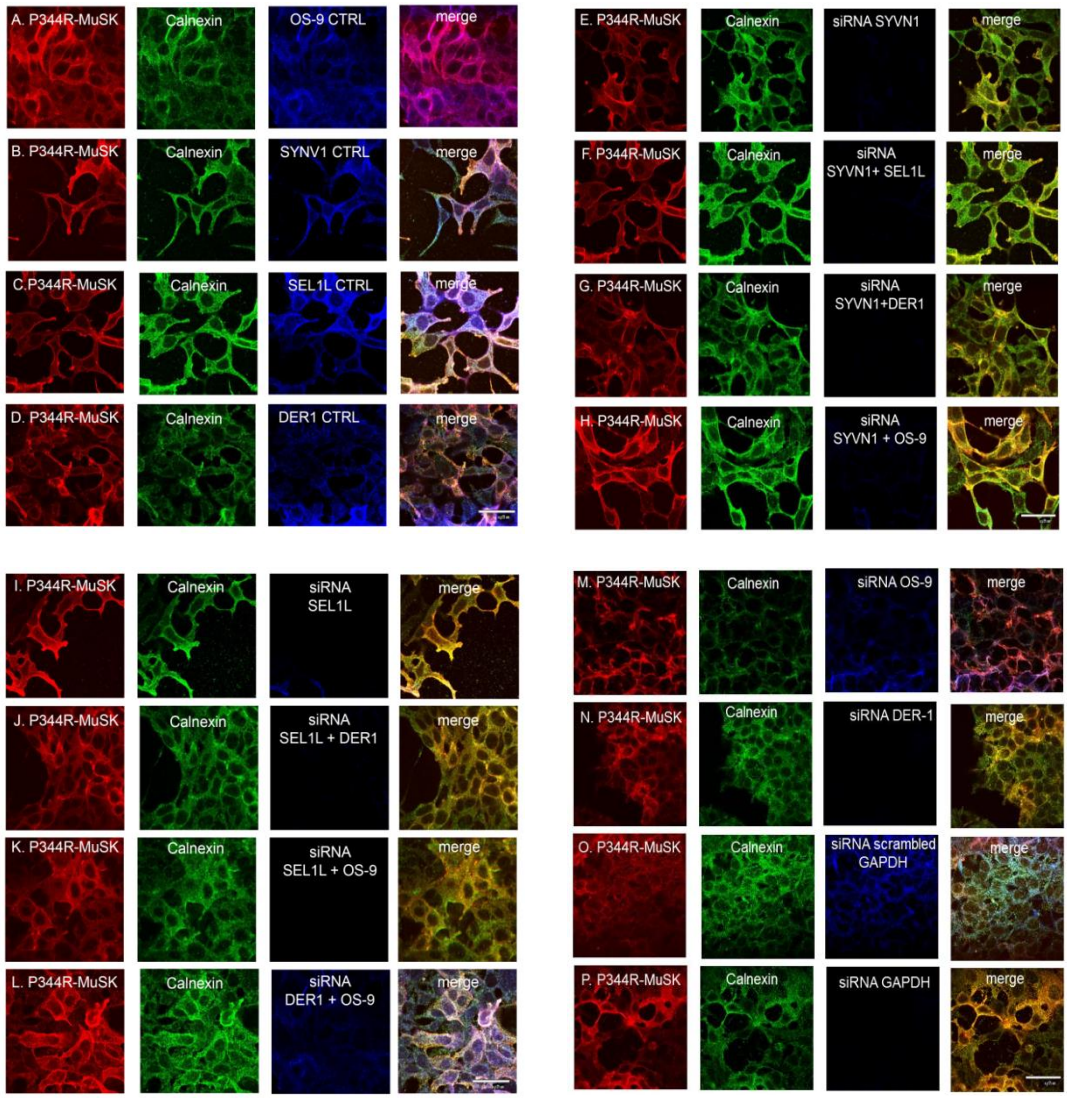


Figure 4.4.4. The effect of siRNA of ERAD components on stable HEK293 cell lines of P344R-MuSK mutant's localization in the ER. FLAG-tagged P344R-MuSK protein is seen as red fluorescence whereas calnexin is seen as green signals. The ERAD components are shown as blue signals. Panel A-D shows four controls for each of the ERAD components SYVN1, SEL1L, OS-9 and DER1 respectively under non-silencing conditions. Panel E shows the effects of silencing SYVN1 alone; panel F SYVN1 and SEL1L; panel G SYVN1 and DER1; panel H SYVN1 and OS-9 pair. SYVN1 and OS-9 pair caused a portion of P344R-MuSK rescue to the plasma membrane. Panel I shows the effect of silencing SEL1L; Panel J SEL1L and DER1; Panel K SEL1L and OS-9 and the synergistic effect of DER1 and OS-9. No rescue was seen in any of these panels. Panel M and N show the silencing of OS-9 and Der1 alone showing no rescue. Scrambled sequences were used as controls; panel o with staining of GAPDH in blue and panel P showing effect of siRNA GAPDH as a control. Objective lens 40X; Scale bar 25µm.

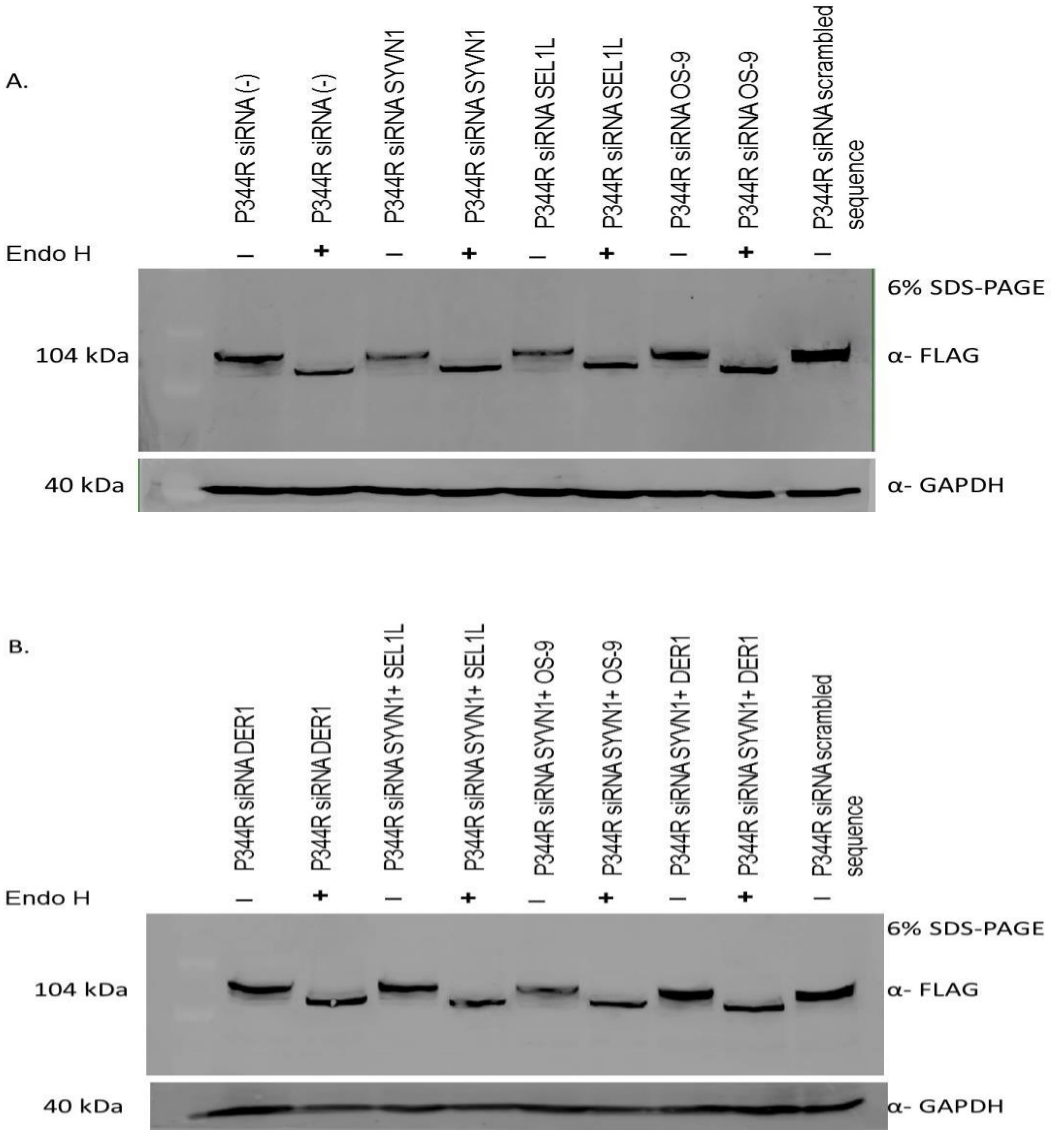


Figure 4.4.5. *N*-glycosylation profile of P344R-MuSK stable cell lines. P344R-MuSK was subjected to Endo H treatment (section 3.4.10). After silencing the aforementioned ERAD components outlined in 4.4.7.2. The protein was run on a 6% SDS-PAGE. (A) Untreated protein is shown in the far left first two lanes, (-) not treated with ENDO H and (+) means treated with ENDO H. The scrambled sequence of P344R-MuSK served as a control for the expression of MuSK and GAPDH a loading control. A representative result shown in blots A and B show that silencing of selected ERAD components alone or in-pairs had no effect on the maturation of P344R-MuSK.

#### 4.4.7.3 The Immunoprecipitation of P344R-MuSK mutant failed to pull-down SYVN1, SEL1L, OS-9 or DER1

I next examined whether there are interactions between SYVN1, SEL1L, OS-9 and/or DER1 with P344R-MuSK mutant. The stably expressed P344R-MuSK mutant was immunoprecipitated with anti-FLAG antibody and the immunoprecipitates were probed with anti-SYVN1, anti-SEL1L, anti-OS-9 and anti-DER1 anti-bodies as shown in Figure 4.4.6. From this experiment it seems that there is no evidence of interaction between P344R-MuSK mutant and SYVN1, SEL1L, OS-9 and/or DER1. This negative result may be due to weak or transient interactions that did not withstand the nature of an IP.

### 4.4.8 Discussion

Misfolded or unassembled proteins, retained in the ER, are eventually degraded by the proteasomes through ERAD [56]. Ubiquitin ligases embedded in the membrane of the ER ubiquitinate misfolded proteins by addition of PUCs during substrate retrotranslocation from the ER to the cytosol [230]. Hrd1p/Der3p ubiquitin-ligase is shown to ubiquitinate ERAD substrates in *S. cerevisiae*.

My results show that P344R-MuSK does not appear to interact with any of the following ERAD components. Endogenous SYVN1, SEL1L, OS-9 and DER1 in HEK293 cells. This was seen by immunoprecipitation and by confocal imaging. When silenced, the P344R-MuSK localization remained in the ER and P344R-MuSK did not traffic to the cell surface. This was further verified with endoglycosidase H digestion.

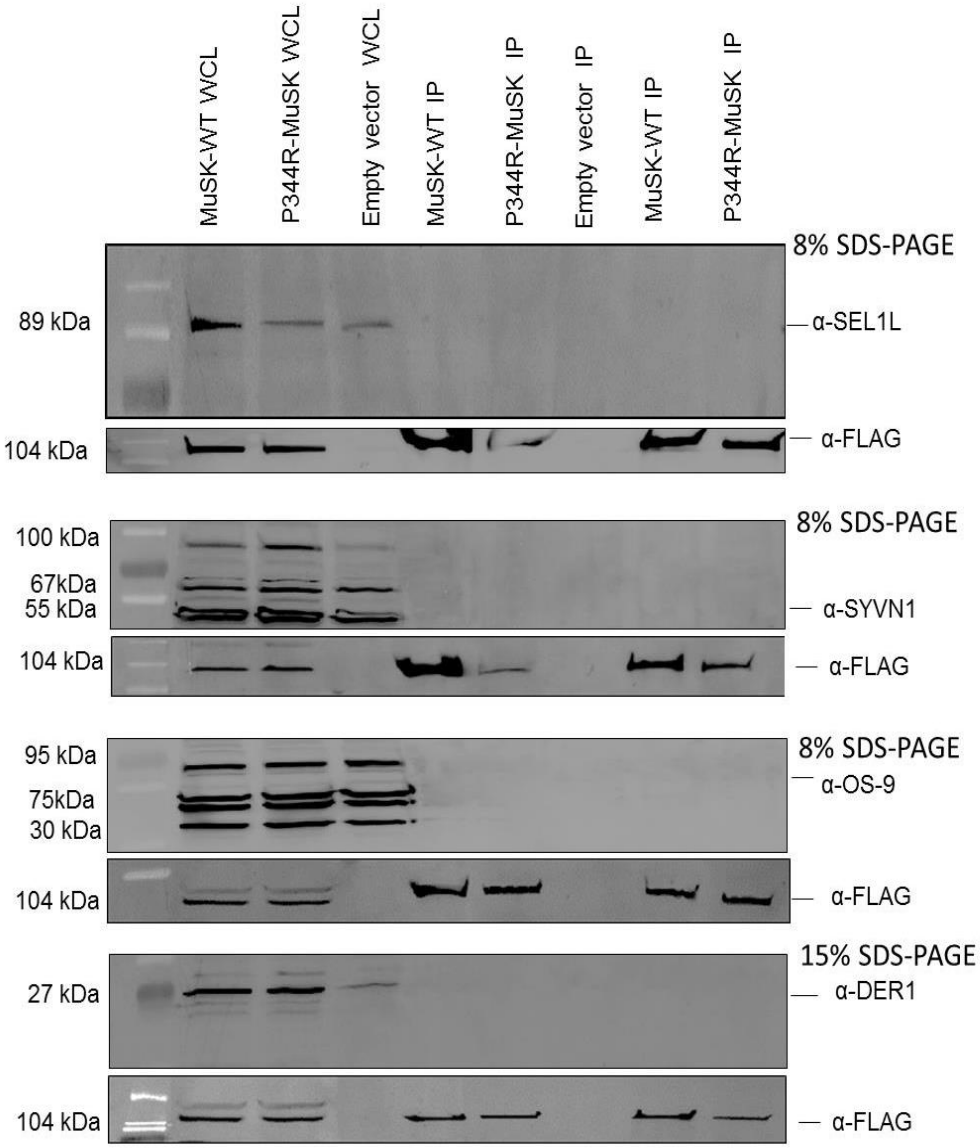


Figure 4.4.6. Immunoprecipitation of P344R-MuSK and SEL1L, SYVN1, OS-9 and Der1 interaction *in vitro*. P344R-MuSK protein was extracted and a proportion of the WCL was subjected to IP as described in the methods. Following IP, the protein was run on different gradients of SDS-PAGE as shown. MuSK-WT, P344R-MuSK and empty vector controls WCL were run as a control for the presence of the proteins SEL1L, SYVN1, OS9 and DER1 in the HEK293-P344R stable cell lines. Next, the IP of MuSK WT, P344R-MuSK and empty vector in duplicates using two different IP methods: SDS elution from the beads (far left), and glycine elution using low PH (far right) for comparison. The blots were probed with each of the antibodies: SEL1L, SYVN1, OS-9 and Der1. The blots were then stripped and re-probed with anti-FLAG to detect the presence of MuSK-WT, P344R-MuSK in WCL and in the IP product. The IP of both MuSK-WT, acting as a control, and the P344R-MuSK failed to pull down any of the four proteins SEL1L, SYVN1, OS-9 and Der1.

Simply put, ERAD is a multifaceted pathway with many different players displaying substrate specificity. The complexity of ERAD is just beginning to emerge and its diversity has been contrasted to its yeast counterpart. The conformation of P344R-MuSK may require a different E3 ligase; as a range of misfolded conformations are possible in the ER [279]. E3 ligases have been shown to show preference for one substrate over others. A more subtle approach would be to isolate the ER organelle within this cell line and study all interacting partners or chaperones interacting with P344R-MuSK, “a P344R-MuSK interactome”. Silencing of these specific individual partners as with ΔF508-CFTR was able to rescue the ΔF508-CFTR-functional mutant [201].

Carvalho et al. identified CPY, an ERAD-L substrate, crosslinking with a number of inter-bilayer residues of the SYVN1 transmembrane region [145]. SYVN1 was shown to be required for retrotranslocation however, their model was incomplete. Sato et al. devised a self-destructive ERAD substrate that self ubiquitinates independently of full-length SYVN1. They show that their substrate Hmg1 isozyme of yeast HMGR required only a built-in RING domain, correct E2 and the AAA ATPase complex only for retrotranslocation and degradation [139]. Since *in vivo* and *in vitro* retrotranslocation can occur in an Δ*hrd1*Δ*doa10* double null strain, this indicates that the dislocation channels may not be necessary [140].

Substrate degradation is well characterized in *S. cerevisiae*. There are three distinct pathways with differing ubiquitin ligases involved. ERAD-C substrates with misfolded cytosolic domains are degraded by Doa10p; ERAD-L substrates with misfolded ER-luminal domains are recognized by Hrd1p while ERAD-M substrates with misfolded intramembrane domains also recognized by Hrd1p, however, the final scaffold for dislocation is different. In mammals, the substrate specificity required for E3-ubiquitin ligases remains to be elucidated.

Recently, mammalian ERAD-LS substrates (soluble polypeptides with luminal lesions), were degraded by the HRD1-SEL1L scaffold with the OS-9 and ERLEC1/XTP3-B lectins. The mammalian system has been shown to be much more complex than yeast and has undergone an expansion of the ERAD E3 ligase family, with the *Hrd1p* homologs Hrd1 and Gp78, the *Doa10p* homolog membrane-associated RING finger (C3HC4) 6, E3 ubiquitin protein ligase (MARCH6), RING finger protein 5, E3 ubiquitin protein ligase (RNF5), RING finger protein 139 (RNF139), and STIP1 homology and U-box containing protein 1, E3 ubiquitin protein ligase (STUB1) and the Derlin-1/ (transmembrane protein 129, E3 ubiquitin protein ligase) TMEM129–dependent pathway [280]. There are approximately 600 E3 ligases and their roles remain to be elucidated [273]. Similarities exist between yeast and mammalian ERAD systems. For example, the mammalian homologues of yeast; Yos9p (OS-9 and ERLEC1/XTP3-B) and the ubiquitin conjugating enzyme E2 (UBC6e), have been shown to bind to the ERAD complex [272].

How a luminal protein can cross the lipid bilayer is not known, and the existence of a proteinaceous pore has been suggested for certain substrates such as the class I major histocompatibility complex (MHC) products [277]. Interestingly, a model has been proposed for the involvement of lipid rearrangements in glycoprotein quality control [281]. Regardless, as mentioned earlier, this dislocation channel remains ill-defined and identification of the channel would be a milestone that would unravel questions regarding this fascinating cellular pathway.

Silencing of the small VCP/p97-interacting protein (SVIP), identified it as an ERAD inhibitor that halts substrate ubiquitination and subsequent ERAD steps [282]. This finding has provided hope for misfolded proteins as overexpressing SVIP may allow misfolded proteins an escape to their final destination. Hence, overexpression of the SVIP alongside chemical chaperones may rescue misfolded proteins from their ERAD fate.

Another protein, a heat shock protein like HSP70 (GRP78/BiP), which is an inhibitor of SVIP, and an ubiquitin ligase (E3) has been shown to target ΔF508-CFTR for degradation [283]. HSPA5/BiP interacts with SYVN1, which counteracts its function. Silencing HSPA5/BiP or overexpressing SYVN1 can also result in promising results. Proteasomal inhibitors are currently being studied and have shown promise in certain cancers, however, these inhibitors had an adverse effect on wild-type CFTR and were consequently ineffective for CF treatment [6].

# Chapter 5: Discussion and Conclusions

## 5.1 Summary

Inherited missense mutations altering amino acids in secretory proteins may lead to defective proteins which can not fold properly in the ER. The cell harbours a machinery which disposes of improperly folded proteins which disrupt the homeostasis of the cell and puts it in jeopardy. The cell maintains a high caliber of proteins by selecting glycoproteins that are fit for performing their intended function and are not deleterious to the cell. However, the high stringency of the ERQC system has considered mutant proteins that may be catalytically functional, as unfit to pass the QC standards, and as a consequence, these proteins are disposed of by ERAD. Developing novel therapeutic interventions for certain mutated proteins may allow proper trafficking, with the normal biological function of mutant proteins, alleviating symptoms for patients.

ERAD has been shown to be a common mechanism for many debilitating genetic disorders ranging from cystic fibrosis to hypercholesterolemia [1, 8, 50]. Missense mutations in FZD4, a crucial Wnt receptor [155], disrupt the proper formation of blood vessels in the eye resulting in FEVR. Nine out of the fifteen examined missense mutations are retained by the ERQC and their localization was shown by confocal fluorescent microscopy to be perinuclear and reticular within the ER, in both HeLa and Cos-7 cell lines. In addition, these nine mutations show an immature *N*-glycosylation profile further supporting their ER-trafficking defects and lack of maturation to some degree. They were found to be tagged with PUCs indicating their interaction with the ubiquitin/proteasomal systems. In short, the mutated proteins are degraded by ERAD and lead to the loss-of-function of the proteins. These mutations cause disease in heterozygous states and my results suggest haploinsufficiency of the FZD4 wild-type allele as a consequence leading to FEVR.

A P344R-MuSK protein was shown to be immature, underglycosylated and localized to the ER in HeLa, Cos-7 and Hek293 cell lines. It was found to be tagged with PUCs and is degraded by the proteasome. Its half-life was shown to be reduced compared to MuSK-WT. It is a thermosensitve protein which is rescued by a range of chemical chaperones and retains its autophosphorylated state which implies that it may retain some biological activity if expressed at the cell-surface. M105T-FZD4, C204Y-FZD4 mutations were also thermosenstive and show maturation and exit out of the ER with chemical chaperone treatment to a lesser degree. Knockdown of prominent ERAD components did not rescue P344R-MuSK to the cell surface.

## 5.2 Outlook and perspectives

Fz-CRD missense mutations are emerging in the literature. However little is known about the importance of the Fz-CRD in disease development. Eight of the nine FZD4 mutations were found in the highly conserved Fz-CRD domain, vital for the folding and function of Wnt receptors. The main class of Wnt receptors is the seven-pass transmembrane frizzled receptors. The clustering of FEVR-causing mutations in the extracellular Fz-CRD of FZD4 suggests a stringent requirement for the correct folding of this domain prior to export of FZD4 from the ER to the plasma membrane. The positions of the missense mutations found within the Fz-CRD of FZD4 are highly conserved in homologs and orthologs alike [210, 221, 233].

Two tyrosine kinase (TK) receptors, MuSK and ROR2 have been reported as non-conventional Wnt receptors. The P344R-MuSK mutation is also found at the heart of the CRD and shares the same Fz-CRD homology as the frizzled family of receptors (Fz1-Fz8) [21, 246]. Deletion studies of full-length *MUSK* lacking the Fz-CRD was expressed in *MUSK*$^{-/-}$ myotubes. As a result, MuSK was unable to co-cluster with rapsyn and AChRs [284]. The crystal structure of the MuSK Fz-CRD is

glycosylated and this contributes to a stabilized MuSK dimer [21] with the potential for MuSK oligomerization to elicit certain biological responses.

The RORs share significant domain similarity to MuSK receptor [285]. ROR2 contains a Fz-CRD which binds Wnt5a for activation [148]. TK receptors are activated by ligand-induced homo- and/or hetero-dimerization [286] and therefore, it is plausible that Wnt5a activates Ror2 through dimerization via the CRD [22]. Missense mutations in the Fz-CRD domain of ROR2 were also found to traffic abnormally to the ER [148].

A recent study reported a S472G missense mutation located within the first Fz-CRD of the corin protein. This missense mutation was shown to result in corin misfolding and ER-retention in preeclamptic patients [287].

The cellular mechanism of the mutations in both FZD4 and MuSK Wnt receptors has not been previously characterized. Delineating the pathogenesis of disease may have profound values for patients and the research community. The understanding of how missense mutations cause changes in a proteins structure and its maturation and how this collectively contributes to disease; helps to further unravel what lies beneath the cell. It opens doors for genetic manipulation, as discussed below, with the aim of developing new drugs or technologies that aim at treating and/or alleviating the root cause of the disease symptoms not the consequences of the disease.

Folding is a very precise process requiring fine tuning alongside chaperones in the ER. Missense mutations superimiposed on proteins change the amino acid residues which expose hydrophobic amino acid residues and therefore change the native structure of the protein as is seen with the FZD4-mutants (Table 4.1.1) and also affect the presence of a particular N-linked glycan causing misfolding or a misassembled protein as is seen with P344R-MuSK mutant. Inherited missense mutations in both FZD4 and MuSK show that there is more going on in the Fz-CRD

imposed by these missense mutations on the native structure of the protein, resulting in their mistrafficking to the ER and consequent proteasomal degradation.

The therapeutic rescue of ER-trafficking mutants has been beneficial for some mutations. Efforts in understanding how the Fz-CRD folds as previously described with other proteins such as the low density lipoprotein receptor (LDLR) [288] may be necessary to understand how chemical chaperones can target this region and prevent misfolding. This may still be as starting point for therapy. However, since these proteins harbor a common Fz-CRD motif; it is plausible to research chemical chaperones or pharmacological chaperones that target the specific cysteine residues, to preserve the pattern and support the structural disulfide bonds and cysteine residues, so as to prevent misfolding altogether.

It may be useful to adjust the reduction-oxidation potential within the ER to allow the cysteines in the Fz-CRD to fold more efficiently. The addition of an oxidizing agent in the microsomes of dogs was able to enter the ER lumen and act as cysteine reducing and oxidizing agent for influenza hemagglutinin (HA). Protein folding of HA was enhanced either by direct oxidation of disulfide bonds or by further assisting the oxidative enzymes such as the disulfide isomerase in the ER lumen [289].

The adaptive UPR could be targeted with therapeutic agents to increase the transcriptional activation of chaperones that may further support folding of the protein. It can also transiently increase protein synthesis. This will inevitably open the door for treatment. It is important to understand further how genomic elements' functional relationship has a role in phenotype formation and disease pathogenesis. In our post-genomic era, methods allowing genomic DNA sequences manipulation, visualization and regulation of gene expression are rapidly evolving. Genome editing such as TALEN (Transcription Activator-Like Effector Nucleases) [290-292] and CRISPR (Clustered Regulatory Interspaced Short Palindromic Repeats)/Cas9

systems [290, 292, 293] are reliable tools for genome engineering. They are useful for cell-based human hereditary disease modeling [290]. Here one could make a cell based model with the desired mutation incorporated in the appropriate cell lines. This would allow the visualization of the cellular processes such as chemical chaperone treatment and siRNA knowdown of ERAD components.

The method used in this study could be useful for screening missense mutations to observe which mutants are thermosensitive and therefore can be engineered for further therapeutic purposes. It also provides the groundwork for supporting and developing the search for chemical chaperones that work in the cellular milieu to promote protein folding and maturation.

## 5.3 Future work

The next step would is a major challenge in cell biology. It would be to understand the role of protein energetics and chaperone function necessary in the folding of cargo for export from the ER. Complete or partial siRNA of co-chaperone partners is a novel way to rescue the ER-retained protein. Proteomics is a growing field and has been used to assess CFTR protein interactions also known as the CFTR interactome. Wang et al. proposed the reason that ΔF508-CFTR failed to fold correctly was because the mutant was unable to fold under the dynamics set forth by the ER-chaperone folding environment known as the “chaperome”. The steady-state dynamics of the ER folding machinery were not in its favor. As a consequence, the Hsp90 co-chaperone which was shown to interact with CFTR’s protein folding in the ER was silenced to restore the energetically favorable environment for this mutant [201].

Academic laboratories are already coming together to collate and discuss the classic model for this group of trafficking conformational diseases, ΔF508-CFTR [27]. It is not enough to delineate a cellular pathogenic mechanism of disease let

alone find a novel mutation. It is more important to understand all aspects on how the mutant protein behaves *in vivo*; energetically with its chaperones, its thermodynamic properties and kinetics of folding, within its special environment. This in turn will enable researchers to fully understand how to therapeutically target the misfold or its interacting partners to promote its rescue and maturation offering a new paradigm with the aim of providing therapy for this class of proteins.

Chemical chaperones that rescued ΔF508-CFTR mutant were a result of high-throughput screening for drug discovery [294]. The extensive work carried out on the CFTR protein by researchers has made it possible to reach therapeutic targets faster than in other conformational diseases and consequently achieve greater results. This has been achieved by understanding the underlying cellular, molecular mechanisms and signaling pathways as an entity within the cell that governs ER-retained inherited diseases.

Insights from this basic research show how FEVR causing P33S, G36D, H69Y, M105T, M105V, C181R, C204R, C204Y, and G488D-FZD4 mutants and P344R-MuSK mutant cause disease. The mechanism has been delineated however, further studies will be required to finish details. Testing of the FEVR-causing mutations in *FZD4* deficient retinal cell lines and the P344R-MuSK on *MuSK* deficient myotubules are necessary to further understand how each mutant interacts in its own cellular milieu; to appreciate both the folding of Fz-CRD in the presence of the mutant and observe the stability of the mutant Fz-CRD with chemical chaperones. With the aid of current computer–based stimulations and bioinformatic tools, this is feasible. The importance of the proteins' interplay with chaperones in the ER is vital for siRNA knockdown as a target for therapy. It is important to further study interacting partners and whether these mutants interact with general chaperones, such as Bip, or specific chaperones such as the CFTR's Aha chaperone and the

Boca chaperone specific for the LRP5/6's homologue arrow in *Drosophila melanogaster;* needed for wingless signal transduction [295].

From this work, it is envisioned that more molecular players in the FZD4 and MuSK pathway will be discovered and the folding of Fz-CRD will be sought after to design molecules for improving expression and stability of the mutant proteins at the cell surface. It could possibly pave the way for discovering new molecular chaperones, pharmacological chaperones and/or chemical correctors that specifically improve the mutant expression at the cell surface and consequently offer an alternative therapeutic measure for FEVR and CMS patients, the novelty of which is mutation specific which makes it personalized or alternatively targets disorders of Fz-CRD, allowing it to target more than one disease with one treatment.

# Bibliography


1. Aridor, M., *Visiting the ER: the endoplasmic reticulum as a target for therapeutics in traffic related diseases.* Adv Drug Deliv Rev, 2007. **59**(8): p. 759-81.

2. Kleizen, B. and I. Braakman, *Protein folding and quality control in the endoplasmic reticulum.* Curr Opin Cell Biol, 2004. **16**(4): p. 343-9.

3. Helenius, A., T. Marquardt, and I. Braakman, *The endoplasmic reticulum as a protein-folding compartment.* Trends Cell Biol, 1992. **2**: p. 227-31.

4. Welch, W.J., *Role of quality control pathways in human diseases involving protein misfolding.* Semin Cell Dev Biol, 2004. **15**(1): p. 31-8.

5. de Silva, A.M., W.E. Balch, and A. Helenius, *Quality control in the endoplasmic reticulum: folding and misfolding of vesicular stomatitis virus G protein in cells and in vitro.* J Cell Biol, 1990. **111**(3): p. 857-66.

6. Araki, K. and K. Nagata, *Protein folding and quality control in the ER.* Cold Spring Harb Perspect Biol, 2011. **3**(11): p. a007526.

7. Ferris, S.P., V.K. Kodali, and R.J. Kaufman, *Glycoprotein folding and quality-control mechanisms in protein-folding diseases.* Dis Model Mech, 2014. **7**(3): p. 331-41.

8. Guerriero, C.J. and J.L. Brodsky, *The delicate balance between secreted protein folding and endoplasmic.* Physiol Rev, 2012. **92**(2): p. 537-76.

9. Nakatsukasa, K. and J.L. Brodsky, *The recognition and retrotranslocation of misfolded proteins from the endoplasmic.* Traffic, 2008. **9**(6): p. 861-70.

10. Vembar, S.S. and J.L. Brodsky, *One step at a time: endoplasmic reticulum-associated degradation.* Nat Rev Mol Cell Biol, 2008. **9**(12): p. 944-957.

11. McCracken, A.A. and J.L. Brodsky, *Assembly of ER-associated protein degradation in vitro: dependence on cytosol, calnexin, and ATP.* J Cell Biol, 1996. **132**(3): p. 291-8.

12. Ahner, A. and J.L. Brodsky, *Checkpoints in ER-associated degradation: excuse me, which way to the proteasome?* Trends Cell Biol, 2004. **14**(9): p. 474-8.

13. Sitia, R. and I. Braakman, *Quality control in the endoplasmic reticulum protein factory.* Nature, 2003. **426**(6968): p. 891-4.

14. Aridor, M. and L.A. Hannan, *Traffic jam: a compendium of human diseases that affect intracellular transport processes.* Traffic, 2000. **1**(11): p. 836-51.

15. Aridor, M. and L.A. Hannan, *Traffic jams II: an update of diseases of intracellular transport.* Traffic, 2002. **3**(11): p. 781-90.

16. Kopito, R.R., *Aggresomes, inclusion bodies and protein aggregation.* Trends Cell Biol, 2000. **10**(12): p. 524-30.

17. Kaufman, R.J., et al., *The unfolded protein response in nutrient sensing and differentiation.* Nat Rev Mol Cell Biol, 2002. **3**(6): p. 411-21.

18. Chen, Y., et al., *ER-associated protein degradation is a common mechanism underpinning numerous monogenic diseases including Robinow syndrome.* Hum Mol Genet, 2005. **14**(17): p. 2559-69.

19. Dann, C.E., et al., *Insights into Wnt binding and signalling from the structures of two Frizzled cysteine-rich domains.* Nature, 2001. **412**(6842): p. 86-90.

20. Kaykas, A., et al., *Mutant Frizzled 4 associated with vitreoretinopathy traps wild-type Frizzled in the endoplasmic reticulum by oligomerization.* Nat Cell Biol, 2004. **6**(1): p. 52-8.

21. Stiegler, A.L., S.J. Burden, and S.R. Hubbard, *Crystal structure of the frizzled-like cysteine-rich domain of the receptor tyrosine kinase MuSK.* J Mol Biol, 2009. **393**(1): p. 1-9.

22. Janda, C.Y., et al., *Structural basis of Wnt recognition by Frizzled.* Science, 2012. **337**: p. 59-64.

23. Kumar, S., et al., *Molecular dissection of Wnt3a-Frizzled8 interaction reveals essential and modulatory determinants of Wnt signaling activity.* BMC Biol, 2014. **12**: p. 44.

24. Pei, J. and N.V. Grishin, *Cysteine-rich domains related to Frizzled receptors and Hedgehog-interacting proteins.* Protein Sci, 2012. **21**: p. 1172-84.

25. Green, J.L., S.G. Kuntz, and P.W. Sternberg, *Ror receptor tyrosine kinases: orphans no more.* Trends Cell Biol, 2008. **18**: p. 536-44.

26. Amaral, M.D., *Novel personalized therapy for cystic fibrosis: treating the basic defect in all patients.* J Intern Med, 2014.

27. Peters, K.W., et al., *CFTR Folding Consortium: methods available for studies of CFTR folding and correction.* Methods Mol Biol, 2011. **742**: p. 335-53.

28. Sato, S., et al., *Glycerol reverses the misfolding phenotype of the most common cystic fibrosis mutation.* J Biol Chem, 1996. **271**(2): p. 635-8.

29. Amaral, M.D., *Therapy through chaperones: sense or antisense? Cystic fibrosis as a model disease.* J Inherit Metab Dis, 2006. **29**(2-3): p. 477-87.

30. Denning, G.M., et al., *Processing of mutant cystic fibrosis transmembrane conductance regulator is temperature-sensitive.* Nature, 1992. **358**(6389): p. 761-4.

31. Brown, C.R., et al., *Chemical chaperones correct the mutant phenotype of the delta F508 cystic.* Cell Stress Chaperones, 1996. **1**(2): p. 117-25.

32. Li, C., et al., *The cystic fibrosis mutation (delta F508) does not influence the chloride channel.* Nat Genet, 1993. **3**(4): p. 311-6.

33. Kim Chiaw, P., et al., *A chemical corrector modifies the channel function of F508del-CFTR.* Mol Pharmacol, 2010. **78**(3): p. 411-8.

34. Schwieger, I., et al., *Derlin-1 and p97/valosin-containing protein mediate the endoplasmic reticulum-associated degradation of human V2 vasopressin receptors.* Mol Pharmacol, 2007. **73**: p. 697-708.

35. Gautherot, J., et al., *Effects of cellular, chemical, and pharmacological chaperones on the rescue of a trafficking-defective mutant of the ATP-binding cassette transporter proteins ABCB1/ABCB4.* J Biol Chem, 2012. **287**(7): p. 5070-8.

36. Castanotto, D. and J.J. Rossi, *The promises and pitfalls of RNA-interference-based therapeutics.* Nature, 2009. **457**(7228): p. 426-33.

37. Sommer, T. and S. Jentsch, *A protein translocation defect linked to ubiquitin conjugation at the endoplasmic reticulum.* Nature, 1993. **365**: p. 176-9.

38. Pickart, C.M., *Mechanisms underlying ubiquitination.* Annu Rev Biochem, 2001. **70**: p. 503-33.

39. Hiller, M.M., et al., *ER degradation of a misfolded luminal protein by the cytosolic ubiquitin-proteasome pathway.* Science, 1996. **273**: p. 1725-8.

40. Jensen, T.J., et al., *Multiple proteolytic systems, including the proteasome, contribute to CFTR processing.* Cell, 1995. **83**: p. 129-35.

41. Ward, C.L., S. Omura, and R.R. Kopito, *Degradation of CFTR by the ubiquitin-proteasome pathway.* Cell, 1995. **83**: p. 121-7.

42. Jo, Y., I.Z. Hartman, and R.A. Debose-Boyd, *Ancient Ubiquitous Protein-1 Mediates Sterol-Induced Ubiquitination of HMG CoA Reductase in Lipid Droplet-Associated Endoplasmic Reticulum Membranes.* Mol Biol Cell, 2012.

43. Foresti, O., et al., *Sterol homeostasis requires regulated degradation of squalene monooxygenase by the ubiquitin ligase Doa10/Teb4.* Elife, 2013. **2**: p. e00953.

44. Pollier, J., et al., *The protein quality control system manages plant defence compound synthesis.* Nature, 2013. **504**(7478): p. 148-52.

45. Cho, J.A., et al., *Insights on the trafficking and retro-translocation of glycosphingolipid-binding bacterial toxins.* Front Cell Infect Microbiol, 2012. **2**: p. 51.

46. Taxis, C., et al., *Use of modular substrates demonstrates mechanistic diversity and reveals differences in chaperone requirement of ERAD.* J Biol Chem, 2003. **278**: p. 35903-13.

47. Christianson, J.C., et al., *Defining human ERAD networks through an integrative mapping strategy.* Nat Cell Biol, 2012. **14**(1): p. 93-105.

48. Powers, T. and P. Walter, *A ribosome at the end of the tunnel.* Science, 1997. **278**(5346): p. 2072-3.

49. Johnson, A.E. and M.A. van Waes, *The translocon: a dynamic gateway at the ER membrane.* Annu Rev Cell Dev Biol, 1999. **15**: p. 799-842.

50. Braakman, I. and D.N. Hebert, *Protein folding in the endoplasmic reticulum.* Cold Spring Harb Perspect Biol, 2013. **5**: p. a013201.

51. Saraogi, I. and S.O. Shan, *Molecular mechanism of co-translational protein targeting by the signal recognition particle.* Traffic, 2011. **12**(5): p. 535-42.

52. Woolhead, C.A., P.J. McCormick, and A.E. Johnson, *Nascent membrane and secretory proteins differ in FRET-detected folding far inside the ribosome and in their exposure to ribosomal proteins.* Cell, 2004. **116**: p. 725-36.

53. Wang, N., R. Daniels, and D.N. Hebert, *The cotranslational maturation of the type I membrane glycoprotein tyrosinase: the heat shock protein 70 system hands off to the lectin-based chaperone system.* Mol Biol Cell, 2005. **16**: p. 3740-52.

54. Land, A., D. Zonneveld, and I. Braakman, *Folding of HIV-1 envelope glycoprotein involves extensive isomerization of disulfide bonds and conformation-dependent leader peptide cleavage.* Faseb j, 2003. **17**: p. 1058-67.

55. Bonfanti, R., et al., *Insulin gene mutations as cause of diabetes in children negative for five type 1 diabetes autoantibodies.* Diabetes Care, 2008. **32**: p. 123-5.

56. Ellgaard, L. and A. Helenius, *Quality control in the endoplasmic reticulum.* Nat Rev Mol Cell Biol, 2003. **4**(3): p. 181-91.

57. Helenius, A. and M. Aebi, *Intracellular functions of N-linked* glycans*.* Science, 2001. **291**(5512): p. 2364-9.

58. Braakman, I. and D.N. Hebert, *Protein folding in the endoplasmic reticulum.* Cold Spring Harb Perspect Biol, 2013. **5**(5): p. a013201.

59. Gidalevitz, T., F. Stevens, and Y. Argon, *Orchestration of secretory protein folding by ER chaperones.* Biochim Biophys Acta, 2013. **1833**: p. 2410-24.

60. Schroder, M. and R.J. Kaufman, *The mammalian unfolded protein response.* Annu Rev Biochem, 2005. **74**: p. 739-89.

61. Ellis, R.J. and F.U. Hartl, *Principles of protein folding in the cellular environment.* Curr Opin Struct Biol, 1999. **9**: p. 102-10.

62. Kuznetsov, G., L.B. Chen, and S.K. Nigam, *Multiple molecular chaperones complex with misfolded large oligomeric glycoproteins in the endoplasmic reticulum.* J Biol Chem, 1997. **272**: p. 3057-63.

63. Helenius, A., *How N-linked oligosaccharides affect glycoprotein folding in the endoplasmic reticulum.* Mol Biol Cell, 1994. **5**(3): p. 253-65.

64. Kornfeld, R. and S. Kornfeld, *Assembly of asparagine-linked oligosaccharides.* Annu Rev Biochem, 1985. **54**: p. 631-64.

65. Allen, S., H.Y. Naim, and N.J. Bulleid, *Intracellular folding of tissue-type plasminogen activator. Effects of disulfide bond formation on N-linked glycosylation and secretion.* J Biol Chem, 1995. **270**(9): p. 4797-804.

66. Schulz, B.L., et al., *Oxidoreductase activity of oligosaccharyltransferase subunits Ost3p and Ost6p defines site-specific glycosylation efficiency.* Proc Natl Acad Sci U S A, 2009. **106**(27): p. 11061-6.

67. Jaeken, J., *Congenital disorders of glycosylation.* Ann N Y Acad Sci, 2010. **1214**: p. 190-8.

68. Zielinska, D.F., et al., *Precision mapping of an in vivo N-glycoproteome reveals rigid topological and sequence constraints.* Cell, 2010. **141**(5): p. 897-907.

69. Dejgaard, S., et al., *The ER glycoprotein quality control system.* Curr Issues Mol Biol, 2004. **6**(1): p. 29-42.

70. Mohorko, E., R. Glockshuber, and M. Aebi, *Oligosaccharyltransferase: the central enzyme of N-linked protein glycosylation.* J Inherit Metab Dis, 2011. **34**(4): p. 869-78.

71. Hebert, D.N. and M. Molinari, *Flagging and docking: dual roles for N*-glycans *in protein quality control and cellular proteostasis.* Trends Biochem Sci, 2012. **37**: p. 404-10.

72. Helenius, A. and M. Aebi, *Roles of N-linked* glycans *in the endoplasmic reticulum.* Annu Rev Biochem, 2004. **73**: p. 1019-49.

73. Hanson, S.R., et al., *The core trisaccharide of an N-linked glycoprotein intrinsically accelerates folding and enhances stability.* Proc Natl Acad Sci U S A, 2009. **106**: p. 3131-6.

74. Schrag, J.D., et al., *Lectin control of protein folding and sorting in the secretory pathway.* Trends Biochem Sci, 2003. **28**(1): p. 49-57.

75. Pearse, B.R. and D.N. Hebert, *Lectin chaperones help direct the maturation of glycoproteins in the endoplasmic reticulum.* Biochim Biophys Acta, 2010. **1803**(6): p. 684-93.

76. Schallus, T., et al., *Malectin: a novel carbohydrate-binding protein of the endoplasmic reticulum and a candidate player in the early steps of protein N-glycosylation.* Mol Biol Cell, 2008. **19**(8): p. 3404-14.

77. Olson, L.J., et al., *Structure of the lectin mannose 6-phosphate receptor homology (MRH) domain of glucosidase II, an enzyme that regulates glycoprotein folding quality control in the endoplasmic reticulum.* J Biol Chem, 2013. **288**: p. 16460-75.

78. Hammond, C., I. Braakman, and A. Helenius, *Role of N-linked oligosaccharide recognition, glucose trimming, and calnexin in glycoprotein folding and quality control.* Proc Natl Acad Sci U S A, 1994. **91**(3): p. 913-7.

79. Schrag, J.D., et al., *The Structure of calnexin, an ER chaperone involved in quality control of protein folding.* Mol Cell, 2001. **8**: p. 633-44.

80. Wang, W.A., J. Groenendyk, and M. Michalak, *Calreticulin signaling in health and disease.* Int J Biochem Cell Biol, 2012. **44**: p. 842-6.

81. Kozlov, G., et al., *Structural basis of carbohydrate recognition by calreticulin.* J Biol Chem, 2010. **285**: p. 38612-20.

82. Molinari, M., et al., *Contrasting functions of calreticulin and calnexin in glycoprotein folding and ER quality control.* Mol Cell, 2004. **13**: p. 125-35.

83. Van den Berg, B., et al., *X-ray structure of a protein-conducting channel.* Nature, 2003. **427**: p. 36-44.

84. Chouquet, A., et al., *X-ray structure of the human calreticulin globular domain reveals a peptide-binding area and suggests a multi-molecular mechanism.* PLoS One, 2011. **6**: p. e17886.

85. Frickel, E.M., et al., *TROSY-NMR reveals interaction between ERp57 and the tip of the calreticulin P-domain.* Proc Natl Acad Sci U S A, 2002. **99**: p. 1954-9.

86. Kozlov, G., et al., *Structural basis of cyclophilin B binding by the calnexin/calreticulin P-domain.* J Biol Chem, 2010. **285**: p. 35551-7.

87. Bukau, B., J. Weissman, and A. Horwich, *Molecular chaperones and protein quality control.* Cell, 2006. **125**: p. 443-51.

88. Tu, B.P. and J.S. Weissman, *Oxidative protein folding in eukaryotes: mechanisms and consequences.* J Cell Biol, 2004. **164**: p. 341-6.

89. Goldberger, R.F., C.J. Epstein, and C.B. Anfinsen, *Acceleration of reactivation of reduced bovine pancreatic ribonuclease by a microsomal system from rat liver.* J Biol Chem, 1963. **238**: p. 628-35.

90. Oka, O.B., et al., *ERdj5 is the ER reductase that catalyzes the removal of non-native disulfides and correct folding of the LDL receptor.* Mol Cell, 2013. **50**: p. 793-804.

91. Frand, A.R. and C.A. Kaiser, *Ero1p oxidizes protein disulfide isomerase in a pathway for disulfide bond formation in the endoplasmic reticulum.* Mol Cell, 1999. **4**: p. 469-77.

92. Benham, A.M., et al., *Ero1-PDI interactions, the response to redox flux and the implications for disulfide bond formation in the mammalian endoplasmic reticulum.* Philos Trans R Soc Lond B Biol Sci, 2013. **368**(1617): p. 20110403.

93. van Anken, E., et al., *Sequential waves of functionally related proteins are expressed when B cells prepare for antibody secretion.* Immunity, 2003. **18**: p. 243-53.

94. Klappa, P., R.B. Freedman, and R. Zimmermann, *Protein disulphide isomerase and a lumenal cyclophilin-type peptidyl prolyl cis-trans isomerase are in transient contact with secretory proteins during late stages of translocation.* Eur J Biochem, 1995. **232**: p. 755-64.

95. Barik, S., *Immunophilins: for the love of proteins.* Cell Mol Life Sci, 2006. **63**(24): p. 2889-900.

96. Pappenberger, G., et al., *Nonprolyl cis peptide bonds in unfolded proteins cause complex folding kinetics.* Nat Struct Biol, 2001. **8**: p. 452-8.

97. D'Alessio, C., J.J. Caramelo, and A.J. Parodi, *UDP-GlC:glycoprotein glucosyltransferase-glucosidase II, the ying-yang of the ER quality control.* Semin Cell Dev Biol, 2010. **21**: p. 491-9.

98. Sousa, M. and A.J. Parodi, *The molecular basis for the recognition of misfolded glycoproteins by the UDP-Glc:glycoprotein glucosyltransferase.* Embo j, 1995. **14**: p. 4196-203.

99. Ritter, C. and A. Helenius, *Recognition of local glycoprotein misfolding by the ER folding sensor UDP-glucose:glycoprotein glucosyltransferase.* Nat Struct Biol, 2000. **7**: p. 278-80.

100. Taylor, S.C., et al., *The ER protein folding sensor UDP-glucose glycoprotein-glucosyltransferase modifies substrates distant to local changes in glycoprotein conformation.* Nat Struct Mol Biol, 2004. **11**: p. 128-34.

101. Zapun, A., et al., *Enhanced catalysis of ribonuclease B folding by the interaction of calnexin or calreticulin with ERp57.* J Biol Chem, 1998. **273**(11): p. 6009-12.

102. Xu, C., et al., *Futile protein folding cycles in the ER are terminated by the unfolded protein O-mannosylation pathway.* Science, 2013. **340**: p. 978-81.

103. Kleizen, B. and I. Braakman, *Cell biology. A sweet send-off.* Science, 2013. **340**: p. 930-1.

104. Sekijima, Y., et al., *The biological and chemical basis for tissue-selective amyloid disease.* Cell, 2005. **121**(1): p. 73-85.

105. Brodsky, J.L. and A.A. McCracken, *ER protein quality control and proteasome-mediated protein degradation.* Semin Cell Dev Biol, 1999. **10**(5): p. 507-13.

106. Warren, G. and I. Mellman, *Bulk flow redux?* Cell, 1999. **98**: p. 125-7.

107. Moremen, K.W., *Golgi alpha-mannosidase II deficiency in vertebrate systems: implications for asparagine-linked oligosaccharide processing in mammals.* Biochim Biophys Acta, 2002. **1573**: p. 225-35.

108. Arvan, P., et al., *Secretory pathway quality control operating in Golgi, plasmalemmal, and endosomal systems.* Traffic, 2002. **3**: p. 771-80.

109. Barlowe, C., *Signals for COPII-dependent export from the ER: what's the ticket out?* Trends Cell Biol, 2003. **13**(6): p. 295-300.

110. Kostova, Z. and D.H. Wolf, *For whom the bell tolls: protein quality control of the endoplasmic reticulum and the ubiquitin-proteasome connection.* EMBO J, 2003. **22**(10): p. 2309-17.

111. Plemper, R.K. and D.H. Wolf, *Retrograde protein translocation: ERADication of secretory proteins in health and disease.* Trends Biochem Sci, 1999. **24**(7): p. 266-70.

112. Sommer, T. and D.H. Wolf, *Endoplasmic reticulum degradation: reverse protein flow of no return.* FASEB J, 1997. **11**(14): p. 1227-33.

113. Tsai, Y.C. and A.M. Weissman, *The Unfolded Protein Response, Degradation from Endoplasmic Reticulum and Cancer.* Genes Cancer, 2010. **1**(7): p. 764-778.

114. Niforou, K., C. Cheimonidou, and I.P. Trougakos, *Molecular chaperones and proteostasis regulation during redox imbalance.* Redox Biol, 2014. **2**: p. 323-32.

115. Wang, S. and R.J. Kaufman, *The impact of the unfolded protein response on human disease.* J Cell Biol, 2012. **197**(7): p. 857-67.

116. Ruggiano, A., O. Foresti, and P. Carvalho, *Quality control: ER-associated degradation: protein quality control and beyond.* J Cell Biol, 2014. **204**(6): p. 869-79.

117. Bernasconi, R. and M. Molinari, *ERAD and ERAD tuning: disposal of cargo and of ERAD regulators from the mammalian ER.* Current Opinion in Cell Biology, 2011. **23**(2): p. 176-183.

118. Fewell, S.W., et al., *The action of molecular chaperones in the early secretory pathway.* Annu Rev Genet, 2001. **35**: p. 149-91.

119. Malhotra, J.D. and R.J. Kaufman, *The endoplasmic reticulum and the unfolded protein response.* Semin Cell Dev Biol, 2007. **18**(6): p. 716-31.

120. Bertolotti, A., et al., *Dynamic interaction of BiP and ER stress transducers in the unfolded-protein response.* Nat Cell Biol, 2000. **2**(6): p. 326-32.

121. Yoshida, H., et al., *XBP1 mRNA is induced by ATF6 and spliced by IRE1 in response to ER stress to produce a highly active transcription factor.* Cell, 2001. **107**(7): p. 881-91.

122. Zinszner, H., et al., *CHOP is implicated in programmed cell death in response to impaired function of the endoplasmic reticulum.* Genes Dev, 1998. **12**(7): p. 982-95.

123. Haze, K., et al., *Mammalian transcription factor ATF6 is synthesized as a transmembrane protein and activated by proteolysis in response to endoplasmic reticulum stress.* Mol Biol Cell, 1999. **10**(11): p. 3787-99.

124. Oda, Y., et al., *Derlin-2 and Derlin-3 are regulated by the mammalian unfolded protein response and are required for ER-associated degradation.* J Cell Biol, 2006. **172**(3): p. 383-93.

125. Maattanen, P., et al., *Protein quality control in the ER: the recognition of misfolded proteins.* Semin Cell Dev Biol, 2010. **21**(5): p. 500-11.

126. Anelli, T. and R. Sitia, *Protein quality control in the early secretory pathway.* EMBO J, 2008. **27**(2): p. 315-27.

127. Olzmann, J.A., R.R. Kopito, and J.C. Christianson, *The mammalian endoplasmic reticulum-associated degradation system.* Cold Spring Harb Perspect Biol, 2012. **5**.

128. Gonzalez, D.S., et al., *Identification, expression, and characterization of a cDNA encoding human endoplasmic reticulum mannosidase I, the enzyme that catalyzes the first mannose trimming step in mammalian Asn-linked oligosaccharide biosynthesis.* J Biol Chem, 1999. **274**: p. 21375-86.

129. Olivari, S. and M. Molinari, *Glycoprotein folding and the role of EDEM1, EDEM2 and EDEM3 in degradation of folding-defective glycoproteins.* FEBS Lett, 2007. **581**: p. 3658-64.

130. Kanehara, K., S. Kawaguchi, and D.T. Ng, *The EDEM and Yos9p families of lectin-like ERAD factors.* Semin Cell Dev Biol, 2007. **18**: p. 743-50.

131. Hosokawa, N., et al., *Human XTP3-B forms an endoplasmic reticulum quality control scaffold with the HRD1-SEL1L ubiquitin ligase complex and BiP.* J Biol Chem, 2008. **283**(30): p. 20914-24.

132. Deshaies, R.J. and C.A. Joazeiro, *RING domain E3 ubiquitin ligases.* Annu Rev Biochem, 2009. **78**: p. 399-434.

133. Gardner, R.G., et al., *Endoplasmic reticulum degradation requires lumen to cytosol signaling. Transmembrane control of Hrd1p by Hrd3p.* J Cell Biol, 2000. **151**(1): p. 69-82.

134. Schulman, B.A. and J.W. Harper, *Ubiquitin-like protein activation by E1 enzymes: the apex for downstream signalling pathways.* Nat Rev Mol Cell Biol, 2009. **10**: p. 319-31.

135. Lemus, L. and V. Goder, *Regulation of Endoplasmic Reticulum-Associated Protein Degradation (ERAD) by Ubiquitin.* Cells, 2014. **3**: p. 824-47.

136. Hirsch, C., et al., *The ubiquitylation machinery of the endoplasmic reticulum.* Nature, 2009. **458**: p. 453-60.

137. Gauss, R., T. Sommer, and E. Jarosch, *The Hrd1p ligase complex forms a linchpin between ER-lumenal substrate selection and Cdc48p recruitment.* Embo j, 2006. **25**(9): p. 1827-35.

138. Kostova, Z., Y.C. Tsai, and A.M. Weissman, *Ubiquitin ligases, critical mediators of endoplasmic reticulum-associated degradation.* Semin Cell Dev Biol, 2007. **18**: p. 770-9.

139. Garza, R.M., B.K. Sato, and R.Y. Hampton, *In vitro analysis of Hrd1p-mediated retrotranslocation of its multispanning membrane substrate 3-hydroxy-3-methylglutaryl (HMG)-CoA reductase.* J Biol Chem, 2009. **284**: p. 14710-22.

140. Hampton, R.Y. and T. Sommer, *Finding the will and the way of ERAD substrate retrotranslocation.* Curr Opin Cell Biol, 2012. **24**: p. 460-6.

141. Wahlman, J., et al., *Real-time fluorescence detection of ERAD substrate retrotranslocation in a mammalian in vitro system.* Cell, 2007. **129**: p. 943-55.

142. Schafer, A. and D.H. Wolf, *Sec61p is part of the endoplasmic reticulum-associated degradation machinery.* Embo j, 2009. **28**: p. 2874-84.

143. Wilcox, A.J. and J.D. Laney, *A ubiquitin-selective AAA-ATPase mediates transcriptional switching by remodelling a repressor-promoter DNA complex.* Nat Cell Biol, 2009. **11**: p. 1481-6.

144. Elsasser, S. and D. Finley, *Delivery of ubiquitinated substrates to protein-unfolding machines.* Nat Cell Biol, 2005. **7**: p. 742-9.

145. Carvalho, P., A.M. Stanley, and T.A. Rapoport, *Retrotranslocation of a misfolded luminal ER protein by the ubiquitin-ligase Hrd1p.* Cell, 2010. **143**(4): p. 579-91.

146. Romisch, K. and B.R. Ali, *Similar processes mediate glycopeptide export from the endoplasmic reticulum in mammalian cells and Saccharomyces cerevisiae.* Proc Natl Acad Sci U S A, 1997. **94**(13): p. 6730-4.

147. Cabral, C.M., Y. Liu, and R.N. Sifers, *Dissecting glycoprotein quality control in the secretory pathway.* Trends Biochem Sci, 2001. **26**(10): p. 619-24.

148. Ali, B.R., et al., *Novel Robinow syndrome causing mutations in the proximal region of the frizzled-like domain of ROR2 are retained in the endoplasmic reticulum.* Hum Genet, 2007. **122**(3-4): p. 389-95.

149. Ali, B.R., et al., *Trafficking defects and loss of ligand binding are the underlying causes of all reported DDR2 missense mutations found in SMED-SL patients.* Hum Mol Genet, 2010. **19**(11): p. 2239-50.

150. Afzal, A.R., et al., *Recessive Robinow syndrome, allelic to dominant brachydactyly type B, is caused by mutation of ROR2.* Nat Genet, 2000. **25**(4): p. 419-22.

151. Ali, B.R., et al., *Endoplasmic reticulum quality control is involved in the mechanism of endoglin-mediated hereditary haemorrhagic telangiectasia.* PLoS One, 2011. **6**(10): p. e26206.

152. Logan, C.Y. and R. Nusse, *The Wnt signaling pathway in development and disease.* Annu Rev Cell Dev Biol, 2004. **20**: p. 781-810.

153. Bhat, R.A., et al., *Wnt3-frizzled 1 chimera as a model to study canonical Wnt signaling.* J Cell Biochem, 2010. **109**(5): p. 876-84.

154. Jing, L., et al., *Wnt signals organize synaptic prepattern and axon guidance through the zebrafish unplugged/MuSK receptor.* Neuron, 2009. **61**: p. 721-33.

155. Speese, S.D. and V. Budnik, *Wnts: up-and-coming at the synapse.* Trends Neurosci, 2007. **30**: p. 268-75.

156. Tatzelt, J., S.B. Prusiner, and W.J. Welch, *Chemical chaperones interfere with the formation of scrapie prion protein.* Embo j, 1996. **15**: p. 6363-73.

157. Brown, C.R., et al., *Chemical chaperones correct the mutant phenotype of the delta F508 cystic fibrosis transmembrane conductance regulator protein.* Cell Stress Chaperones, 1996. **1**: p. 117-25.

158. Burrows, J.A., L.K. Willis, and D.H. Perlmutter, *Chemical chaperones mediate increased secretion of mutant alpha 1-antitrypsin (alpha 1-AT) Z: A potential pharmacological strategy for prevention of liver injury and emphysema in alpha 1-AT deficiency.* Proc Natl Acad Sci U S A, 2000. **97**: p. 1796-801.

159. Tamarappoo, B.K. and A.S. Verkman, *Defective aquaporin-2 trafficking in nephrogenic diabetes insipidus and correction by chemical chaperones.* J Clin Invest, 1998. **101**: p. 2257-67.

160. Robben, J.H., et al., *Rescue of vasopressin V2 receptor mutants by chemical chaperones: specificity and.* Mol Biol Cell, 2006. **17**(1): p. 379-86.

161. Chapple, J.P., et al., *Unfolding retinal dystrophies: a role for molecular chaperones?* Trends Mol Med, 2001. **7**: p. 414-21.

162. Tachikawa, M., et al., *Mislocalization of fukutin protein by disease-causing missense mutations can be rescued with treatments directed at folding amelioration.* Journal of Biological Chemistry, 2012. **287**(11): p. 8398-8406.

163. Chaudhuri, T.K. and S. Paul, *Protein-misfolding diseases and chaperone-based therapeutic approaches.* Febs j, 2006. **273**(7): p. 1331-49.

164. Loo, T.W. and D.M. Clarke, *Correction of defective protein kinesis of human P-glycoprotein mutants by substrates and modulators.* J Biol Chem, 1997. **272**: p. 709-12.

165. Mendes, F., et al., *Establishment and characterization of a novel polarized MDCK epithelial cellular model for CFTR studies.* Cell Physiol Biochem, 2005. **16**(4-6): p. 281-90.

166. Chu, C.Y., et al., *Functional rescue of a kidney anion exchanger 1 trafficking mutant in renal epithelial cells.* PLoS One, 2013. **8**(2): p. e57062.

167. Egan, M.E., et al., *Calcium-pump inhibitors induce functional surface expression of Delta F508-CFTR.* Nat Med, 2002. **8**(5): p. 485-92.

168. Al-Fageeh, M.B., et al., *The cold-shock response in cultured mammalian cells: harnessing the response for the improvement of recombinant protein production.* Biotechnol Bioeng, 2006. **93**(5): p. 829-35.

169. Rieder, C.L. and R.W. Cole, *Cold-shock and the Mammalian cell cycle.* Cell Cycle, 2002. **1**(3): p. 169-75.

170. Tachikawa, M., et al., *Mislocalization of fukutin protein by disease-causing missense mutations can be.* J Biol Chem, 2012. **287**(11): p. 8398-406.

171. Yu, R., et al., *Rescue of a pathogenic mutant human glucagon receptor by pharmacological chaperones.* J Mol Endocrinol, 2012. **49**: p. 69-78.

172. Ding, W.G., et al., *Improved functional expression of human cardiac kv1.5 channels and trafficking-defective mutants by low temperature treatment.* PLoS One, 2014. **9**(3): p. e92923.

173. Gekko, K. and S.N. Timasheff, *Mechanism of protein stabilization by glycerol: preferential hydration in glycerol-water mixtures.* Biochemistry, 1981. **20**: p. 4667-76.

174. Leandro, P., et al., *Glycerol increases the yield and activity of human phenylalanine hydroxylase mutant enzymes produced in a prokaryotic expression system.* Mol Genet Metab, 2001. **73**: p. 173-8.

175. Sawano, H., et al., *Efficient in vitro folding of the three-disulfide derivatives of hen lysozyme in the presence of glycerol.* FEBS Lett, 1992. **303**: p. 11-4.

176. Shelanski, M.L., F. Gaskin, and C.R. Cantor, *Microtubule assembly in the absence of added nucleotides.* Proc Natl Acad Sci U S A, 1973. **70**: p. 765-8.

177. Fuller, W. and A.W. Cuthbert, *Post-translational disruption of the delta F508 cystic fibrosis transmembrane conductance regulator (CFTR)-molecular chaperone complex with geldanamycin stabilizes delta F508 CFTR in the rabbit reticulocyte lysate.* J Biol Chem, 2000. **275**: p. 37462-8.

178. Choo-Kang, L.R. and P.L. Zeitlin, *Induction of HSP70 promotes DeltaF508 CFTR trafficking.* Am J Physiol Lung Cell Mol Physiol, 2001. **281**: p. L58-68.

179. Shearer, A.G. and R.Y. Hampton, *Structural control of endoplasmic reticulum-associated degradation: effect of chemical chaperones on 3-hydroxy-3-methylglutaryl-CoA reductase.* J Biol Chem, 2003. **279**: p. 188-96.

180. Fan, Y.Q., et al., *Effects of osmolytes on human brain-type creatine kinase folding in dilute solutions and crowding systems.* Int J Biol Macromol, 2012. **51**(5): p. 845-58.

181. Zhang, X.M., et al., *Organic solutes rescue the functional defect in delta F508 cystic fibrosis.* J Biol Chem, 2003. **278**(51): p. 51232-42.

182. Song, J.L. and D.T. Chuang, *Natural osmolyte trimethylamine N-oxide corrects assembly defects of mutant.* J Biol Chem, 2001. **276**(43): p. 40241-6.

183. Egan, M.E., et al., *Curcumin, a major constituent of turmeric, corrects cystic fibrosis defects.* Science, 2004. **304**(5670): p. 600-2.

184. Roy, S., B. Jana, and B. Bagchi, *Dimethyl sulfoxide induced structural transformations and non-monotonic concentration dependence of conformational fluctuation around active site of lysozyme.* J Chem Phys, 2012. **136**: p. 115103.

185. Yoshida, H., et al., *Chemical chaperones reduce aggregate formation and cell death caused by the truncated Machado-Joseph disease gene product with an expanded polyglutamine stretch.* Neurobiol Dis, 2002. **10**: p. 88-99.

186. Simoes-Correia, J., et al., *Endoplasmic reticulum quality control: a new mechanism of E-cadherin regulation and its implication in cancer.* Hum Mol Genet, 2008. **17**: p. 3566-76.

187. Lee, S.A., O.V. Belyaeva, and N.Y. Kedishvili, *Evidence that proteosome inhibitors and chemical chaperones can rescue the activity of retinol dehydrogenase 12 mutant T49M.* Chem Biol Interact, 2011. **191**: p. 55-9.

188. Yu, Y.C., et al., *Curcumin and genistein additively potentiate G551D-CFTR.* J Cyst Fibros, 2011. **10**(4): p. 243-52.

189. Mall, M. and K. Kunzelmann, *Correction of the CF defect by curcumin: hypes and disappointments.* Bioessays, 2005. **27**(1): p. 9-13.

190. Hafner-Bratkovic, I., et al., *Curcumin binds to the alpha-helical intermediate and to the amyloid form of prion protein - a new mechanism for the inhibition of PrP(Sc) accumulation.* J Neurochem, 2007. **104**: p. 1553-64.

191. Ono, K. and M. Yamada, *Antioxidant compounds have potent anti-fibrillogenic and fibril-destabilizing effects for alpha-synuclein fibrils in vitro.* J Neurochem, 2006. **97**: p. 105-15.

192. Yu, W., P. Kim Chiaw, and C.E. Bear, *Probing conformational rescue induced by a chemical corrector of F508del-cystic fibrosis transmembrane conductance regulator (CFTR) mutant.* J Biol Chem, 2011. **286**(28): p. 24714-25.

193. Ren, H.Y., et al., *VX-809 corrects folding defects in cystic fibrosis transmembrane conductance regulator protein through action on membrane-spanning domain 1.* Mol Biol Cell, 2013. **24**: p. 3016-24.

194. Odolczyk, N., et al., *Discovery of novel potent DeltaF508-CFTR correctors that target the nucleotide binding domain.* EMBO Mol Med, 2013. **5**: p. 1484-501.

195. Pedemonte, N., et al., *Small-molecule correctors of defective DeltaF508-CFTR cellular processing identified by high-throughput screening.* J Clin Invest, 2005. **115**: p. 2564-71.

196. Van Goor, F., et al., *Rescue of DeltaF508-CFTR trafficking and gating in human cystic fibrosis airway primary cultures by small molecules.* Am J Physiol Lung Cell Mol Physiol, 2006. **290**: p. L1117-30.

197. Clancy, J.P., et al., *Results of a phase IIa study of VX-809, an investigational CFTR corrector compound, in subjects with cystic fibrosis homozygous for the F508del-CFTR mutation.* Thorax, 2011. **67**: p. 12-8.

198. Fan, J.Q., et al., *Accelerated transport and maturation of lysosomal alpha-galactosidase A in Fabry.* Nat Med, 1999. **5**(1): p. 112-5.

199. Hamanaka, R., et al., *Rescue of mutant alpha-galactosidase A in the endoplasmic reticulum by.* Biochim Biophys Acta, 2008. **1782**(6): p. 408-13.

200. Merulla, J., et al., *Specificity and regulation of the endoplasmic reticulum-associated degradation machinery.* Traffic, 2013. **14**(7): p. 767-77.

201. Wang, X., et al., *Hsp90 cochaperone Aha1 downregulation rescues misfolding of CFTR in cystic fibrosis.* Cell, 2006. **127**(4): p. 803-15.

202. Harada, K., et al., *Curcumin enhances cystic fibrosis transmembrane regulator expression by down-regulating calreticulin.* Biochem Biophys Res Commun, 2007. **353**(2): p. 351-6.

203. Ali, B.R., et al., *A novel statin-mediated "prenylation block-and-release" assay provides insight into the membrane targeting mechanisms of small GTPases.* Biochem Biophys Res Commun, 2010. **397**: p. 34-41.

204. Schindelin, J., et al., *Fiji: an open-source platform for biological-image analysis.* Nat Methods, 2012. **9**(7): p. 676-82.

205. Patrick, G.N., et al., *p35, the neuronal-specific activator of cyclin-dependent kinase 5 (Cdk5) is degraded by the ubiquitin-proteasome pathway.* J Biol Chem, 1998. **273**: p. 24057-64.

206. Swerdlow, P.S., D. Finley, and A. Varshavsky, *Enhancement of immunoblot sensitivity by heating of hydrated filters.* Anal Biochem, 1986. **156**(1): p. 147-53.

207. Pendergast, S.D., et al., *Study of the Norrie disease gene in 2 patients with bilateral persistent hyperplastic primary vitreous.* Arch Ophthalmol, 1998. **116**(3): p. 381-2.

208. Norrie, G., *Causes of blindness in children.* Acta Ophthalmology, 1927. **5**(1-3): p. 357-386.

209. van Nouhuys, C.E., *Signs, complications, and platelet aggregation in familial exudative vitreoretinopathy.* Am J Ophthalmol, 1991. **111**(1): p. 34-41.

210. Kondo, H., et al., *Frizzled 4 gene (FZD4) mutations in patients with familial exudative vitreoretinopathy with variable expressivity.* Br J Ophthalmol, 2003. **87**(10): p. 1291-5.

211. Zhang, K., et al., *An essential role of the cysteine-rich domain of FZD4 in Norrin/Wnt signaling and.* J Biol Chem, 2011. **286**(12): p. 10210-5.

212. Ye, X., Y. Wang, and J. Nathans, *The Norrin/Frizzled4 signaling pathway in retinal vascular development and.* Trends Mol Med, 2010. **16**(9): p. 417-25.

213. Ye, X., et al., *Norrin, frizzled-4, and Lrp5 signaling in endothelial cells controls a genetic.* Cell, 2009. **139**(2): p. 285-98.

214. Smallwood, P.M., et al., *Mutational analysis of Norrin-Frizzled4 recognition.* J Biol Chem, 2007. **282**(6): p. 4057-68.

215. Stenson, P.D., et al., *Human Gene Mutation Database (HGMD): 2003 update.* Hum Mutat, 2003. **21**(6): p. 577-81.

216. Kondo, H., et al., *Severe form of familial exudative vitreoretinopathy caused by homozygous R417Q mutation in frizzled-4 gene.* Ophthalmic Genet, 2007. **28**(4): p. 220-3.

217. Lemma, V., et al., *A disorder-to-order structural transition in the COOH-tail of Fz4 determines misfolding of the L501fsX533-Fz4 mutant.* Sci Rep, 2013. **3**: p. 2659.

218. Li, P., et al., *Karyotype-phenotype insights from 11q14.1-q23.2 interstitial deletions: FZD4 haploinsufficiency and exudative vitreoretinopathy in a patient with a complex chromosome rearrangement.* Am J Med Genet A, 2006. **140**(24): p. 2721-9.

219. MacDonald, M.L., et al., *Genetic variants of frizzled-4 gene in familial exudative vitreoretinopathy and advanced retinopathy of prematurity.* Clin Genet, 2005. **67**(4): p. 363-6.

220. Toomes, C., et al., *Spectrum and frequency of FZD4 mutations in familial exudative vitreoretinopathy.* Invest Ophthalmol Vis Sci, 2004. **45**(7): p. 2083-90.

221. Omoto, S., et al., *Autosomal dominant familial exudative vitreoretinopathy in two Japanese families with FZD4 mutations (H69Y and C181R).* Ophthalmic Genet, 2004. **25**(2): p. 81-90.

222. Nikopoulos, K., et al., *Overview of the mutation spectrum in familial exudative vitreoretinopathy and Norrie disease with identification of 21 novel variants in FZD4, LRP5, and NDP.* Hum Mutat, 2010. **31**(6): p. 656-66.

223. Nallathambi, J., et al., *Identification of novel FZD4 mutations in Indian patients with familial exudative vitreoretinopathy.* Mol Vis, 2006. **12**: p. 1086-92.

224. Xu, Q., et al., *Vascular development in the retina and inner ear: control by Norrin and Frizzled-4, a high-affinity ligand-receptor pair.* Cell, 2004. **116**(6): p. 883-95.

225. Robitaille, J., et al., *Mutant frizzled-4 disrupts retinal angiogenesis in familial exudative vitreoretinopathy.* Nat Genet, 2002. **32**(2): p. 326-30.

226. Burrus, L.W. and A.P. McMahon, *Biochemical analysis of murine Wnt proteins reveals both shared and distinct properties.* Exp Cell Res, 1995. **220**(2): p. 363-73.

227. Devesa, I., G. Fernandez-Ballester, and A. Ferrer-Montiel, *Targeting protein-protein interactions to rescue Deltaf508-cftr: a novel corrector approach to treat cystic fibrosis.* EMBO Mol Med, 2013. **5**(10): p. 1462-4.

228. Hanrahan, J.W., H.M. Sampson, and D.Y. Thomas, *Novel pharmacological strategies to treat cystic fibrosis.* Trends Pharmacol Sci, 2013. **34**(2): p. 119-25.

229. Rowe, S.M. and A.S. Verkman, *Cystic fibrosis transmembrane regulator correctors and potentiators.* Cold Spring Harb Perspect Med, 2013. **3**(7).

230. Plemper, R.K., et al., *Genetic interactions of Hrd3p and Der3p/Hrd1p with Sec61p suggest a retro-translocation complex mediating protein transport for ER degradation.* J Cell Sci, 1999. **112 ( Pt 22)**: p. 4123-34.

231. Petersen, T.N., et al., *SignalP 4.0: discriminating signal peptides from transmembrane regions.* Nat Methods, 2011. **8**(10): p. 785-6.

232. Rajan, S., et al., *In vitro processing and secretion of mutant insulin proteins that cause permanent neonatal diabetes.* Am J Physiol Endocrinol Metab, 2009. **298**: p. E403-10.

233. Jia, L.Y., et al., *Novel frizzled-4 gene mutations in chinese patients with familial exudative vitreoretinopathy.* Arch Ophthalmol, 2010. **128**(10): p. 1341-9.

234. Ke, J., et al., *Structure and function of Norrin in assembly and activation of a Frizzled 4-Lrp5/6 complex.* Genes Dev, 2013. **27**(21): p. 2305-19.

235. Carron, C., et al., *Frizzled receptor dimerization is sufficient to activate the Wnt/beta-catenin pathway.* J Cell Sci, 2003. **116**(Pt 12): p. 2541-50.

236. Thrower, J.S., et al., *Recognition of the polyubiquitin proteolytic signal.* Embo j, 2000. **19**(1): p. 94-102.

237. Engel, A.G., *Current status of the congenital myasthenic syndromes.* Neuromuscul Disord, 2011.

238. Maselli, R.A., et al., *Mutations in MUSK causing congenital myasthenic syndrome impair MuSK-Dok-7 interaction.* Hum Mol Genet, 2010. **19**(12): p. 2370-9.

239. Chevessier, F., et al., *MUSK, a new target for mutations causing congenital myasthenic syndrome.* Hum Mol Genet, 2004. **13**(24): p. 3229-40.

240. Mihaylova, V., et al., *Refinement of the clinical phenotype in musk-related congenital myasthenic syndromes.* Neurology, 2009. **73**(22): p. 1926-8.

241. Ben Ammar, A., et al., *A mutation causes MuSK reduced sensitivity to agrin and congenital myasthenia.* PLoS One, 2013. **8**(1): p. e53826.

242. Eymard, B., D. Hantai, and B. Estournet, *Congenital myasthenic syndromes.* Handb Clin Neurol, 2013. **113**: p. 1469-80.

243. Masiakowski, P. and G.D. Yancopoulos, *The Wnt receptor CRD domain is also found in MuSK and related orphan receptor tyrosine kinases.* Curr Biol, 1998. **8**(12): p. R407.

244. Jennings, C.G., S.M. Dyer, and S.J. Burden, *Muscle-specific trk-related receptor with a kringle domain defines a distinct class of receptor tyrosine kinases.* Proc Natl Acad Sci U S A, 1993. **90**(7): p. 2895-9.

245. Xu, Y.K. and R. Nusse, *The Frizzled CRD domain is conserved in diverse proteins including several receptor tyrosine kinases.* Curr Biol, 1998. **8**(12): p. R405-6.

246. DeChiara, T.M., et al., *The receptor tyrosine kinase MuSK is required for neuromuscular junction formation in vivo.* Cell, 1996. **85**(4): p. 501-12.

247. Strochlic, L., et al., *Wnt4 participates in the formation of vertebrate neuromuscular junction.* PLoS One, 2012. **7**(1): p. e29976.

248. Kim, N., et al., *Lrp4 is a receptor for Agrin and forms a complex with MuSK.* Cell, 2008. **135**(2): p. 334-42.

249. Gallenmuller, C., et al., *Salbutamol-responsive limb-girdle congenital myasthenic syndrome due to a novel missense mutation and heteroallelic deletion in MUSK.* Neuromuscul Disord, 2014. **24**(1): p. 31-5.

250. Milhem, R.M., et al., *Identification of the cellular mechanisms that modulate trafficking of Frizzled Family Receptor 4 (FZD4) missense mutants associated with FEVR.* Invest Ophthalmol Vis Sci, 2014.

251. Till, J.H., et al., *Crystal structure of the MuSK tyrosine kinase: insights into receptor autoregulation.* Structure, 2002. **10**(9): p. 1187-96.

252. Stein, A., et al., *Key Steps in ERAD of Luminal ER Proteins Reconstituted with Purified Components.* Cell, 2014. **158**(6): p. 1375-88.

253. Stiegler, A.L., S.J. Burden, and S.R. Hubbard, *Crystal structure of the agrin-responsive immunoglobulin-like domains 1 and 2 of the receptor tyrosine kinase MuSK.* J Mol Biol, 2006. **364**: p. 424-33.

254. Okada, K., et al., *The muscle protein Dok-7 is essential for neuromuscular synaptogenesis.* Science, 2006. **312**(5781): p. 1802-5.

255. Wedemeyer, W.J., E. Welker, and H.A. Scheraga, *Proline cis-trans isomerization and protein folding.* Biochemistry, 2002. **41**(50): p. 14637-44.

256. Wang, X., et al., *Chemical and biological folding contribute to temperature-sensitive DeltaF508.* Traffic, 2008. **9**(11): p. 1878-93.

257. Glickman, M.H. and A. Ciechanover, *The ubiquitin-proteasome proteolytic pathway: destruction for the sake of construction.* Physiol Rev, 2002. **82**(2): p. 373-428.

258. Ziv, I., et al., *A perturbed ubiquitin landscape distinguishes between ubiquitin in trafficking and in proteolysis.* Mol Cell Proteomics, 2011. **10**(5): p. M111.009753.

259. Vikkula, M., et al., *Vascular dysmorphogenesis caused by an activating mutation in the receptor tyrosine kinase TIE2.* Cell, 1996. **87**: p. 1181-90.

260. Limaye, N., et al., *Somatic mutations in angiopoietin receptor gene TEK cause solitary and multiple.* Nat Genet, 2009. **41**(1): p. 118-24.

261. Wouters, V., et al., *Hereditary cutaneomucosal venous malformations are caused by TIE2 mutations with.* Eur J Hum Genet, 2010. **18**(4): p. 414-20.

262. Dumont, D.J., et al., *tek, a novel tyrosine kinase gene located on mouse chromosome 4, is expressed in endothelial cells and their presumptive precursors.* Oncogene, 1992. **7**: p. 1471-80.

263. Sato, T.N., et al., *Tie-1 and tie-2 define another class of putative receptor tyrosine kinase genes expressed in early embryonic vascular system.* Proc Natl Acad Sci U S A, 1993. **90**: p. 9355-8.

264. Wouters, V., et al., *Hereditary cutaneomucosal venous malformations are caused by TIE2 mutations with widely variable hyper-phosphorylating effects.* Eur J Hum Genet, 2009. **18**: p. 414-20.

265. Calvert, J.T., et al., *Allelic and locus heterogeneity in inherited venous malformations.* Hum Mol Genet, 1999. **8**: p. 1279-89.

266. Boon, L.M., et al., *Assignment of a locus for dominantly inherited venous malformations to chromosome 9p.* Hum Mol Genet, 1994. **3**: p. 1583-7.

267. Gallione, C.J., et al., *A gene for familial venous malformations maps to chromosome 9p in a second large kindred.* J Med Genet, 1995. **32**: p. 197-9.

268. Kontos, C.D., et al., *Tyrosine 1101 of Tie2 is the major site of association of p85 and is required for.* Mol Cell Biol, 1998. **18**(7): p. 4131-40.

269. Brodsky, J.L., *Just a trim, please: refining ER degradation through deubiquitination.* Cell, 2013. **154**: p. 479-81.

270. Neuber, O., et al., *Ubx2 links the Cdc48 complex to ER-associated protein degradation*, in *Nat Cell Biol*. 2005: England. p. 993-8.

271. Sato, B.K., et al., *Misfolded membrane proteins are specifically recognized by the transmembrane domain of the Hrd1p ubiquitin ligase.* Mol Cell, 2009. **34**: p. 212-22.

272. Iida, Y., et al., *SEL1L protein critically determines the stability of the HRD1-SEL1L endoplasmic reticulum-associated degradation (ERAD) complex to optimize the degradation kinetics of ERAD substrates.* J Biol Chem, 2011. **286**(19): p. 16929-39.

273. Mueller, B., et al., *SEL1L nucleates a protein complex required for dislocation of misfolded glycoproteins.* Proc Natl Acad Sci U S A, 2008. **105**: p. 12325-30.

274. Christianson, J.C., et al., *OS-9 and GRP94 deliver mutant alpha1-antitrypsin to the Hrd1-SEL1L ubiquitin ligase complex for ERAD.* Nat Cell Biol, 2008. **10**: p. 272-82.

275. Hosokawa, N., et al., *Human OS-9, a lectin required for glycoprotein endoplasmic reticulum-associated degradation, recognizes mannose-trimmed N*-glycans*.* J Biol Chem, 2009. **284**(25): p. 17061-8.

276. Hosokawa, N., Y. Kamiya, and K. Kato, *The role of MRH domain-containing lectins in ERAD.* Glycobiology, 2010. **20**: p. 651-60.

277. Lilley, B.N. and H.L. Ploegh, *A membrane protein required for dislocation of misfolded proteins from the ER.* Nature, 2004. **429**(6994): p. 834-40.

278. Mehnert, M., T. Sommer, and E. Jarosch, *Der1 promotes movement of misfolded proteins through the endoplasmic reticulum membrane.* Nat Cell Biol, 2013. **16**: p. 77-86.

279. Ishikura, S., A.M. Weissman, and J.S. Bonifacino, *Serine residues in the cytosolic tail of the T-cell antigen receptor alpha-chain mediate ubiquitination and endoplasmic reticulum-associated degradation of the unassembled protein.* J Biol Chem, 2010. **285**: p. 23916-24.

280. van den Boomen, D.J., et al., *TMEM129 is a Derlin-1 associated ERAD E3 ligase essential for virus-induced degradation of MHC-I.* Proc Natl Acad Sci U S A, 2014. **111**: p. 11425-30.

281. Ploegh, H.L., *A lipid-based model for the creation of an escape hatch from the endoplasmic reticulum.* Nature, 2007. **448**: p. 435-8.

282. Ballar, P., et al., *Identification of SVIP as an endogenous inhibitor of endoplasmic reticulum-associated degradation.* J Biol Chem, 2007. **282**(47): p. 33908-14.

283. Ballar, P., et al., *Differential regulation of CFTRDeltaF508 degradation by ubiquitin ligases gp78 and Hrd1.* Int J Biochem Cell Biol, 2010. **42**(1): p. 167-73.

284. Zhou, H., et al., *Distinct domains of MuSK mediate its abilities to induce and to associate with postsynaptic specializations.* J Cell Biol, 1999. **146**: p. 1133-46.

285. Bainbridge, T.W., et al., *Evolutionary divergence in the catalytic activity of the CAM-1, ROR1 and ROR2 kinase domains.* PLoS One, 2014. **9**: p. e102695.

286. Stroud, R.M. and J.A. Wells, *Mechanistic diversity of cytokine receptor signaling across cell membranes.* Sci STKE, 2004. **2004**: p. re7.

287. Dong, N., et al., *Corin mutations K317E and S472G from preeclamptic patients alter zymogen activation and cell surface targeting. [Corrected].* J Biol Chem, 2014. **289**: p. 17909-16.

288. Jansens, A., E. van Duijn, and I. Braakman, *Coordinated nonvectorial folding in a newly synthesized multidomain protein.* Science, 2002. **298**: p. 2401-3.

289. Marquardt, T., D.N. Hebert, and A. Helenius, *Post-translational folding of influenza hemagglutinin in isolated endoplasmic reticulum-derived microsomes.* J Biol Chem, 1993. **268**: p. 19618-25.

290. Nemudryi, A.A., et al., *TALEN and CRISPR/Cas Genome Editing Systems: Tools of Discovery.* Acta Naturae, 2014. **6**: p. 19-40.

291. Peng, Y., et al., *Making designer mutants in model organisms*, in *Development*. 2014, (c) 2014. Published by The Company of Biologists Ltd. p. 4042-4054.

292. Mariano, A., L. Xu, and R. Han, *Highly efficient genome editing via 2A-coupled co-expression of two TALEN monomers.* BMC Res Notes, 2014. **7**: p. 628.

293. Schiml, S., F. Fauser, and H. Puchta, *The CRISPR/Cas system can be used as nuclease for in planta gene targeting and as paired nickases for directed mutagenesis in Arabidopsis resulting in heritable progeny.* Plant J, 2014.

294. Verkman, A.S. and L.J. Galietta, *Chloride channels as drug targets.* Nat Rev Drug Discov, 2009. **8**: p. 153-71.

295. Culi, J. and R.S. Mann, *Boca, an endoplasmic reticulum protein required for wingless signaling and trafficking of LDL receptor family members in Drosophila.* Cell, 2003. **112**: p. 343-54.

# Appendix I

## List of Publications:

Milhem, R.M., Al-Gazali, L., & Ali, B.R. (2015). Improved plasma membrane expression of the trafficking defective P344R mutant of muscle, skeletal, receptor tyrosine kinase (MuSK) causing congenital myasthenic syndrome. The International Journal of Biochemistry and Cell Biology. In Press.

Milhem, R.M., Ben-Salem, S.M., Al-Gazali, L.I., & Ali, B.R. (2014). Identification of the cellular mechanisms that modulate trafficking of Frizzled Family Receptor 4 (FZD4) missense mutants associated with FEVR. *Invest Ophthalmol Vis Sci*. doi: 10.1167/iovs.14-13885

Matlik, H.N., Milhem, R.M., Saadeldin, I.Y., Al-Jaibeji, H.S., Al-Gazali, L., & Ali, B.R. (2014). Clinical and molecular analysis of a novel COLQ missense mutation causing congenital myasthenic syndrome in a Syrian family. *Pediatr Neurol, 51*, 165-169. doi: 10.1016/j.pediatrneurol.2014.03.012

Saadeldin, I.M., Milhem, R.M.. Al-Ghazali, Lihadh. Ali, Bassam. (2013). Novel KCNQ2 Mutation in a Large Emirati Family with Benign Familial Neonatal Seizures. *Pediatr Neurol, 48*, 63-66.

Ali, B.R., Ben-Rebeh, I., John, A., Akawi, N.A., Milhem, R.M., Al-Shehhi, N.A., Al-Gazali, L. (2011). Endoplasmic reticulum quality control is involved in the mechanism of endoglin-mediated hereditary haemorrhagic telangiectasia. *PLoS One, 6*(10), e26206. doi: 10.1371/journal.pone.0026206

## List of Conferences:

R.M.Milhem, L. Al-Ghazali and B.R.Ali; conference speaker

The Rescue of Cellular Trafficking-defective Mutants resulting in Congenital Myasthenic Syndrome and Familial Exudative Vitreoretinopathy; 5th Pan Arab Human Genetics Conference: Genomics into healthcare-November 17-19, 2013, Dubai, UAE

B.R. Ali, A. John, R.M. Milhem; poster

ER retention and degradation of mutated proteins is a common mechanism in numerous loss-of-function genetic conditions. Genomic Disorders 2012: The genomics of rare Diseases, 21-24 March 2012, Hinxton, Cambridge, UK

R.M. Milhem, L. Al-Gazali and B.R. Ali; poster

ER-Retention is a Common Cellular Mechanism Underlying Numerous Human Monogenic Disorders: The Case of Familial Exudative Vitreoretinopathy and Congenital Myasthenic Syndrome. FASEB Science Research Conference on Protein Folding in the Cell. 20-26th July 2014, Saxtons River, VT, USA.